GRAVEL TRANSPORT AND STRATIFICATION ORIGINS, KICKING HORSE RIVER, BRITISH COLUMBIA

GRAVEL TRANSPORT AND STRATIFICATION ORIGINS, KICKING HORSE RIVER, BRITISH COLUMBIA

By

FRANCES J. HEIN, B.S.

A Thesis

Submitted to the School of Graduate Studies

in Partial Fulfilment of the Requirements

for the Degree

Master of Science

McMaster University

September 1974

MASTER OF SCIENCE (1974) McMASTER UNIVERSITY
(Geology) Hamilton, Ontario

TITLE: Gravel Transport and Stratification Origins, Kicking Horse River, British Columbia.

AUTHOR: Frances J. Hein, B.S. (University of Illinois at Chicago Circle Campus)

SUPERVISOR: Professor Roger G. Walker

NUMBER OF PAGES: i-xii; 1-135

ABSTRACT

In the Kicking Horse River systematic changes occur in bar forms from upstream to downstream reaches. In high gradient coarse-grained upstream localities flow is confined to one or two main channels which have a somewhat meandering to braided form. Bedload is transported only during maximum flow conditions as diffuse gravel sheets. In low gradient fine-grained medial to distal reaches flow is carried down anastomosing braided channel complexes with extensive bar development. These differences in bar-and-channel morphologies can be explained as follows. In upstream reaches bars and channels are relict from flood flows, where lower summer flows are incompetent to rework the diffuse sheets into true bars. In finer-grained reaches bars develop from flood-deposited diffuse sheets, where finer sediment is winnowed out under lower flows and transported as bar lobes. Significant lateral exchange of flow between adjacent channel systems produces a complex braided channel pattern.

Diffuse gravel sheets display little sediment sorting and no foreset development. Deposits are massive poorly sorted gravels. Examination of sorting on bar surfaces, suggest that diagonal bar deposits would be lenticular fining-upward

or massive gravels with low angle to horizontal bedding. Deposits associated with transverse bar migration would consist of fining-upward gravels with a few lenses of planar cross-stratified sequences.

Preservability of stratification types estimated from trench sections in the North Saskatchewan River suggest that horizonatally bedded massive gravels are dominant in medial to distal flats. Remaining percentages are largely composed of fining-upward and planar cross-stratified gravels.

Proximal sediments would be coarse-grained, poorly sorted massive deposits. Medial to distal deposits would be predominantly massive (due to extensive bar dissection) with subordinant amounts of fining-upward and planar cross-stratified sequences (associated with bar migrations). Systematic transitions from ill-defined bars in proximal areas to true bars in distal reaches, suggest that massive poorly sorted gravels should decrease downvalley, corresponding to an increase in moderately sorted planar cross-stratified sequences.

ACKNOWLEDGEMENTS

The author is very grateful to Professors R.G. Walker and G.V. Middleton who offered many helpful suggestions. Thanks are extended to Professors D.G. Smith and N.D. Smith who provided stimulating discussions. Finally, I am indebted to several persons who assisted in the field: D.J. Hein, who provided capable field assistance during the majority of the field season; S.P. Fuller and P.N. Hein, who also assisted in the field.

Financial assistance and equipment were provided by the Department of Geology and the Research Board, McMaster University; the bulk of the expenses were covered by a Research Grant from the Geological Society of America and from a National Research Council grant to R.G. Walker. I also thank Mr. T.F. Smith, Department of the Environment, Ottawa, for loan of a stage recorder. Permission from the National and Historic Parks Branch, Department of Indian Affairs and Northern Development of Canada to do field work in Banff and Yoho National Parks is appreciated.

Helen Elliott typed the manuscript and Lynn Franks assisted in preparation of some of the diagrams.

TABLE OF CONTENTS

LIST OF TABLES

LIST OF FIGURES

CHAPTER 1

INTRODUCTION

GENERAL INTRODUCTION

In recent years many workers have examined the sedimentology of coarse-grained braided rivers (Krigström, 1962; Fahnestock, 1963; McDonald and Banerjee, 1971; Boothroyd, 1972; Bradley et al., 1972; Church, 1972; Rust, 1972; N. Smith, 1972; D. Smith, 1973b; N. Smith, 1974). Braided streams can be classified as "deep", greater than 4 m depth, or "shallow", less than 4 m depth (Eynon and Walker, 1974). The deep water model proposed by Eynon and Walker (1974) was based upon sediment facies distributions in Pleistocene glaciofluvial deposits. Most of the shallow braided river models, however, have been solely based upon sediment distribution patterns on outwash flat surfaces. Sedimentary features associated with the dominant gravel facies include massive, coarsening-up, fining-up and cross-stratified sequences. Few studies have tried to correlate bar-and-channel development, hydrology and sediment transport with these sedimentary sequences (Fahnestock, 1963; N. Smith, 1972, 1974). Some workers have constructed facies models

based on proximal-distal trends in surface sedimentary features (Boothroyd, 1972; Rust, 1972). These features were examined only during low-flow exposed conditions; hence, the model is quite interpretive. Due to the many problems associated with mapping bars and channels during high discharges, few previous studies have documented processes of braiding in coarse-grained proximal areas versus braiding processes in more distal fine-grained reaches (Fahnestock, 1963). Other problems with the shallow braided river model include the actual preservability of "characteristic" sedimentary features and their potential of being incorporated in the ancient record.

The primary objective of this project is to try and develop a model for shallow coarse-grained braided river deposition which would enable one to distinguish proximal versus distal sediments. This model is based upon (1) braiding patterns in proximal versus distal areas; (2) sediment sorting on individual bar surfaces, from which a model for the origins of the gravel sequences could be proposed; and, (3) percentages of sedimentary sequences in trench-section of exposed outwash areas.

PLAN OF STUDY

Origins of stratification were investigated in terms of bar-and-channel pattern evolution, hydraulics of bedload transport and bar migration, and sorting of gravel on bar surfaces. These studies were conducted primarily on the Kicking Horse River outwash plain, with supplementary data obtained from the Bath Creek gravel flats. The occurrence and preservability of sedimentary sequences, interpreted from bar behavior in the Kicking Horse River and Bath Creek, were then investigated in trenched cross-sections of recent exposed shallow braided river gravel flats of the North Saskatchewan River. Because of the difficulty in trenching modern outwash sediments, this investigation could only be conducted in one reach. In summary, a model is suggested for shallow braided stream deposits in confined proglacial valleytrain environments.

CHAPTER 2

REGIONAL SETTING

LOCATIONS

Access to most glacier-fed rivers in the Canadian Rockies is commonly difficult. Hence, road access to outwash flats was the main deciding factor in selection of study areas. Two major highways transverse the Park Ranges areas: the Trans Canada highway (No. 1) and the Columbia-Icefields highway (No. 93). These highways bisect several outwash river systems which were deemed suitable for study: (1) the Kicking Horse River, in Yoho National Park near the townsite of Field, B.C.; (2) Bath Creek, in Banff National Park, approximately 5 miles west of the townsite of Lake Louise, Alta., and (3) the North Saskatchewan River, in Banff National Park, Alta., approximately 11 miles southeast of the Banff-Jasper National Park boundary (Figures 1,2,3).

Bar-and-channel braiding patterns and sediment distributions were studied in the Kicking Horse River, with supplementary data obtained from Bath Creek. The Kicking Horse River was thought to be an ideal location for a study

Figure 1. General location map of study areas

Figure 2. Map of Kicking Horse River study area

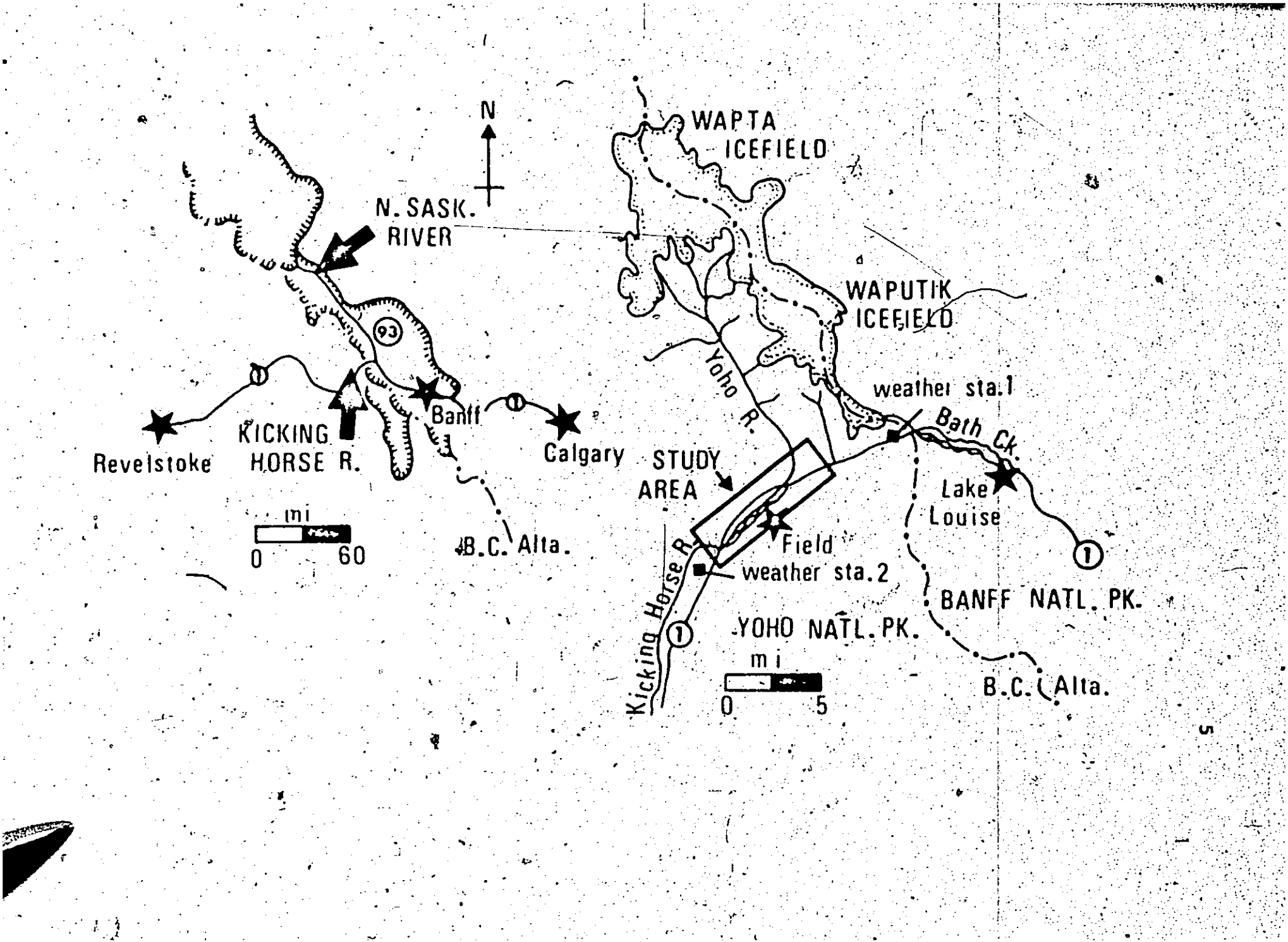
N
WAPTA
ICEFIELD
N. SASK.
RIVER
WAPUTIK
ICEFIELD
93
Yoho R.
weather sta.1
Bath Ck.
Banff
Revelstoke
KICKING
HORSE R.
Calgary
STUDY
AREA
Lake
Louise
mi
0 60
B.C. Alta.
Field
weather sta.2
Kicking Horse R.
BANFF NATL. PK.
YOHO NATL. PK.
mi
0 5
B.C. Alta.

Figure 3. Map of North Saskatchewan River study area

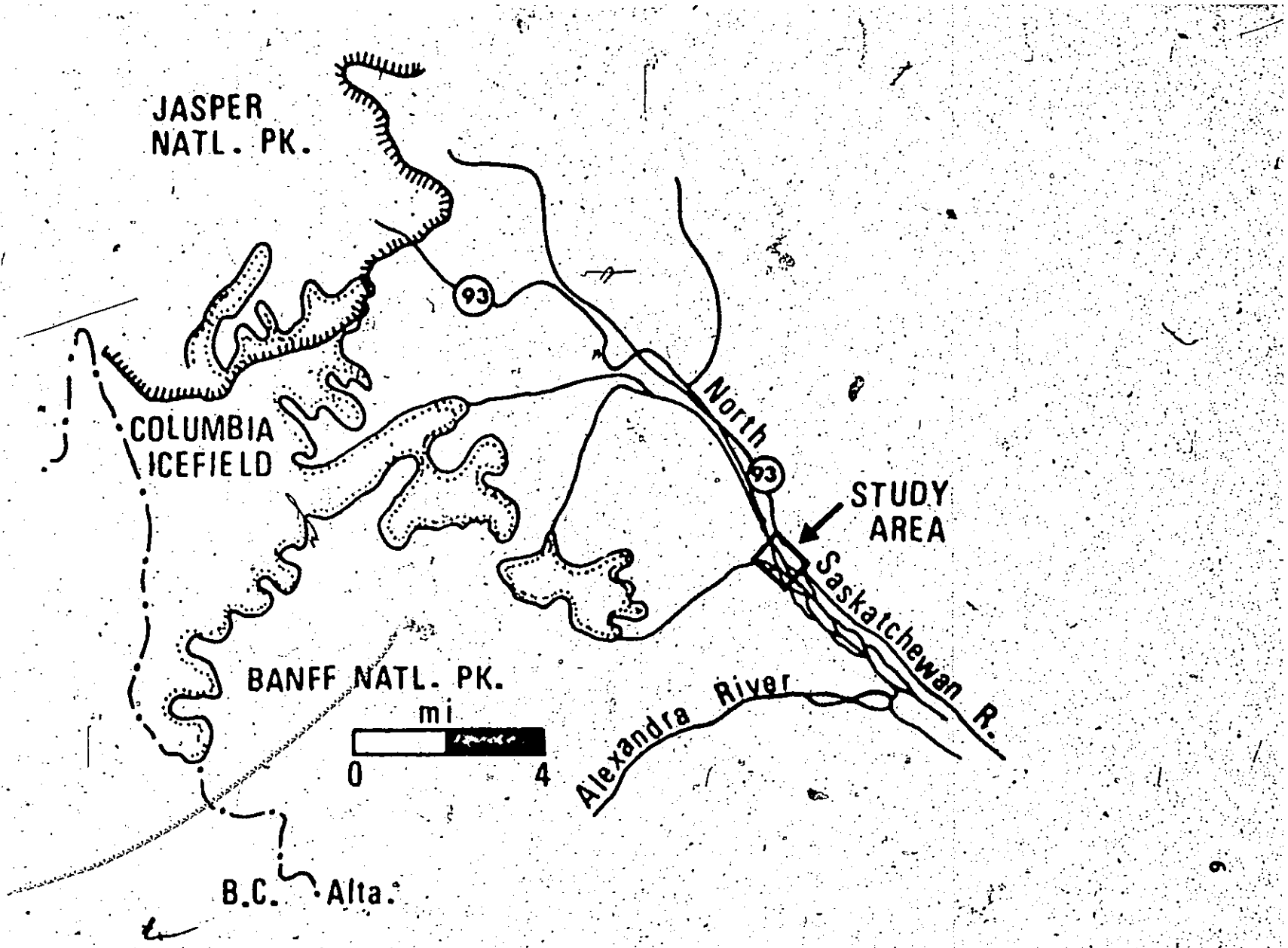
JASPER
NATL. PK.
93
COLUMBIA
ICEFIELD
North
93
STUDY
AREA
Saskatchewan R.
BANFF NATL. PK.
mi
0
4
Alexandra River
B.C.
Alta.

of proximal-distal braiding patterns for the following reasons:

(1) Several bridges span the river which could serve as temporary gauging stations;

(2) Weather stations are maintained by Yoho National Park in the Kicking Horse River area;

(3) The river has a wide range of summer discharges (N. Smith, 1974) which are suitable for studying bar-and-channel evolution during high flows and sediment distribution patterns on outwash surfaces during low flows;

(4) Previous sedimentological studies in this system by N. Smith (1972, 1974) have described general sedimentary, morphologic and hydraulic characteristics of this river. Because these aspects were established, there was sufficient time in one field season to concentrate on the detailed aspects of bar formation, gravel transport and resulting stratification types.

Because the Kicking Horse River flows in a relatively narrow, confined channel system and due to the high summer discharges it is quite difficult to study preserved stratification in section. In contrast, the upper North Saskatchewan is a tributary to the Alexandra-North Saskatchewan

system in terms of discharge, but transports an estimated 95% of the outwash gravels into the system (D. Smith, 1973a). Extensive exposed gravel flats occur northwest of the confluence with the Alexandra River and provided a "high and dry" area to study internal stratification types in trenched sections.

GENERAL GEOLOGY: KICKING HORSE RIVER AREA

The Kicking Horse River is located in the rugged Main Ranges of the Canadian Cordillera, where the local bedrock is composed mainly of Cambrian carbonates. The river flows through a steep, glacially-carved valley, with maximum relief of 6,000 ft (Mt. Stephen). Several alluvial fans contribute small amounts of sediment from the tributaries. Outcrops of the famous Burgess Shale and Mt. Stephen fossil beds have prompted many detailed paleontologic, stratigraphic and structural studies in this area.

In terms of total bedrock composition, there is approximately 5% exposure of the Lower Cambrian Gog quartzite, with the remaining percentages composed of Cambrian carbonates, ranging from the lower Cambrian Mt. Whyte Formation to the Upper Cambrian Arctomys Formation. The fluvial gravels in the Kicking Horse River show a similar composition.

Dominant bed material is sub- to well-rounded gravel, composed of about 98% limestone and dolomite, 2% quartzite and traces of clay shale and chert (N. Smith, 1974).

Allen (1914) briefly described and mapped the glaciofluvial deposits in the Kicking Horse River valley. Pleistocene to Recent deposits of the lower Kicking Horse River valley between Leanchoil and Golden, B.C. were studied by BeMent (1972). These deposits were interpreted as being glaciofluvial to glaciolacustrine in origin. The lower Kicking Horse River valley shows evidence of glaciation 19,000 to 10,000 years B.P. Field observations by BeMent (1972) indicate that ice within the valley was at least 3,500 ft thick. Evidence for only one glacial stage was found in this area, whereas other valleys of central and southern British Columbia indicate from two to four glacial stages (Armstrong and Tipper, 1948; Fulton, 1971).

RIVER HYDROLOGY, MORPHOLOGY AND SEDIMENT: KICKING HORSE RIVER

The author worked as field assistant with N. Smith (1972, 1974) in his studies of bar development and sedimentology of the Kicking Horse River system. Field work was done in August and September, 1971, with additional data obtained in July 1972. Processes involved with bar formation and

growth, and sediment distribution patterns within the system were the main topics covered in N. Smith's study (1972, 1974). The present study is an extension of his work and emphasizes integrated bar-and-channel development and braiding patterns in proximal versus distal reaches of the gravel flats. Field work was done primarily in the months of June through August, 1973, with some preliminary data obtained in July 1972. Data cited pre-1973 in the following section is from N. Smith's study; data obtained during the summer of 1973 is from the present study.

1. Hydrology

The Kicking Horse River system is fed by the Wapta and Waputik Icefields in eastern British Columbia (Figure 3). The Yoho River is the main tributary, which contributes an estimated 80% of the discharge to the Kicking Horse River system. Temporary gauging stations have been monitored under the Field townsite bridge during the summers 1971, 1972 (N. Smith, 1974) and 1973 (this study). As with most glacial meltwater streams, summer discharges depend upon weather conditions over the icefields. Highest flows occurred in August 1971 when local air temperatures were ranging around 90°F (Table 1). During this clear hot period of maximum glacial melting, daily discharge extremes varied by a factor of two. Maximum discharge was calculated at 3,400

Table 1. Maximum river discharges recorded during Summers 1971 to 1973, Kicking Horse River

Date	Maximum Discharge (cfs)	Average Discharge (cfs)	Weather Conditions	Reference
August 1971	3,400	-	Clear, Hot	N. Smith, 1974
July 1972	-	1,700	Cool, Rainy Overcast	
June 1973	2,400	-	Hot, Clear	Present Study
June, August 1973	-	500-800	Cold, Rainy	
July 1973	1,560	-	Hot, Clear	
August 1973	1,225	-	Hot, Clear	

cubic feet per second (cfs). Daily flows were minimal in the late morning with peak discharges occurring around 7.00 p.m. During July 1972 air temperatures were cooler than normal and weather conditions were overcast and rainy. Discharges during this month were fairly constant (approximately 1,700 cfs), with only a slight hint of daily diurnal fluctuations (N. Smith, 1974).

Weather and hydrologic data recorded from May 31 to August 31, 1973 in the present study are summarized in Figures 4,5. Figure 4C shows the average daily discharge, which was computed as the average of the maximum and minimum discharges per day. Three discharge periods could be distinguished: Cold Rainy, Spring Melt and Summer Diurnal Periods (Figure 4C). Continuous discharge and stage height records of typical days within these periods are shown in Figure 5. Cold Rainy Periods have very low discharges (500-800 cfs), with peaks caused by rain runoff and slightly warmer air temperatures (Figure 4). Maximum discharges during the 1973 field season were reached during the Spring Melt Period, characterized by maximum precipitation rates and very high air temperatures (70-90°F). At this time all of the snow in the valley and on adjacent slopes melted. The combined contribution of discharge from tributary streams and a substantial discharge output from the icefields produced the maximum discharge of 2,400 cfs. Three hot Summer Diurnal

Figure 4. Weather and river discharge records, Kicking Horse River, summer 1973.

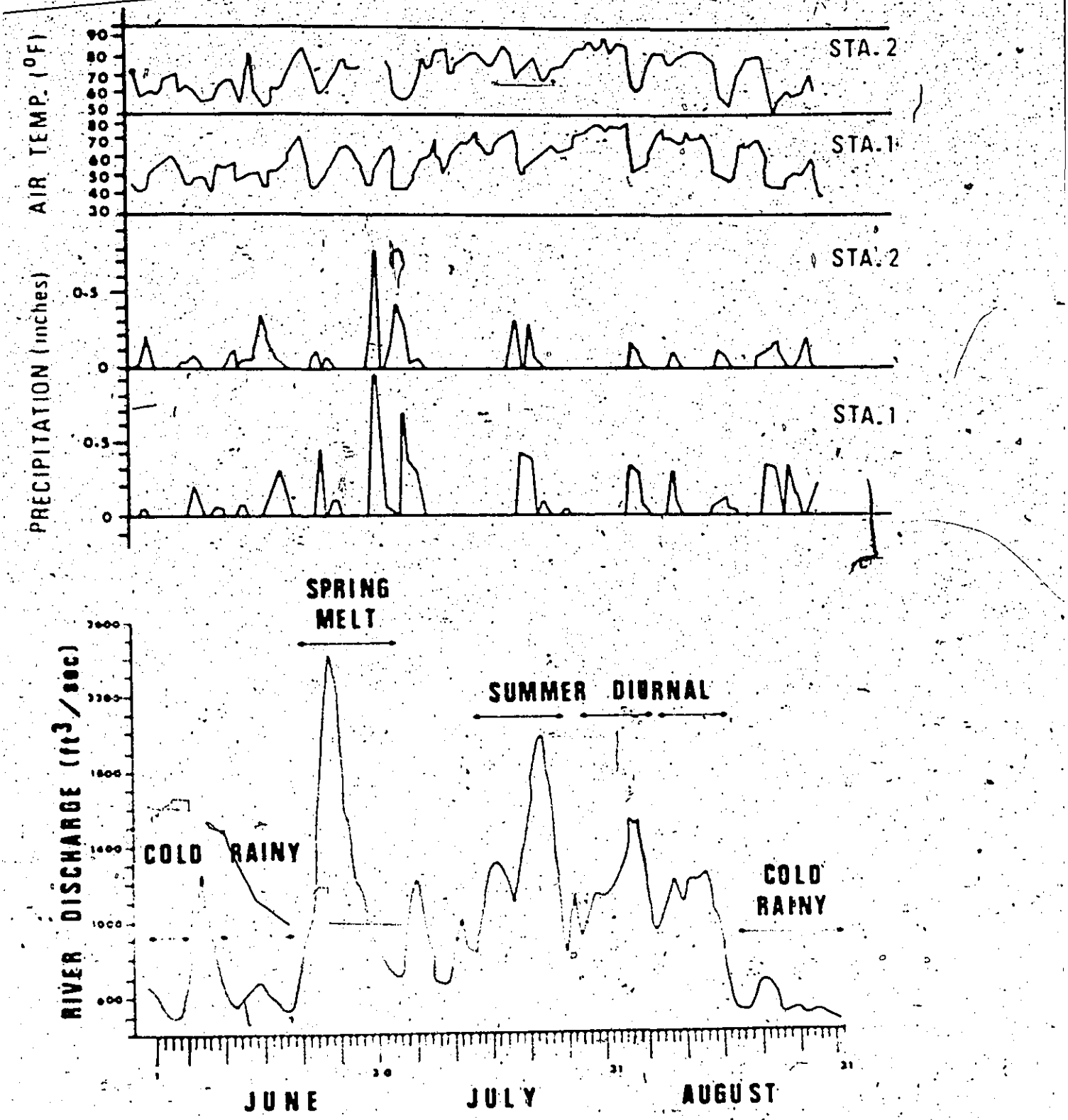
AIR TEMP. (°F)
STA. 2
STA. 1
PRECIPITATION (inches)
STA. 2
STA. 1
SPRING MELT
SUMMER DIURNAL
COLD RAINY
COLD RAINY
RIVER DISCHARGE (ft³/sec)
JUNE
JULY
AUGUST

Figure 5. Typical discharge period records, Kicking Horse River, summer 1973

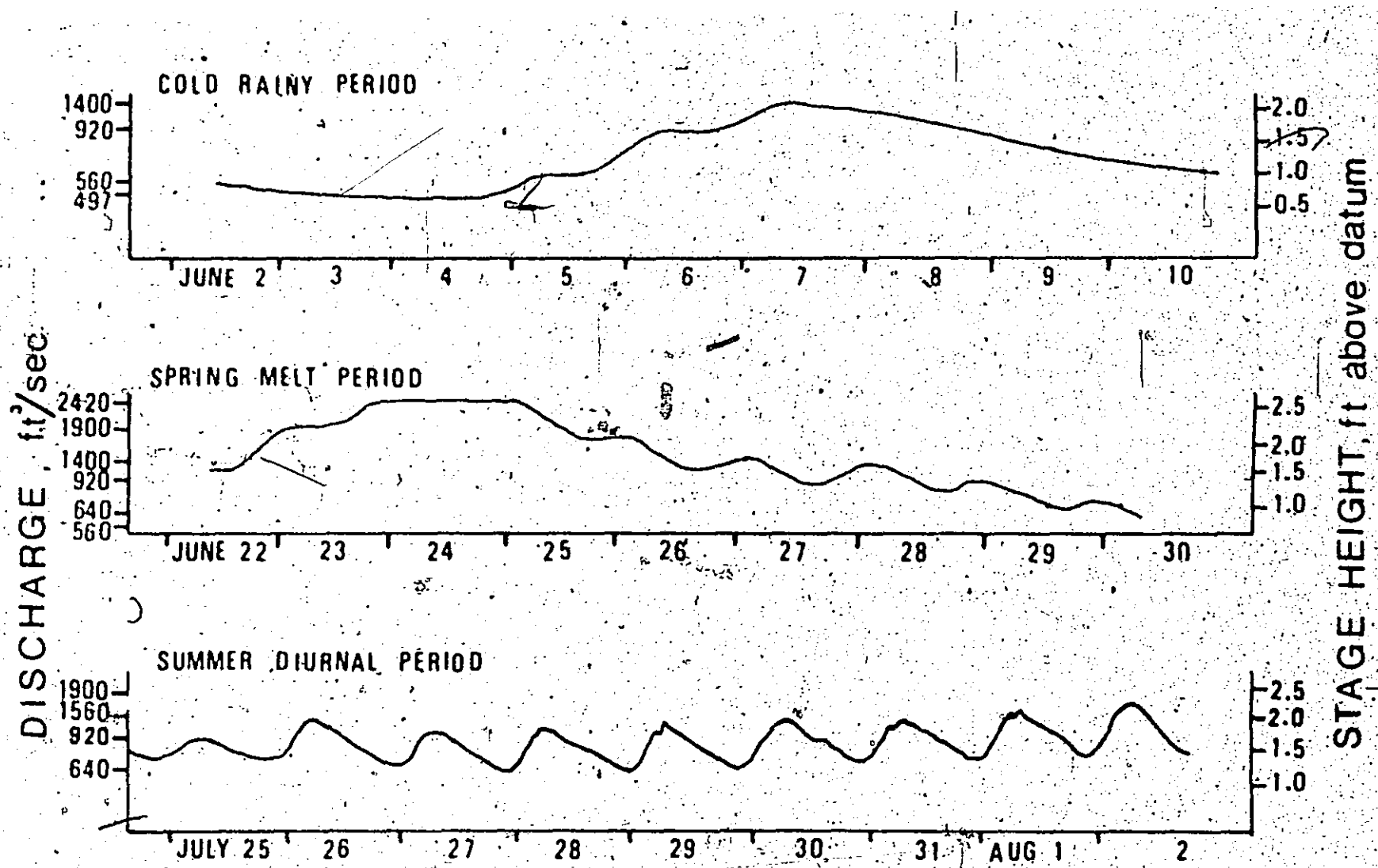
COLD RAINY PERIOD
1400
920
560
497
2.0
1.5
1.0
0.5
JUNE 2
3
4
5
6
7
8
9
10
SPRING MELT PERIOD
2420
1900
1400
920
640
560
2.5
2.0
1.5
1.0
JUNE 22
23
24
25
26
27
28
29
30
SUMMER DIURNAL PERIOD
1900
1560
920
640
2.5
2.0
1.5
1.0
JULY 25
26
27
28
29
30
31
AUG 1
2
DISCHARGE, ft³/sec
STAGE HEIGHT, ft above datum

Periods were observed, each separated by cold periods. Diurnal fluctuations in discharge, which vary by a factor of 1.5 to 2, occur during clear sky and maximum air temperature weather conditions. The August Summer Diurnal Period had much lower discharges (maximum 1,225 cfs), which was probably a function of the colder temperatures and overcast weather conditions observed over the Wapta and Waputik Icefields.

2. Morphology and Sediment

The Kicking Horse River is characterized by alternating gravel flats and narrow channel river patterns. Downstream from the confluence between the Yoho River and Kicking Horse Creek, the Kicking Horse River is confined to a steep narrow channel, which opens up into an extensive gravel flat outwash area (Figures 6,7) downstream from the Trans-Canada Highway bridge. At the townsite of Field, a large alluvial fan constricts the flow to a narrow channel, which then opens up again into a wide plain, approximately 0.5 miles downstream from Field (Figures 6,7). Two miles downstream from Field, the river again becomes a narrow cascading channel, which extends for 2 miles downstream, where again it becomes a broad plain of the lower Kicking Horse River. The alternating gravel flats and narrow channel river pattern is explained by Allen (1914) as follows. The valley is interpreted as being pre-glacial in origin. Upon glaciation basins were gouged out

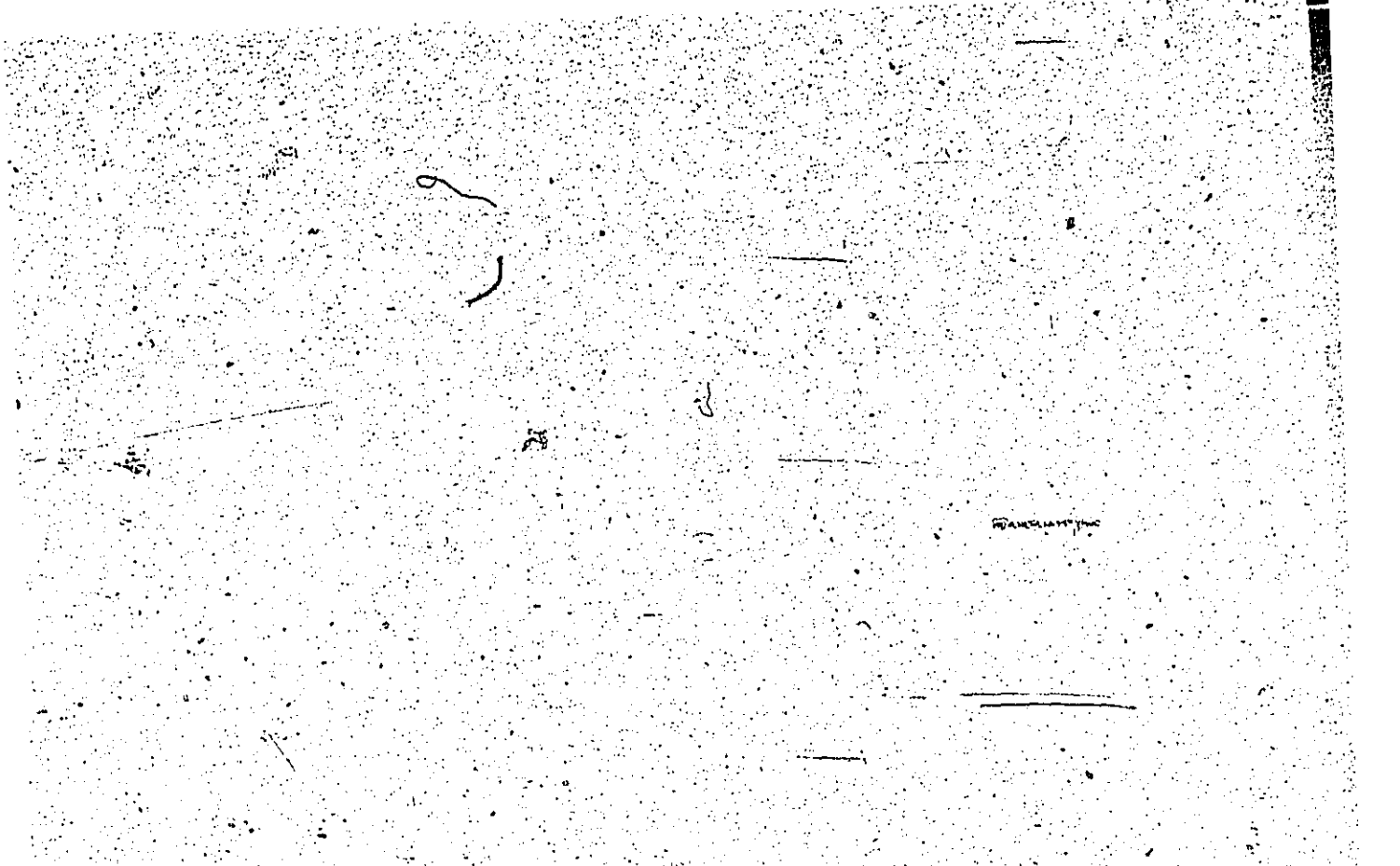

Figure 6. Oblique photo of upper Kicking Horse River taken from Mt. Stephen, Geological Survey of Canada Phbto nos. 2-23-73 to 2-26-73. Flow is from Right to Left.

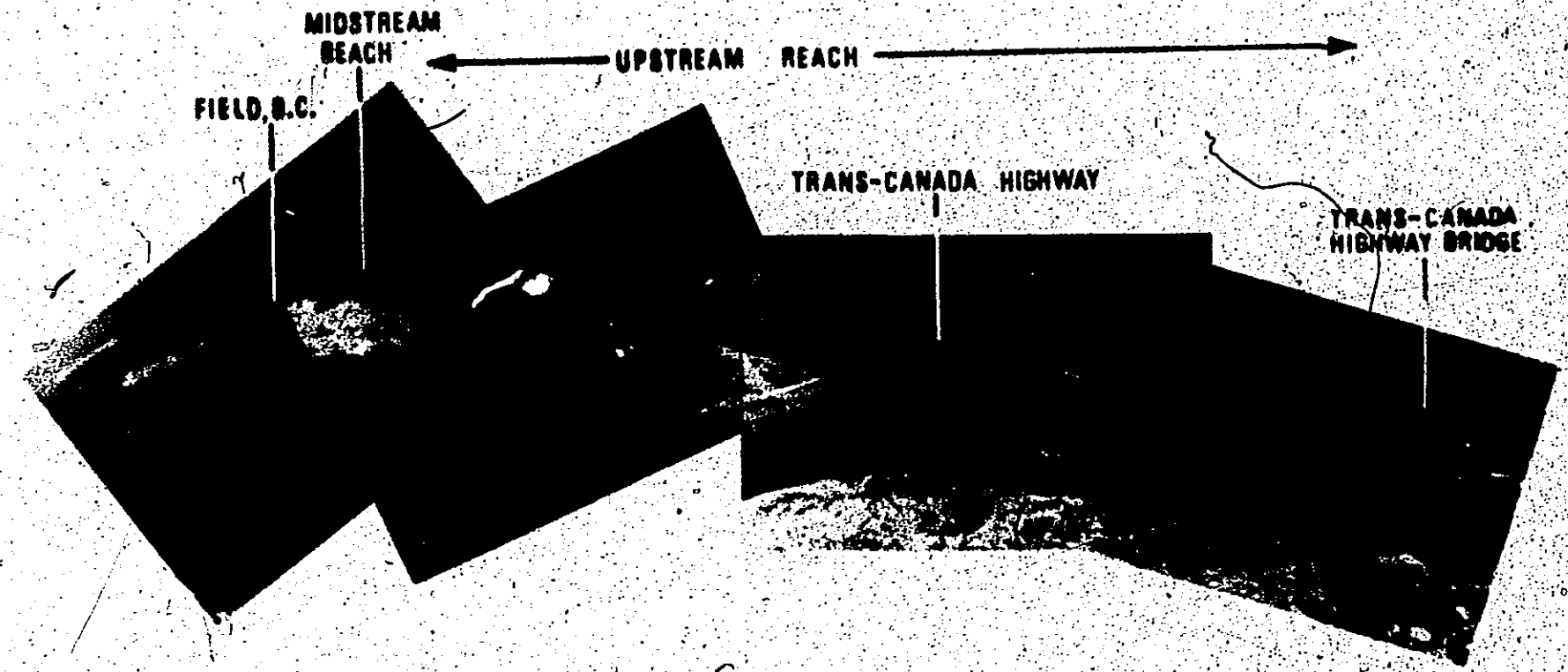

KICKING HORSE RIVER, B.C.

Figure 7. Longitudinal profile of Kicking Horse River outwash plain (modified after N. Smith, 1974)

Figure 8. Downvalley trends in size of bed material, Kicking Horse River (modified after N. Smith, 1974)

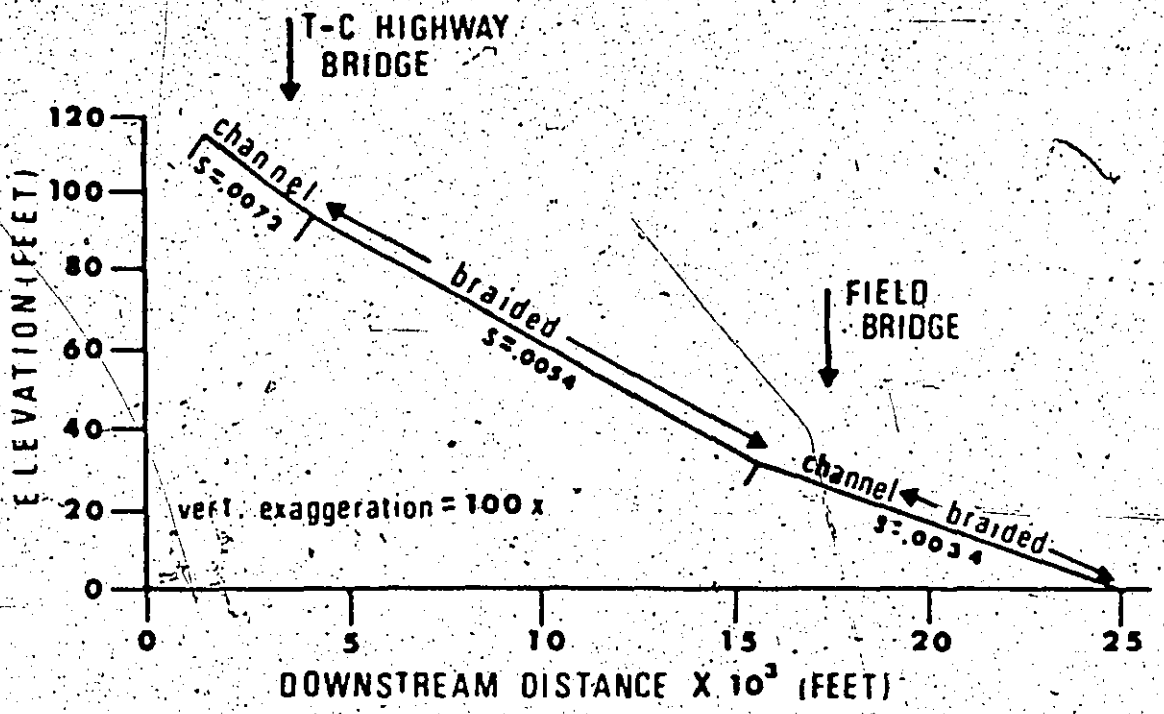
T-C HIGHWAY BRIDGE
FIELD BRIDGE
channel
S=.0073
braided
S=.0054
channel
braided
S=.0034
vert. exaggeration = 100 x
ELEVATION (FEET)
120
100
80
60
40
20
0
0
5
10
15
20
25
DOWNSTREAM DISTANCE X 10³ (FEET)

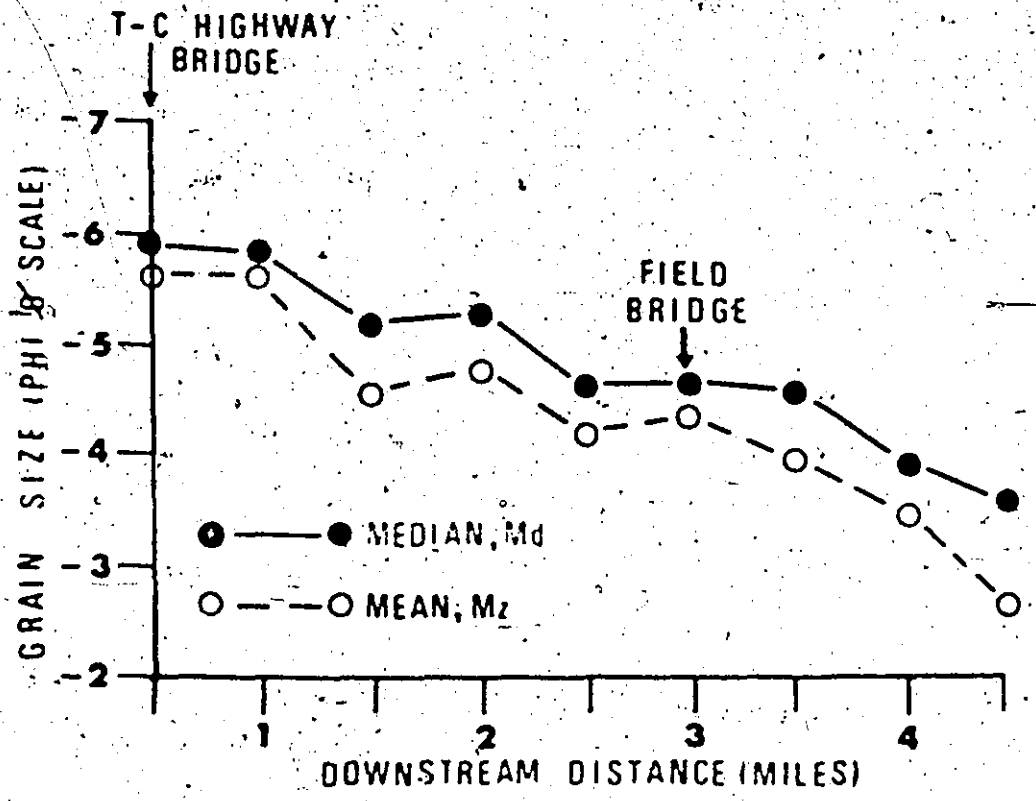
T-C HIGHWAY BRIDGE
FIELD BRIDGE
GRAIN SIZE (PHI SCALE)
-7
-6
-5
-4
-3
-2
MEDIAN, Md
MEAN, Mz
1
2
3
4
DOWNSTREAM DISTANCE (MILES)

of the valley floor and have become filled in with glaciolacustrine and glaciofluvial deposits, forming the extensive gravel flats. The study area is the 4 mile long gravel plain between the Trans-Canada Highway bridge and the narrow channel near Natural Bridge (Figure 3).

Longitudinal profile measurements (N. Smith, 1974) show that the outwash gravel flats in the study area can be approximated by two straight lines (Figure 7). Above the break in slope (which occurs just upstream from the Field bridge), the average gradient of the water surface is 0.0054; whereas downstream from the slope break it is 0.0034. The reason for this slope break is unknown. Extensive gravel dredging operations maintained by Yoho National Park occur on the river flats in this slope break region. Approximately 64,000 tons of gravel have been removed between the years 1970 and 1973 (D. Watson, Pers. Comm.). However, despite the large tonnage of gravel that has been removed, the gravel operations are not thought to be the cause of this slope break, as similar breaks in longitudinal profiles have been observed in Bow and Peyto outwash areas (McDonald and Banerjee, 1971). McDonald and Banerjee (1971) suggest that the slope break may represent the contact between upstream degrading outwash surfaces and downstream aggrading surfaces.

Examination of aerial photographs of the Kicking Horse River gravel flats indicate that braiding patterns change from upstream to midstream and downstream reaches of the 4 mile study reach. In high-slope upstream reaches (Figure 6) flow is transported down one or two major channels, which have a braided to somewhat meandering form. Midstream and downstream reaches have a complex braided channel pattern, where flow is carried down many braided channels which anastomose back and forth across the gravel flats. This change in braid pattern occurs just downstream from the slope break in the longitudinal profile. Corresponding to the downstream reduction in slope there is also a significant decrease in bedload grain size (Figure 8). Upstream reaches have a mean grain size of -5.7ϕ, which decreases to -2.7ϕ in downstream sections (N. Smith, 1974).

GENERAL GEOLOGY: NORTH SASKATCHEWAN RIVER AREA

The North Saskatchewan River flows along the axis of a breached anticline in a glacially carved U-shaped valley, with maximum relief of 6,200 ft (Mt. Saskatchewan). Previous work in this area has been limited. Baird (1970) briefly described this section in his study of the regional geology

of the Canadian Cordillera. Surficial deposits were mapped by McPherson (1970). Rates of aggradation and modes of channel braiding of the Alexandra-North Saskatchewan River system were studied by D. Smith (1973b). Bedrock material ranges in age from Precambrian to Carboniferous and is composed of approximately 70% carbonates and 30% quartzite. Fluvial gravels have essentially the same composition as the bedrock material (D. Smith, 1973a).

Late Pleistocene glaciers reached an average thickness of 3,000 ft in the study area (McPherson, 1970). The last recession occurred 9,000 years B.P. (Westgate and Dreimanis, 1967) and ended the Pleistocene era in this region. There have been three or four minor glacial advances in the Columbia Icefield area in recent time (D. Smith, in prep.).

RIVER HYDROLOGY, MORPHOLOGY AND SEDIMENT: NORTH SASKATCHEWAN RIVER

1. Hydrology

The Columbia Icefield is the major water source for the North Saskatchewan River (Figure 2). As with the Kicking Horse River, summer discharges are a function of weather conditions over the icefield. A temporary gauging station was established by D. Smith (1973a) during the summers 1970, 1971. As with most glacially-fed streams in this region, during warm

summer months marked diurnal fluctuations in discharge occur. Low flows occur in the late morning to early afternoon and peak flows occur between 6.00 and 8.00 p.m. On clear hot days discharge extremes can vary by a factor of two. Maximum discharges measured by D. Smith during the summers 1970, 1971 were 5,400 cfs. In terms of discharge contribution the upper North Saskatchewan River contributes only 40% of the water volume to the Alexandra-North Saskatchewan system; but accounts for an estimated 95% of the bedload contribution (D. Smith, 1973a).

2. Morphology and Sediment

The Alexandra-North Saskatchewan River system valley is characterized by alternate reaches of braided gravel flats and anastomosing predominantly meandering channel complexes. Braided patterns occur in coarse-grained unstable shallow complexes. Anastomosing predominantly meandering patterns occur in areas which are stabilized by vegetation and have extensive floodplain deposition on mid-channel islands. The anastomosing pattern occurs where there is a backwater effect developed in the system. For example, at the confluence between the Alexandra and North Saskatchewan Rivers (Figure 9) the upper North Saskatchewan dumps a huge fan-shaped mass of outwash gravel. This gravel mass constricts the main channel of the Alexandra River to the

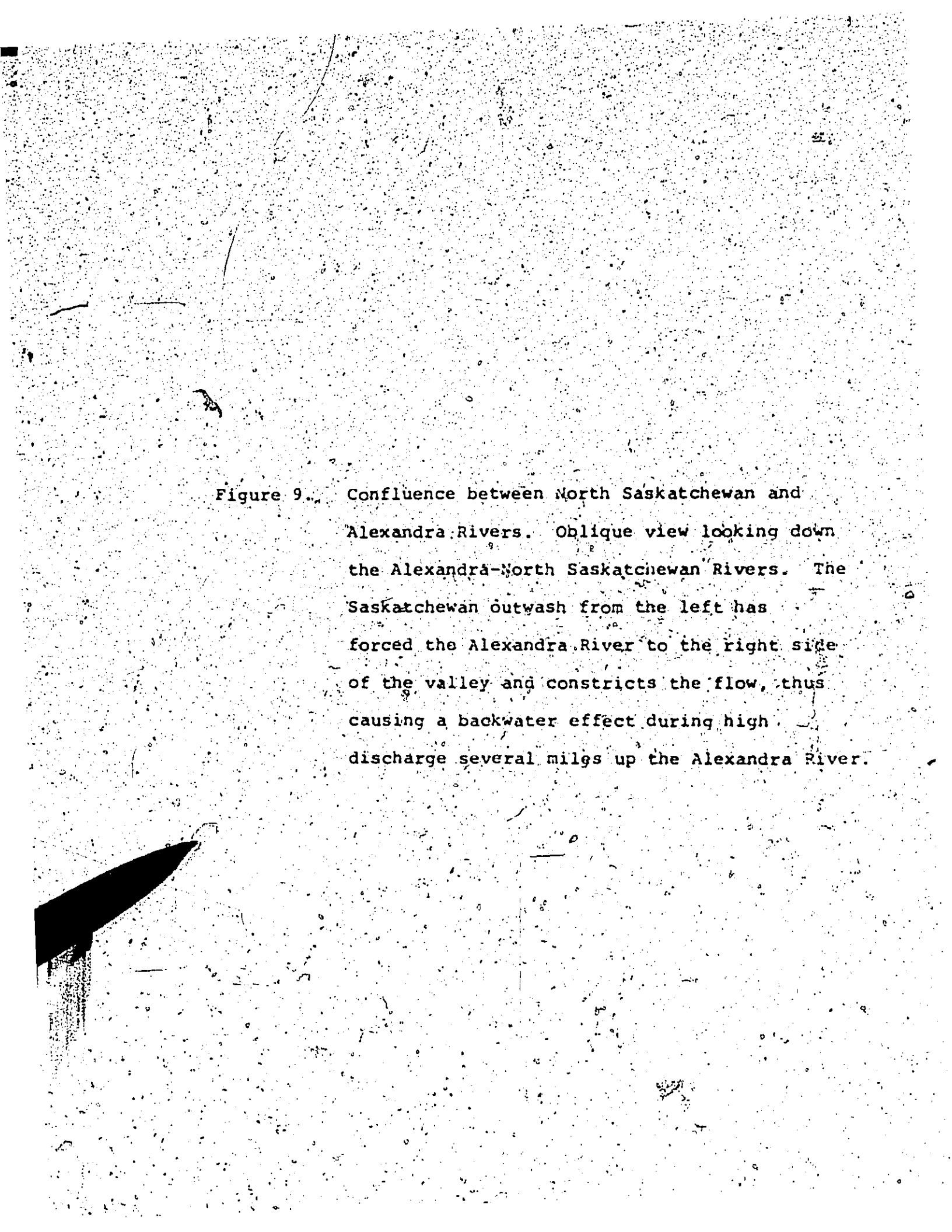

Figure 9. Confluence between North Saskatchewan and Alexandra Rivers. Oblique view looking down the Alexandra-North Saskatchewan Rivers. The Saskatchewan outwash from the left has forced the Alexandra River to the right side of the valley and constricts the flow, thus causing a backwater effect during high discharge several miles up the Alexandra River.

right side of the valley, causing a backwater effect up the Alexandra during high discharge periods, resulting in an anastomosing somewhat meandering channel pattern for several miles up the Alexandra River. Floodplain silts and vegetated islands predominate in backwater reaches. In D. Smith's 10 mile study reach of the Alexandra-North Saskatchewan river system, there are three such backwater reaches of floodplain alluvium which are separated by two fan-shaped outwash gravel flats.

Average rates of aggradation of the outwash flats were estimated by D. Smith (1973a) from C^{14} dating of organic material, from tree-ring dating of buried living trees and the presence of a volcanic ash layer within the outwash deposits. Computed aggradation rates varied from 1 ft in 98 yrs to 1 ft in 480 yrs over the past 2,450 year time period. During this period the thickness of valley fill that was deposited ranged from 4 to 25.5 ft.

Extensive exposed gravel flats occur in the upper North Saskatchewan, approximately 5 miles upstream from the confluence with the Alexandra River. The upper 4 feet of bed sediments in this outwash flat are thought to be temporary bar-and-channel deposits, which are reworked during successive high spring and summer discharge periods (D. Smith, 1973a). These exposed flats afforded the opportunity to study the preservability of stratification and sedimentary features

associated with modern outwash gravels. In this upper braided reach, where stratification studies were conducted, the mean channel slope is 0.0065 and median grain size of bed sediments is -4.7ϕ (D. Smith, 1973a).

CHAPTER 3

BAR MORPHOLOGIES AND BRAIDING PATTERNS: KICKING HORSE RIVER

INTRODUCTION

Most of the bed load gravel in the Kicking Horse River is transported in a modified type of pool-and-riffle sequence (Figure 10), which is termed a "pool-and-bar" sequence (D. Smith, 1973b). Sediment is transported through the pool, up onto the topographically higher bars of the riffle sequence. Depending upon flow conditions sediment is either deposited on the bar surface, deposited on the foreset margin, or transported out of the system to the next pool-and-bar sequence.

Pools are characterized by convergent flow, which is funnelled down the pool by pre-existing active bars and exposed bar-channel remnants. Pools commonly occur at the intersection of two or more flows of equal or unequal strength (Figures 10,11). It must be emphasized that these pool-and-bar sequences differ dramatically from those observed in meandering systems (Keller, 1970, 1971; Keller and Melhorn, 1973). In braided outwash areas, pools are sites of

Figure 10. Idealized sketch of pool-and-bar sequence (modified after D. Smith, 1973b)

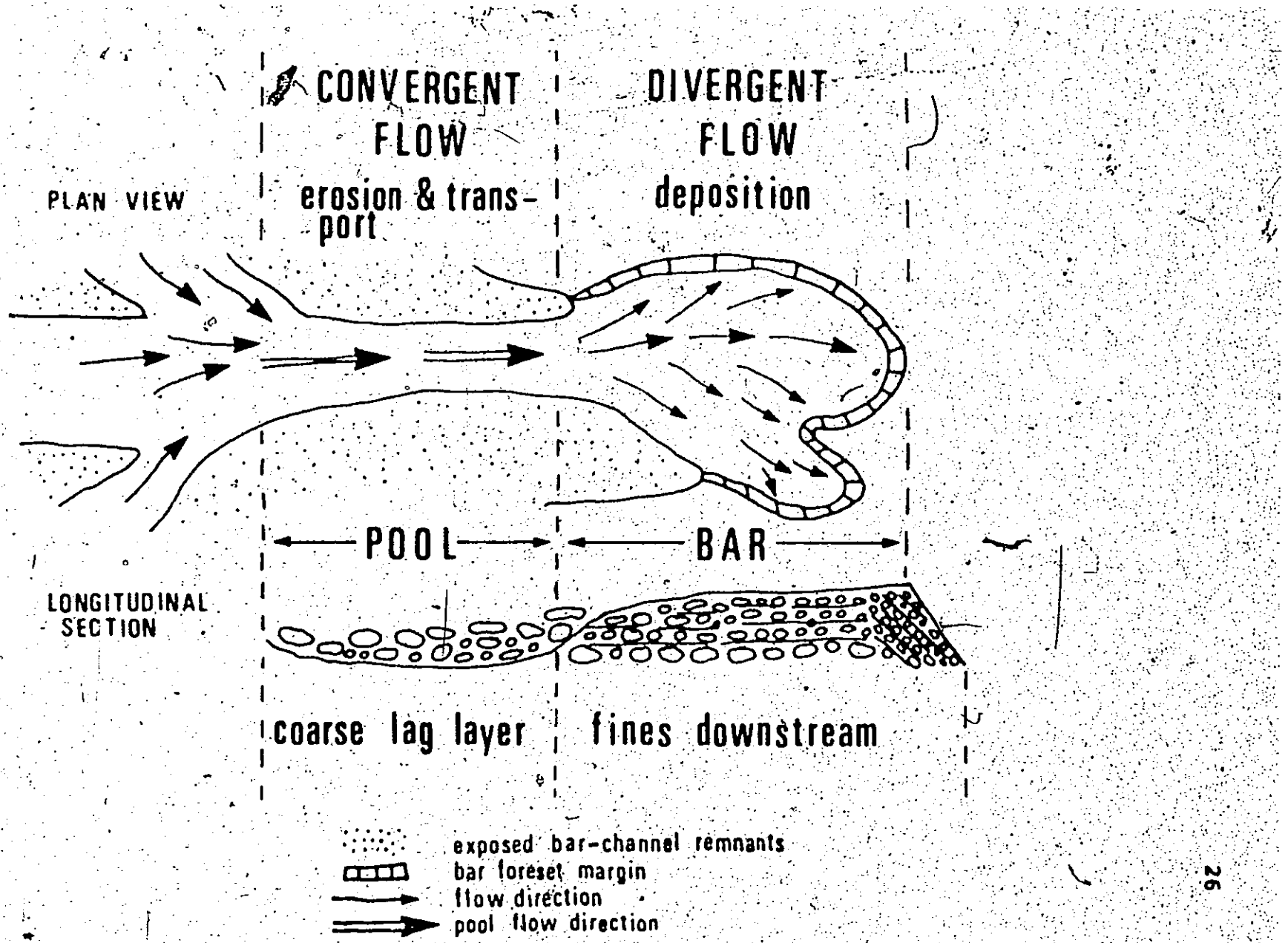
CONVERGENT FLOW
erosion & trans-port
DIVERGENT FLOW
deposition
PLAN VIEW
POOL
BAR
LONGITUDINAL SECTION
coarse lag layer
fines downstream
exposed bar-channel remnants
bar foreset margin
flow direction
pool flow direction

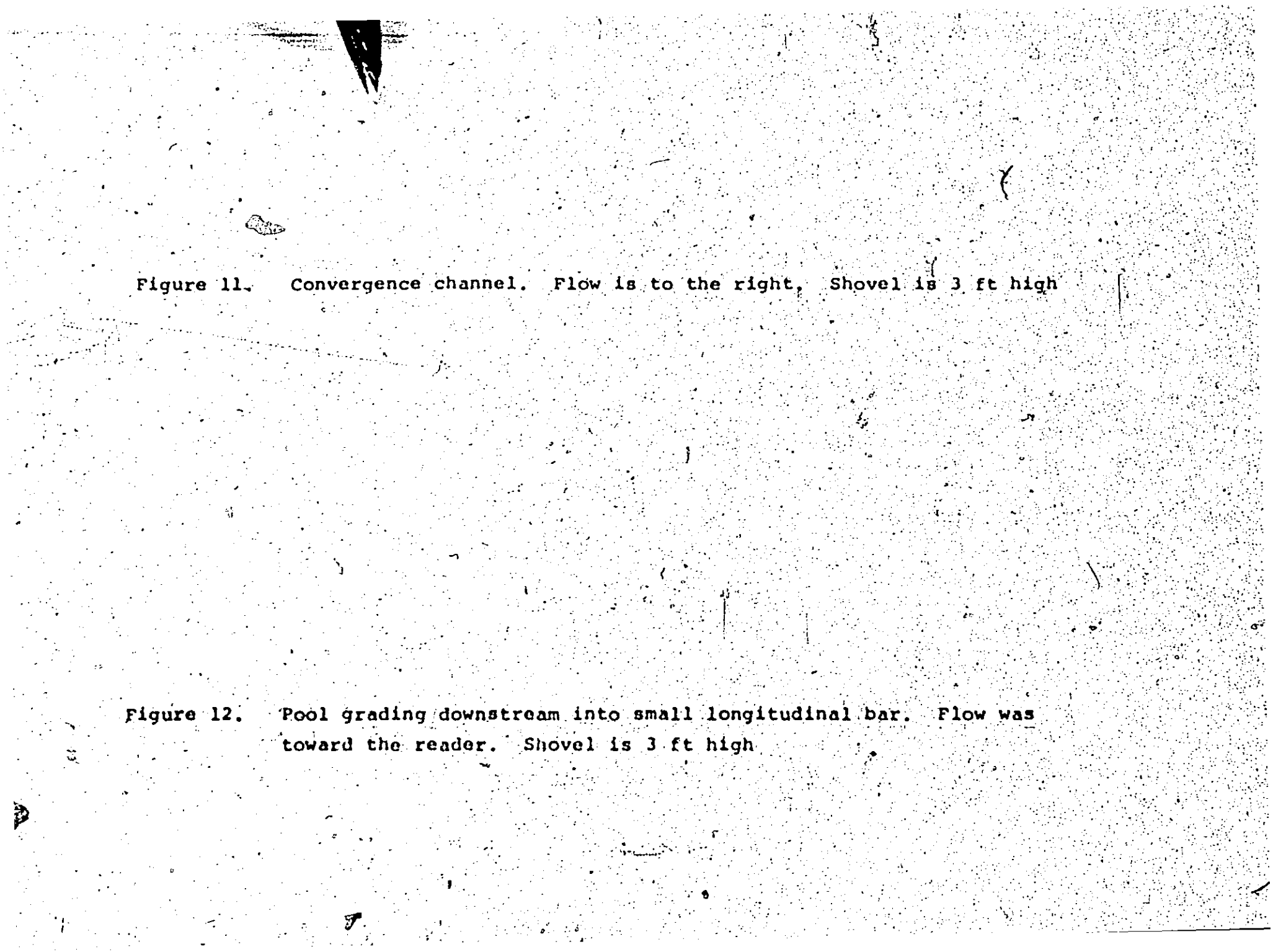

Figure 11. Convergence channel. Flow is to the right. Shovel is 3 ft high

Figure 12. Pool grading downstream into small longitudinal bar. Flow was toward the reader. Shovel is 3 ft high

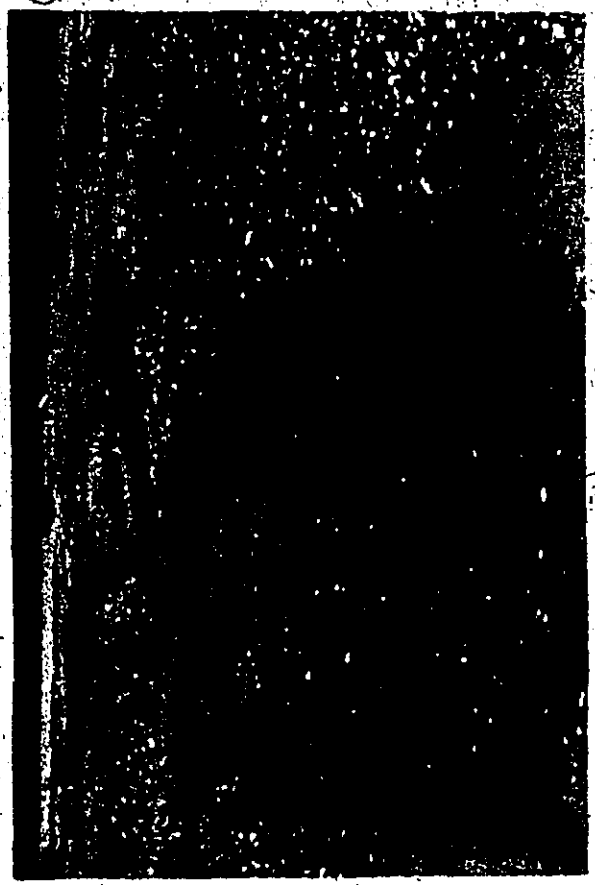

erosion and gravel transport during maximum discharges when channel-bar complexes are active. Water surface slopes in the convergent channels are quite high (S = 3-4°); depths average from 3-4 ft, with a maximum depth of at least 5 ft; widths are quite variable, ranging from 5-30 ft. Most pools are less than 20 ft wide. Due to the funnelling of large quantities of water through a constricted channel, bed velocities are quite high (average bottom velocity = 2.5-3.0 ft/sec). Sediment that remains in a pool following a high discharge period would be a lag deposit too coarse to be moved by the flow in the pool (Figure 10).

Upon downstream channel widening, flow becomes unconfined and diverges. Sediment is then deposited in the form of gravel bars (Figures 10,12). Bars assume a variety of shapes depending upon local flow conditions, proximity to banks, steadiness of flow, duration of flow, curvature and depth of the channel and bank stability.

There is much dispute in the literature about the term "bar". Many workers refer to "braid bars" as those gravel accumulations which divide the channel to cause a braided pattern (Allen, 1970; Blatt et al., 1972; Rust, 1972; Boothroyd, 1972). However, such braid bars may have very complex depositional and erosional histories, as demonstrated by N. Smith (1972, 1974).

The majority of the mid-channel bars are remnants

of bar-channel complexes which at most display faint traces of former bar-and-channel morphologies. Attempts to classify these mid-channel erosional remnants as bars were abandoned due to the very complex morphologic history of these features. The author is following the classification scheme of N. Smith (1974) by using the term "unit bar". This term refers to those bars that have fairly simple morphological developments, where observed bar forms are mainly depositional features with only slight erosional modification.

Using this definition of a braid bar, there are four major types of unit bars in the Kicking Horse River (in order of relative abundance): diagonal, transverse, point and longitudinal unit bars (Figure 13).

Diagonal Unit Bars occur as left (Figure 14A) or right (Figure 14B) diagonal bars (looking downstream flow is deflected to the left or right across the bar surface) (Church, 1972). Main flow directions are oblique to bar long axes and foreset margins commonly migrate at 90° to the main flow direction. Diagonal bars are the most common bar form in the Kicking Horse River. Initiation of bar growth occurs where secondary currents are deflected asymetrically from the main flow. Bars commonly occur in the lee of pre-existing active bars, or downstream from the junction of two channels of unequal strength.

Figure 13. Types of bar morphologies observed in outwash gravel during high discharges, Kicking Horse River.

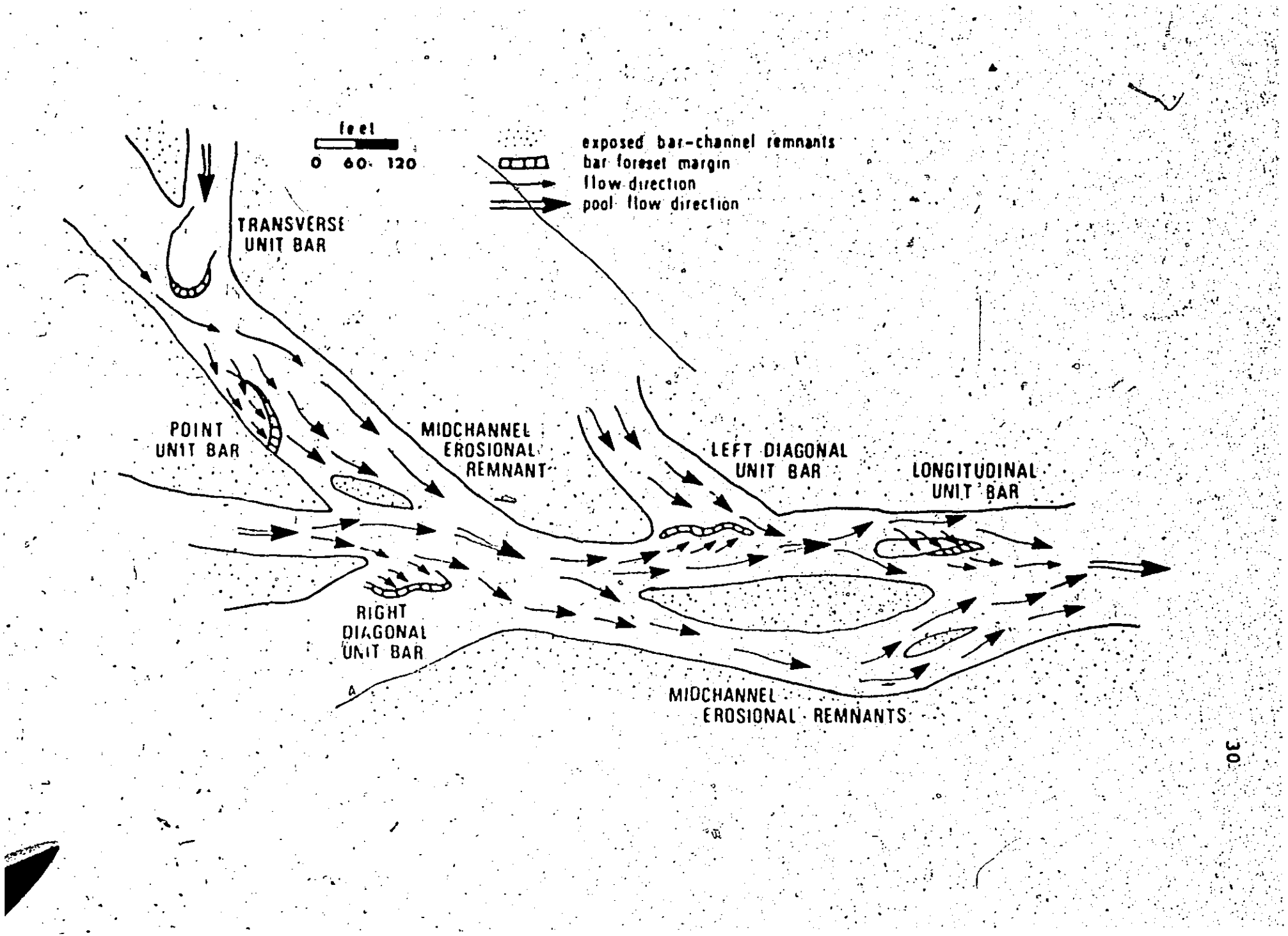
feet
0 60 120
exposed bar-channel remnants
bar foreset margin
flow direction
pool flow direction
TRANSVERSE UNIT BAR
POINT UNIT BAR
MIDCHANNEL EROSIONAL REMNANT
LEFT DIAGONAL UNIT BAR
LONGITUDINAL UNIT BAR
RIGHT DIAGONAL UNIT BAR
MIDCHANNEL EROSIONAL REMNANTS

Figure 14A. Left diagonal bar. Flow is toward the reader and to the right. Stake for scale is 4 ft high.

Figure 14B. Right diagonal bar. Flow is toward the reader and to the left. Stake in the foreground is 3 ft high.

Figure 14C. Transverse bar lobes. Flow is toward the reader. Camper in the background and to the left gives an indication of the scale.


A

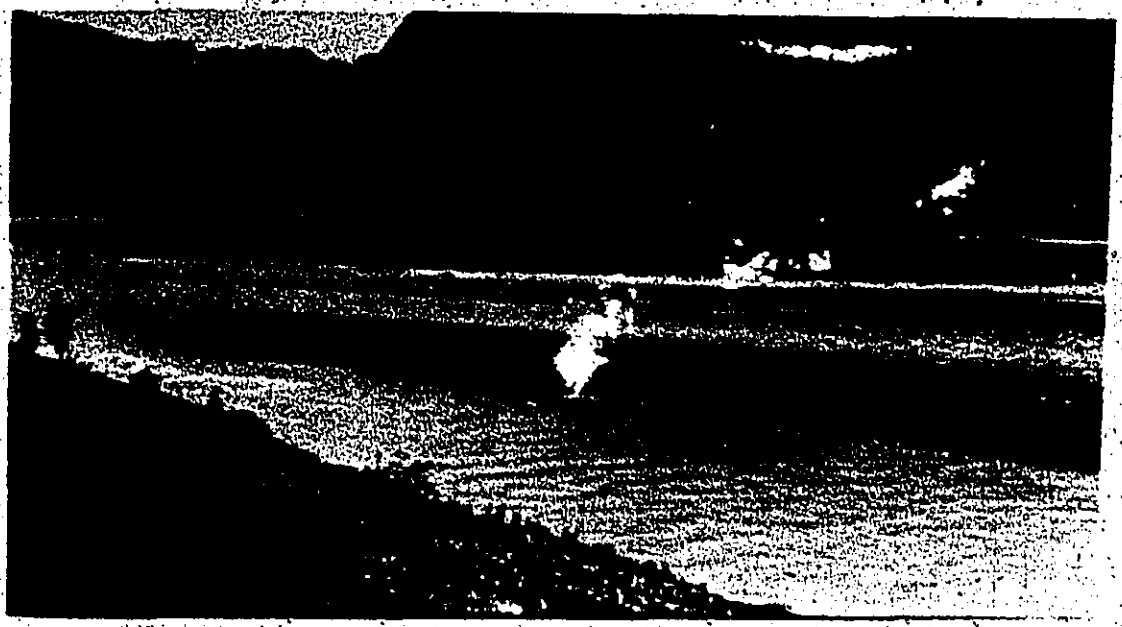
B

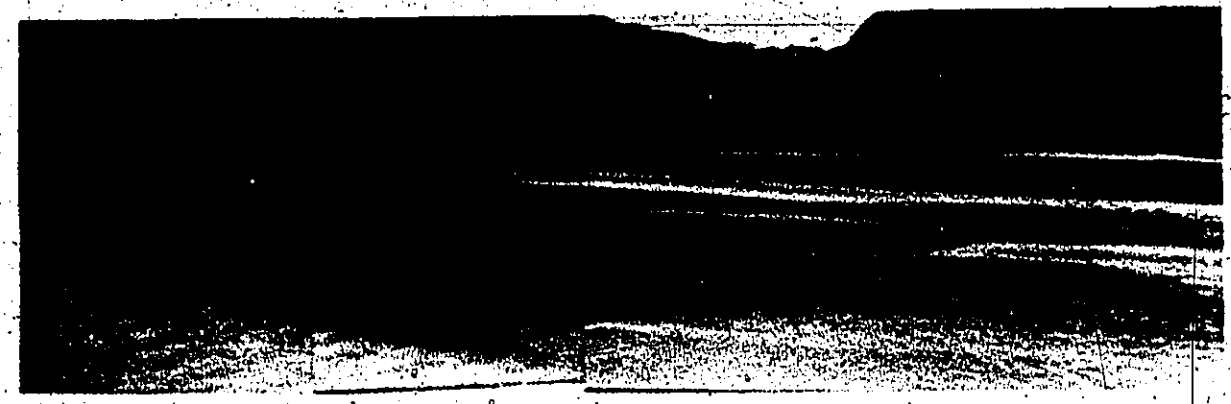
C

Transverse Unit Bars commonly have lobate margins with high angle foresets (N. Smith, 1971) (Figure 14C). Bar long axes are parallel to main flow directions. Transverse bars initiate in expanding flow conditions, in areas where depths increase rapidly, or at the junction of two channels of unequal strength. These bars are identical to the sandy transverse bars described in the braided Platte River system (N. Smith, 1971). Coarse-grained gravel bar lobes have also been described from the North Saskatchewan River (D. Smith, 1972).

Point Unit Bars form in gently convex channels. Bar long axes are parallel to main flow directions. Point bars dip gently toward the outer bank and commonly develop foreset or riffle margins. These bars are analogous to those found in meandering river systems.

Longitudinal Unit Bars form in areas where gravel accumulations are initiated as mid-channel ridges (N. Smith, 1970) (Figure 12). Bars are convex in cross-section and streamlined cigar-shaped in plan view. Bar long axes are parallel to main flow directions. Bars can develop foreset or riffle margins. Longitudinal bar accumulations commonly serve as locus points for riffle or diagonal bar initiation.

Preliminary observations by the author suggested that regional slope and average bed load grain size may strongly influence bar shape. One of the major goals of this project was to study bar-and-channel development as a function of slope and bed load grain size.

PROCEDURE

Successive plane table maps during several discharge cycles were surveyed in 500 ft long reaches of the river. Three sections of the outwash plain of the Upper Kicking Horse River were selected for study: upstream, midstream and downstream sections (Figure 6,15). The original study plan was to correlate bar-channel pattern changes with local discharges, velocity fluctuations and flow distribution patterns in regions of differing regional slope and bed load grain size. However, there were many insurmountable difficulties in using this approach.

Flow conditions fluctuated so rapidly that measured flow data did not correlate with pre-mapped bar-channel patterns. Flows in upstream sections were confined mainly to a single channel. During maximum discharges when bars were mobile, the channel was impassable. Only initial and final bar-channel patterns were mapped in the upstream section,

Figure 15. Map showing study sections, Kicking Horse River

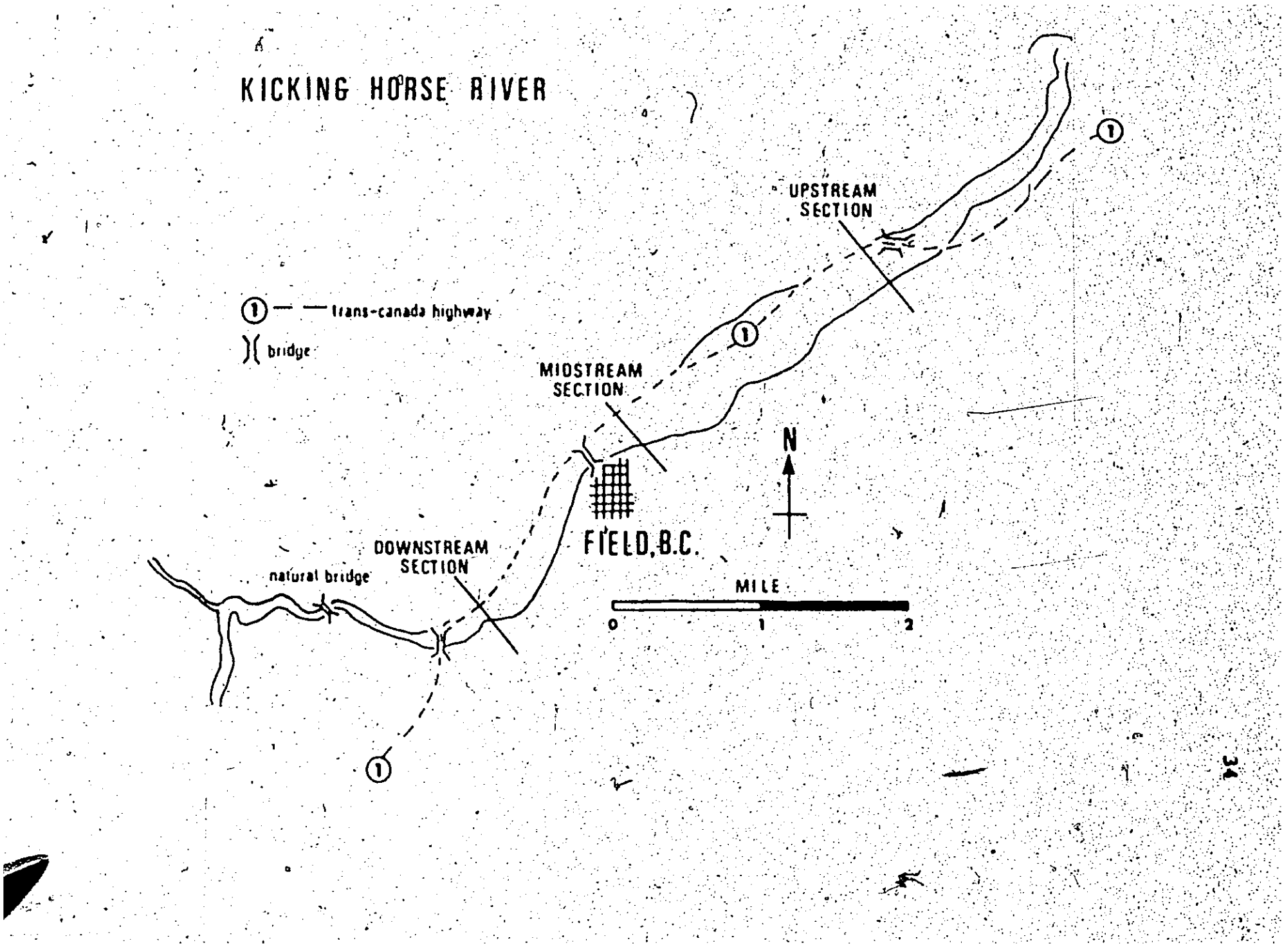
KICKING HORSE RIVER
1 — — trans-canada highway
bridge
UPSTREAM SECTION
MIDSTREAM SECTION
DOWNSTREAM SECTION
natural bridge
FIELD, B.C.
N
MILE
0
1
2

making it difficult to correlate changes with one another.

Midstream and downstream sections have similar braiding patterns. For this reason, survey maps of 500 ft reaches were only made in the more accessible midstream section. In the downstream section individual bar deyelopment and decay were monitored during successive discharge cycles.

DESCRIPTION OF STUDY AREAS

In high-gradient (S = 0.0054) (Figure 7) coarse-grained (Mz = -5.6ø) (Figure 8) upstream sections the flow is confined mainly to a single channel (Figure 16). Channels are deep erosional features with a fairly straight to somewhat meandering form. Bed load is transported predominantly as diffuse gravel sheets, which are commonly one or two pebbles thick and have ill-defined margins. Diagonal bars occur rarely in protected lees of pre-existing bars or bar-channel remnants (Figure 16). Sediment was in transport only during short periods of maximum flow conditions, where discharges exceeded 2,000 cfs (Figure 4C).

By contrast, in the low-gradient (S = 0.0034) (Figure 6) fine-grained (Mz = -4.3ø) midstream and (Mz = -2.7ø) (Figure 8) downstream reaches, channels are

Figure 16. Idealized sketches of bar-channel complexes typical of upstream and downstream reaches, Kicking Horse River.

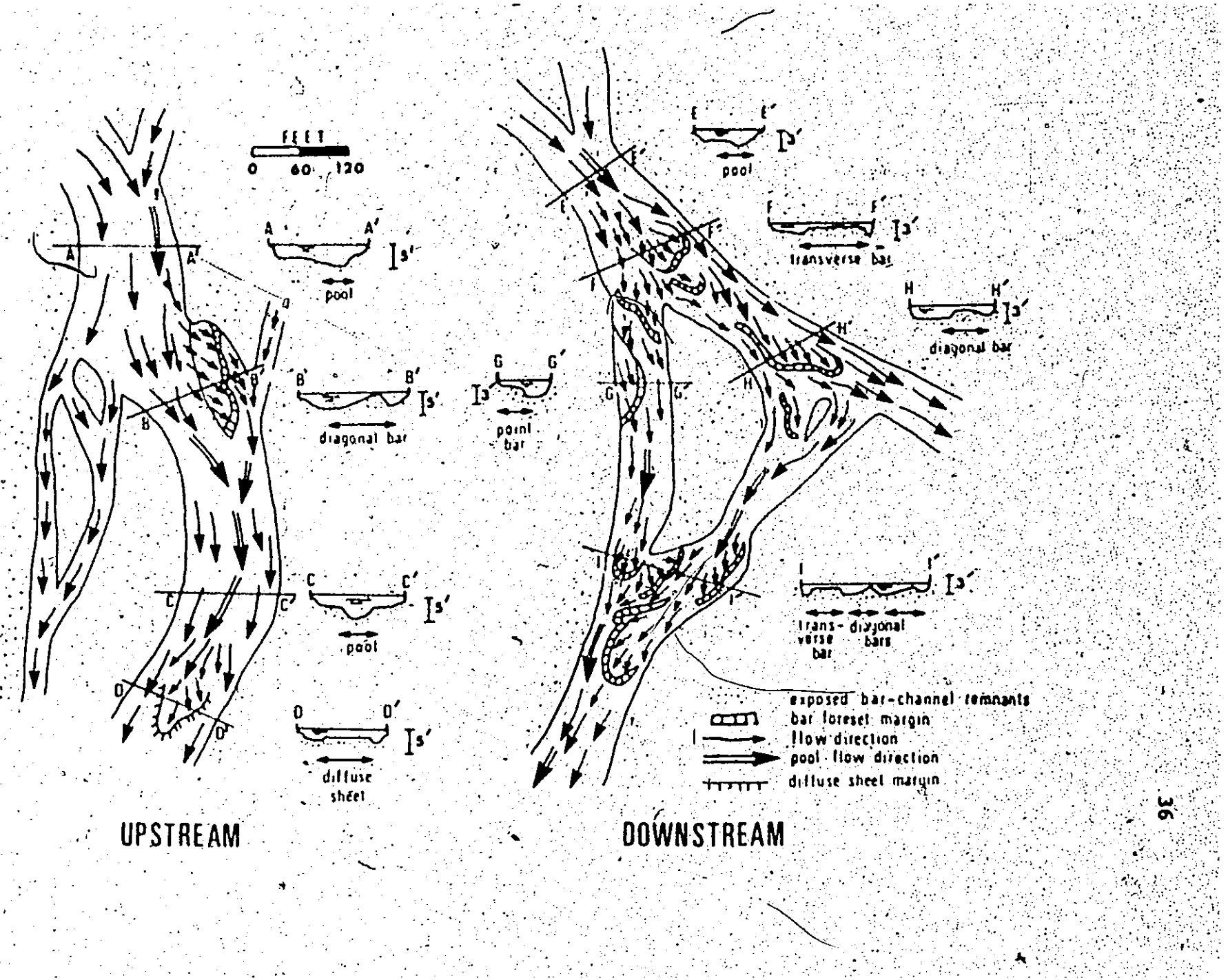
FEET
0 60 120
pool
diagonal bar
pool
diffuse sheet
UPSTREAM
pool
transverse bar
diagonal bar
point bar
trans- verse bar
diagonal bars
exposed bar-channel remnants
bar foreset margin
flow direction
pool flow direction
diffuse sheet margin
DOWNSTREAM

broader and shallower. Flow is not confined to a single main channel, but appears to be equally distributed among many channels, forming anastomosing braided complexes. Diagonal bars dominate in these reaches. Transverse bars are also common (Figure 16). Sediment was in transport during most of the field season, where lower fluid discharges were needed to transport the finer bed material in midstream (Q_{needed} = 1,200 cfs) and downstream (Q_{needed} = 1,000 cfs) sections (Figure 4C).

RESULTS

1. Upstream Section

The upstream section was mapped during rising stages of the Spring Melt discharge period (June 22) (Figure 17A). Pre-existing ridges in the channel modified flow patterns and initiated gravel accumulation and bar growth in the lee of these obstacles. As shown in Figure 17A a pre-existing gravel ridge in the main channel bifurcated the flow. Dominant flows were deflected to the west and east, leaving a low-velocity, low-discharge inactive area. Deposition of gravel occurred in this region as a diffuse gravel lobe (B_1), similar in shape to a transverse bar lobe, but lacking a well-defined margin. This gravel sheet was approximately

Figure 17. Plane table maps of upstream section, Spring Melt Period (June 22 - June 25, 1973)

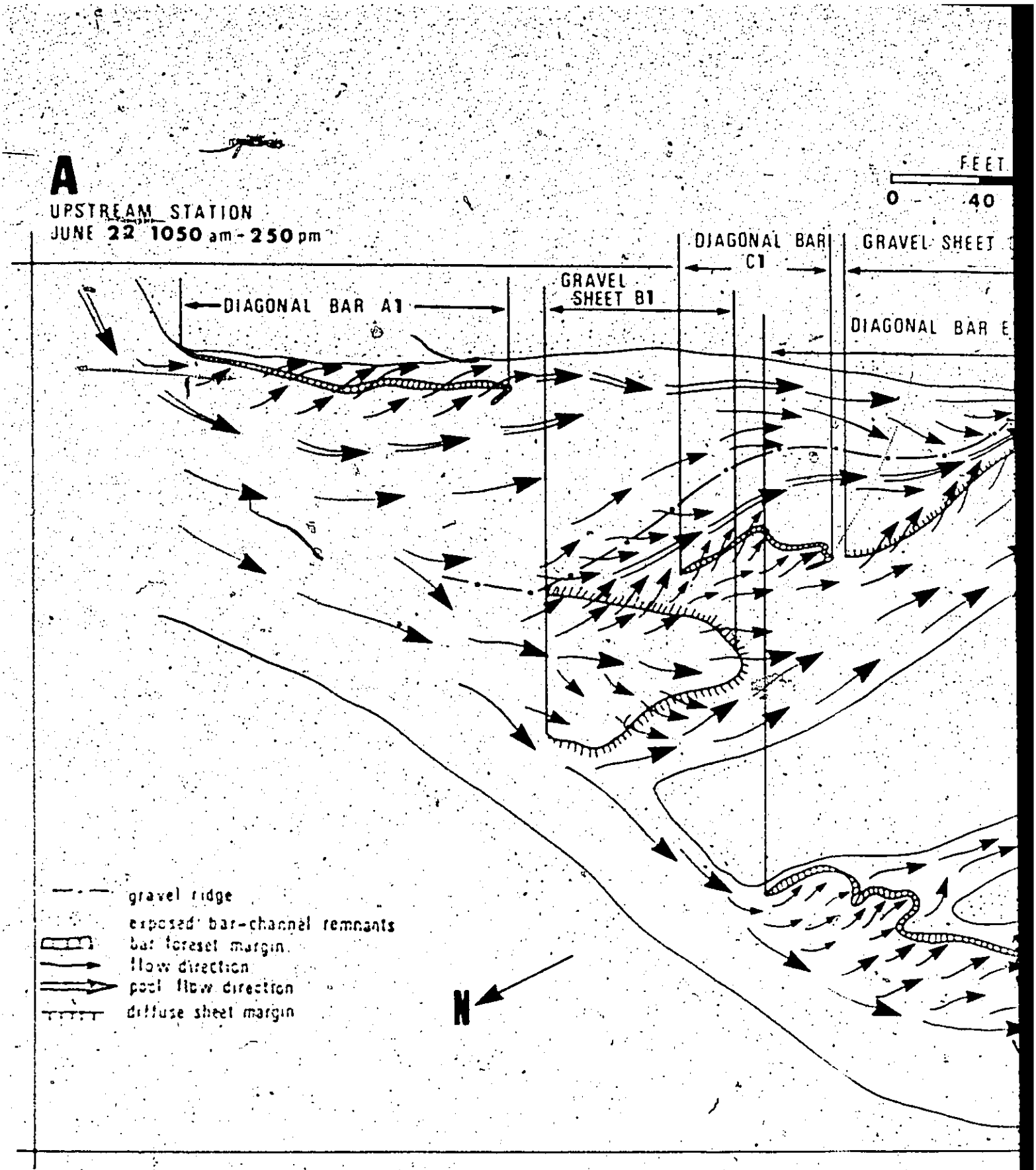
A
UPSTREAM STATION
JUNE 22 1050 am - 250 pm
FEET
0 - 40
DIAGONAL BAR A1
GRAVEL SHEET B1
DIAGONAL BAR C1
GRAVEL SHEET
DIAGONAL BAR E
gravel ridge
exposed bar-channel remnants
bar foreset margin
flow direction
pool flow direction
diffuse sheet margin
N

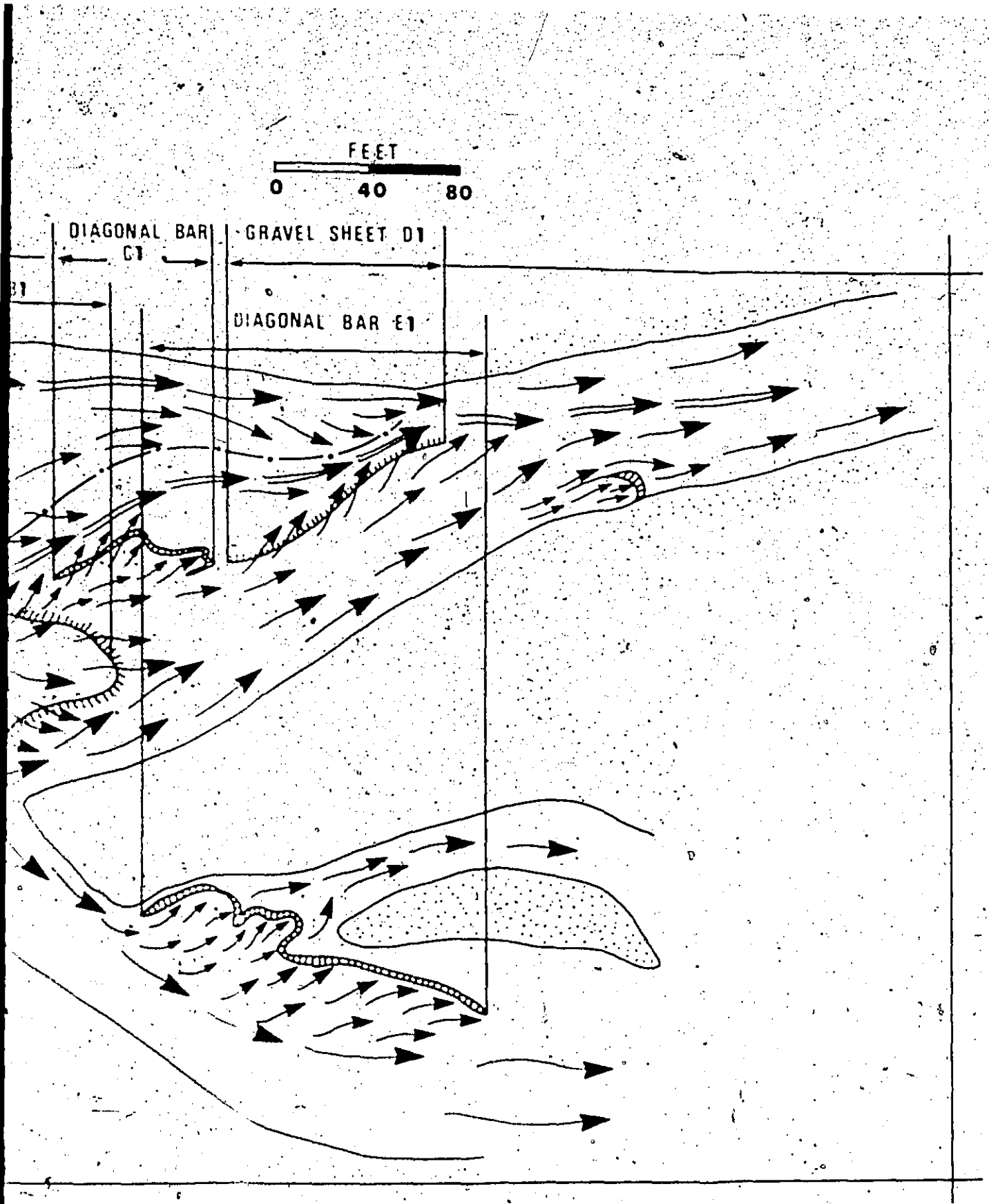
FEET
0
40
80
DIAGONAL BAR C1
GRAVEL SHEET D1
DIAGONAL BAR E1

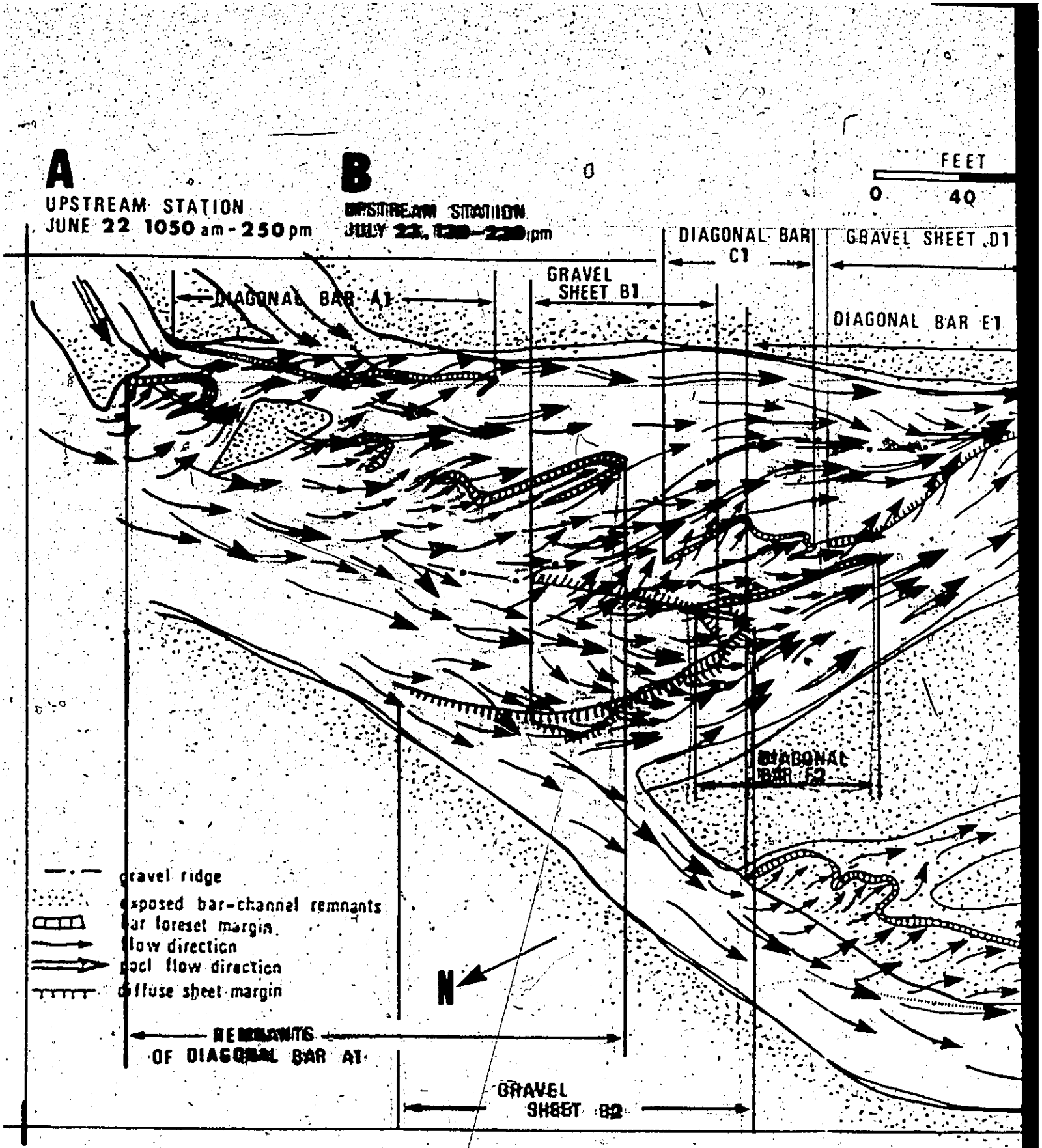
A
UPSTREAM STATION
JUNE 22 1050 am - 250 pm
B
UPSTREAM STATION
JULY 22, 130-230 pm
FEET
0 40
DIAGONAL BAR A1
GRAVEL SHEET B1
DIAGONAL BAR C1
GRAVEL SHEET D1
DIAGONAL BAR E1
DIAGONAL BAR F2
gravel ridge
exposed bar-channel remnants
bar foreset margin
flow direction
local flow direction
diffuse sheet margin
N
REMNANTS OF DIAGONAL BAR A1
GRAVEL SHEET B2

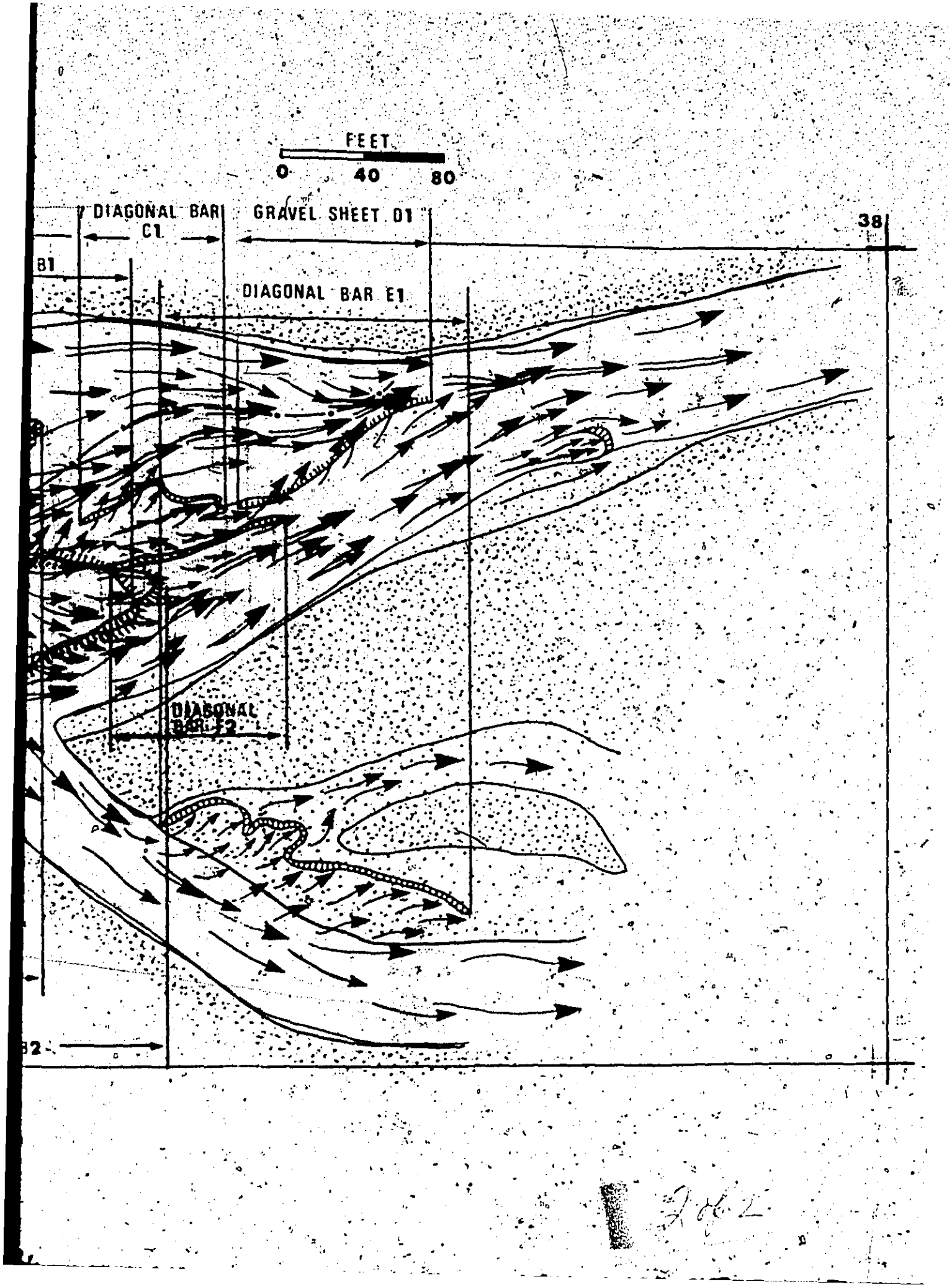
FEET
0
40
80
DIAGONAL BAR C1
GRAVEL SHEET D1
38
B1
DIAGONAL BAR E1
DIAGONAL BAR F2
B2

one or two pebbles high and grain sizes were slightly smaller than the adjacent channel areas. Formation of this diffuse gravel sheet then deflected flows toward the main bank. There were some back eddies and reflection of secondary flows into the lee of the sheet, resulting in the formation of a small diagonal bar (C_1). Flow between the pre-existing gravel ridge and the diffuse gravel sheet was convergent, forming a pool with very high velocities (greater than 4 ft/sec) and high water surface slope (S = 5°). This convergence channel was floored with a cobble-size lag layer. This channel joined the main flow downstream from the gravel ridge, forming a much deeper and swifter pool, which persisted downstream approximately 75 ft. Two small diagonal bars formed in protective lees of exposed bar remnants, where secondary currents were deflected from the main flow (A_1, E_1). The only mappable diffuse sheet was bar B_2. However, large volumes of cobbles and large pebbles were in active transport as bed load in the main channel. Due to the large depths and high suspended sediment concentration of the water, it was impossible to discern the position of these sheets.

During increased flows, the gravel sheet B_1 and the small diagonal bar C_1 were eroded away. The diagonal bar A_1 extended downstream and began to influence the main channel flow directions during falling stage. Main flows were

diverted to the east. The pre-existing gravel ridge again deflected flows, resulting in a low-velocity sheet-wash divergent flow pattern in the lee of the ridge. Large to medium pebbles were deposited in this area as a diffuse gravel sheet (B_2), which in turn diverted flows and created a protective lee, where a right diagonal bar formed (F_2). The left diagonal bar (A_1) became dissected during decreasing flows (Figure 17B, Bar A_2). Bar remnants of this diagonal bar then diverted flows and became the nuclei for foreset development. After June 25 flows were not competent to transport the large bed load sediment of this upstream reach and bar remnants as seen in Figure 17B remained intact during the remainder of the field season.

2. Midstream Section

The midstream section was mapped during high diurnal summer glacial melt discharges between July 18 and July 24. In contrast to the upstream section where main flows were restricted to somewhat meandering channels, in the midstream section channels are highly anastomosing complexes (Figures 18A, 18B). During the highest summer discharge (July 21) flow was almost sheet-like.

Shallow reaches are characterized by diffuse gravel sheets and small transverse-diagonal unit bar complexes. Bar lobes overlap one another and during highest flows seem

Figure 18. Plane table maps of midstream section, Summer Diurnal Period (July 18 - July 24, 1973)

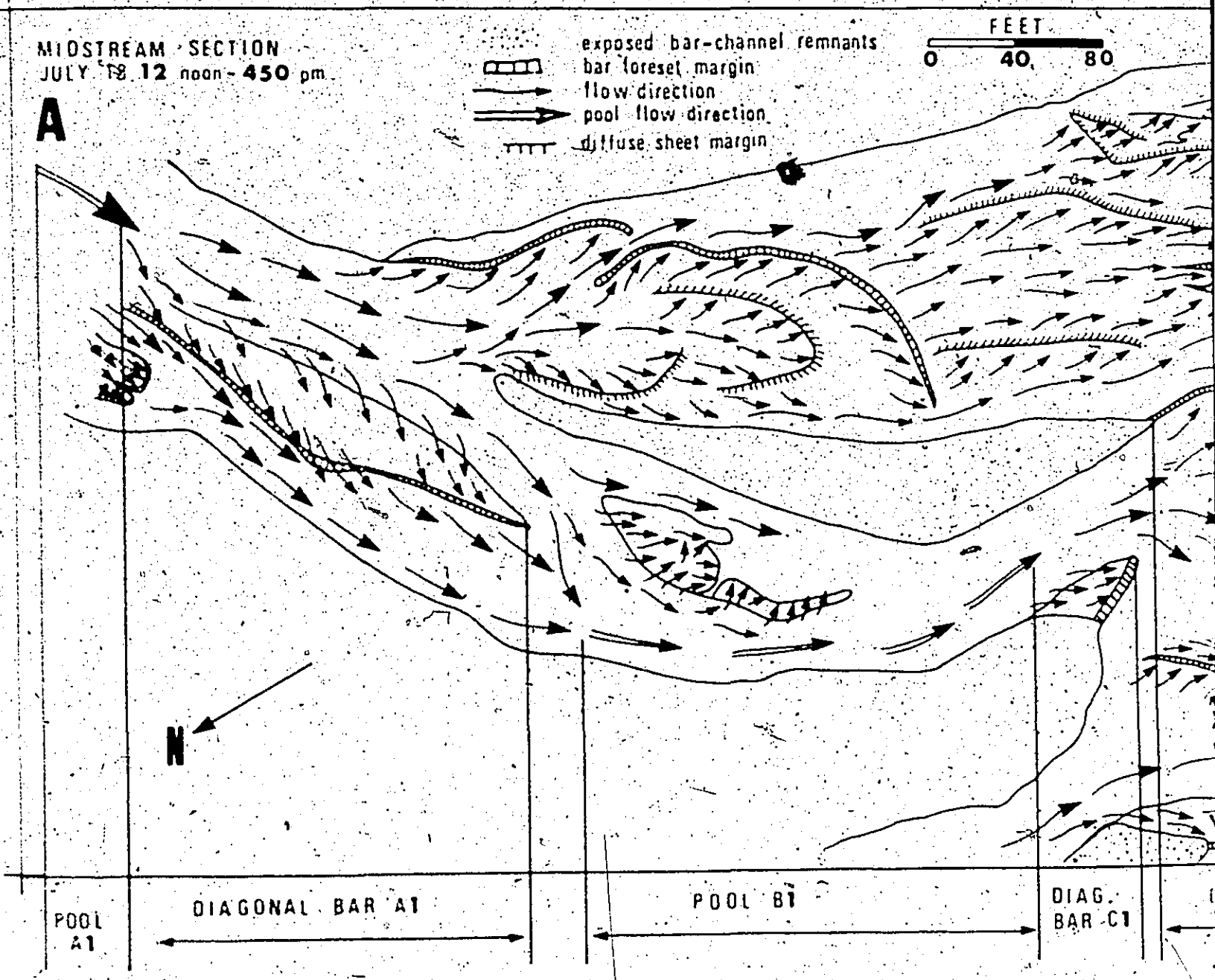
MIDSTREAM SECTION
JULY 18 12 noon - 450 pm
A
exposed bar-channel remnants
bar foreset margin
flow direction
pool flow direction
diffuse sheet margin
FEET
0 40 80
N
POOL A1
DIAGONAL BAR A1
POOL B1
DIAG. BAR C1

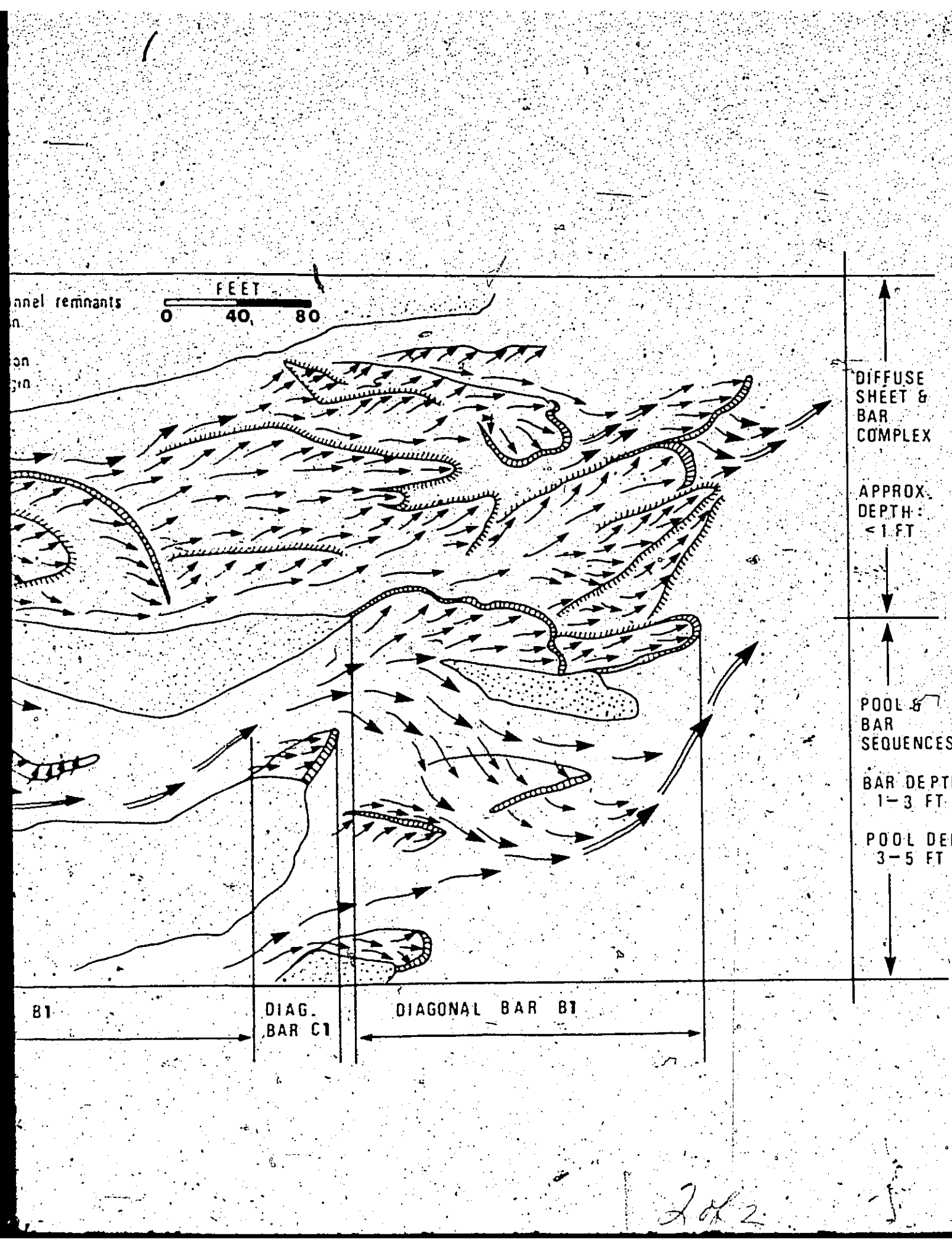
nnel remnants
n
on
in
FEET
0 40 80
DIFFUSE SHEET & BAR COMPLEX
APPROX. DEPTH: < 1 FT
POOL & BAR SEQUENCES
BAR DEPTHS: 1–3 FT
POOL DEPTHS: 3–5 FT
B1
DIAG. BAR C1
DIAGONAL BAR B1

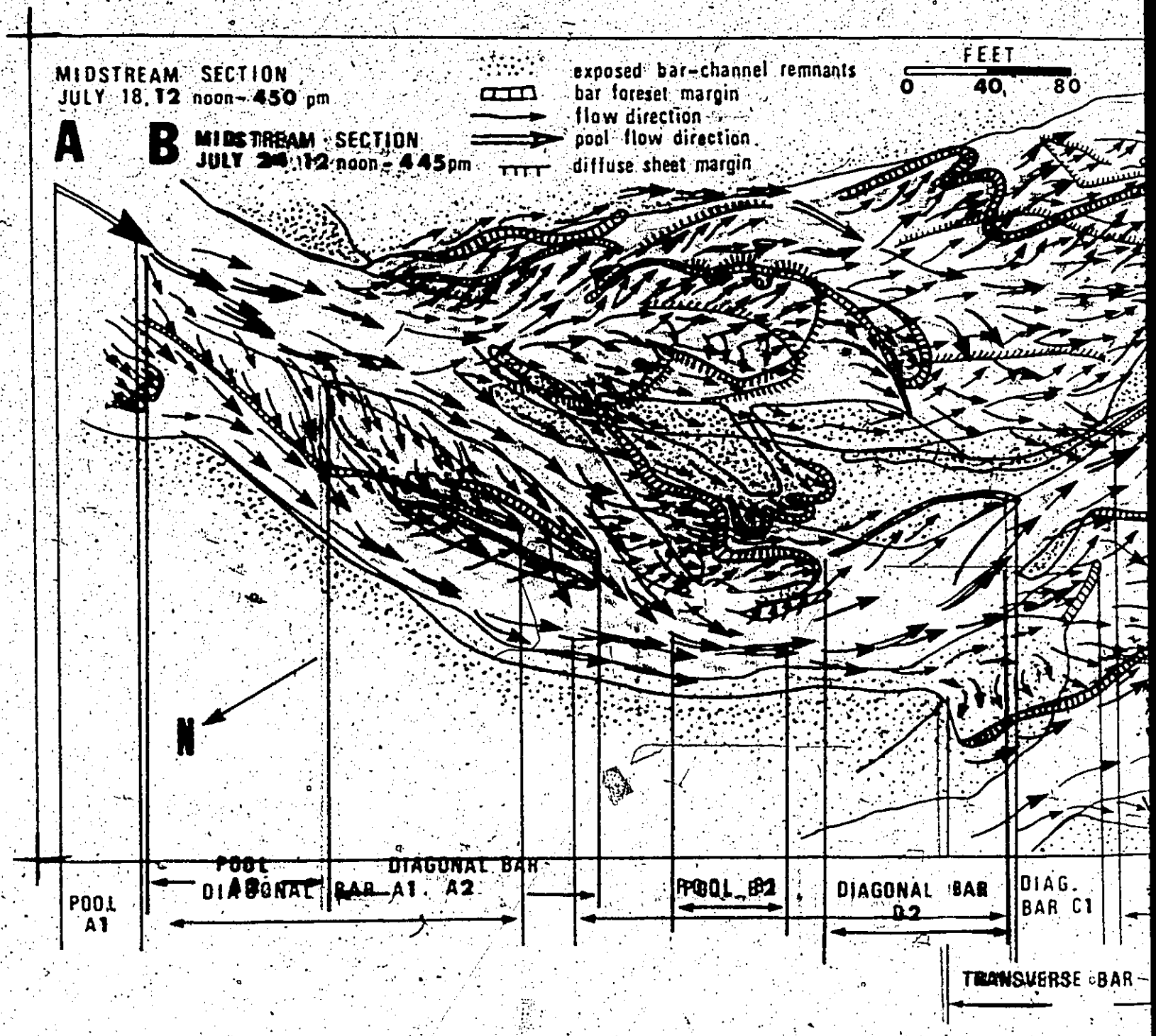
MIDSTREAM SECTION
JULY 18, 12 noon - 4.50 pm
A
B
MIDSTREAM SECTION
JULY 24, 12 noon - 4.45pm
exposed bar-channel remnants
bar foreset margin
flow direction
pool flow direction
diffuse sheet margin
FEET
0
40
80
N
POOL A1
DIAGONAL BAR A1, A2
POOL B2
DIAGONAL BAR B2
DIAG. BAR C1
TRANSVERSE BAR

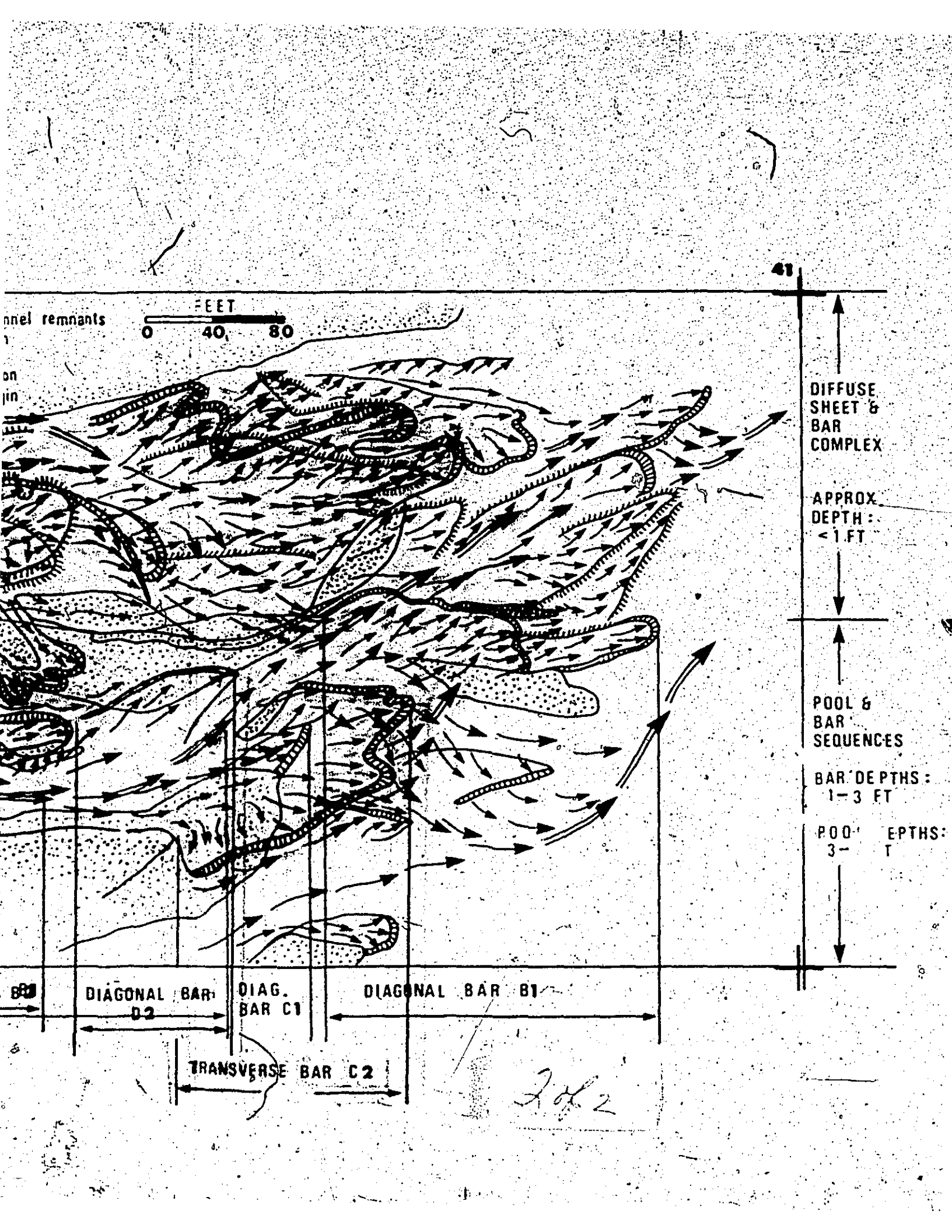
41
nnel remnants
FEET
0 40 80
DIFFUSE SHEET & BAR COMPLEX
APPROX. DEPTH: < 1 FT
POOL & BAR SEQUENCES
BAR DEPTHS: 1–3 FT
POOL DEPTHS: 3– FT
DIAGONAL BAR B2
DIAG. BAR C1
DIAGONAL BAR B1
TRANSVERSE BAR C2

to display a somewhat periodic spacing. Bars in the shallow complex have little or no foreset development. They are commonly 1-3 pebbles thick. Bars initiate as diffuse gravel sheets, and with an adequate basin depth into which they are migrating, they will develop a foreset margin.

Pool-and-bar sequences occur in the deeper channels. As in the upstream section diagonal bars form in areas where secondary currents are deflected from the flow (Figure 18A, Bar A_1). Small diagonal bars in the main channel form in the protective lee of pre-existing active bars (Figure 18B, Bar A_2). On July 21 the main flow in the deeper channel shifted to the south, thereby leaving a low velocity zone where flows became divergent. The transverse bar C_2 (Figure 18B) initiated as a diffuse gravel sheet, which then developed a well-defined foreset margin. With declining discharge, flows converged on the bar surface to a single channel which then gradually eroded the original bar surface. Diagonal Bar A_2 also became extremely dissected.

3. Downstream Section

Major flow was not concentrated in a single channel in the downstream section. Dominant flows may be carried down one channel during several discharge cycles, then flows would gradually shift directions and occupy a different channel. Shifts back and forth between adjacent channel

systems occurred three times during the field season (May 23 to September 5). Because of the unpredictability of the position of the flows capable of transporting gravel, the method of making successive maps of a given 500 ft study reach was abandoned. Rather, small bar-channel complexes were mapped during successive discharge cycles to see what factors promote or discourage bar development and growth.

As in the previous sections studied, bars initiate as diffuse gravel sheets during high flows in areas where flow competence is reduced. Transverse bars commonly form in regions where confined flows fan out into wider channels (Figure 19A). With further downstream and lateral growth, the bar develops a well-defined foreset margin (Figure 19B). During decreasing flow conditions (due to a shift in the direction of the main flow), flows entering the bar mouth became incapable of transporting gravel across the entire bar surface. An incipient convergent channel formed on the bar surface (Figure 19B). With further convergence of flow into this channel, the bar surface became highly dissected. The downstream lobe was eroded out and sediment was redeposited as a series of small gravel lobes (Figure 19C). Secondary flows continued to occupy the southeastern limb of the lobe and were competent to transport small pebbles. This limb then behaved as a left diagonal bar. Upon subsequent reoccupation of this channel by the main flow the bar remnants

Figure 19. Plane table maps of downstream section, Spring Melt Period (June 25 - June 29, 1973).

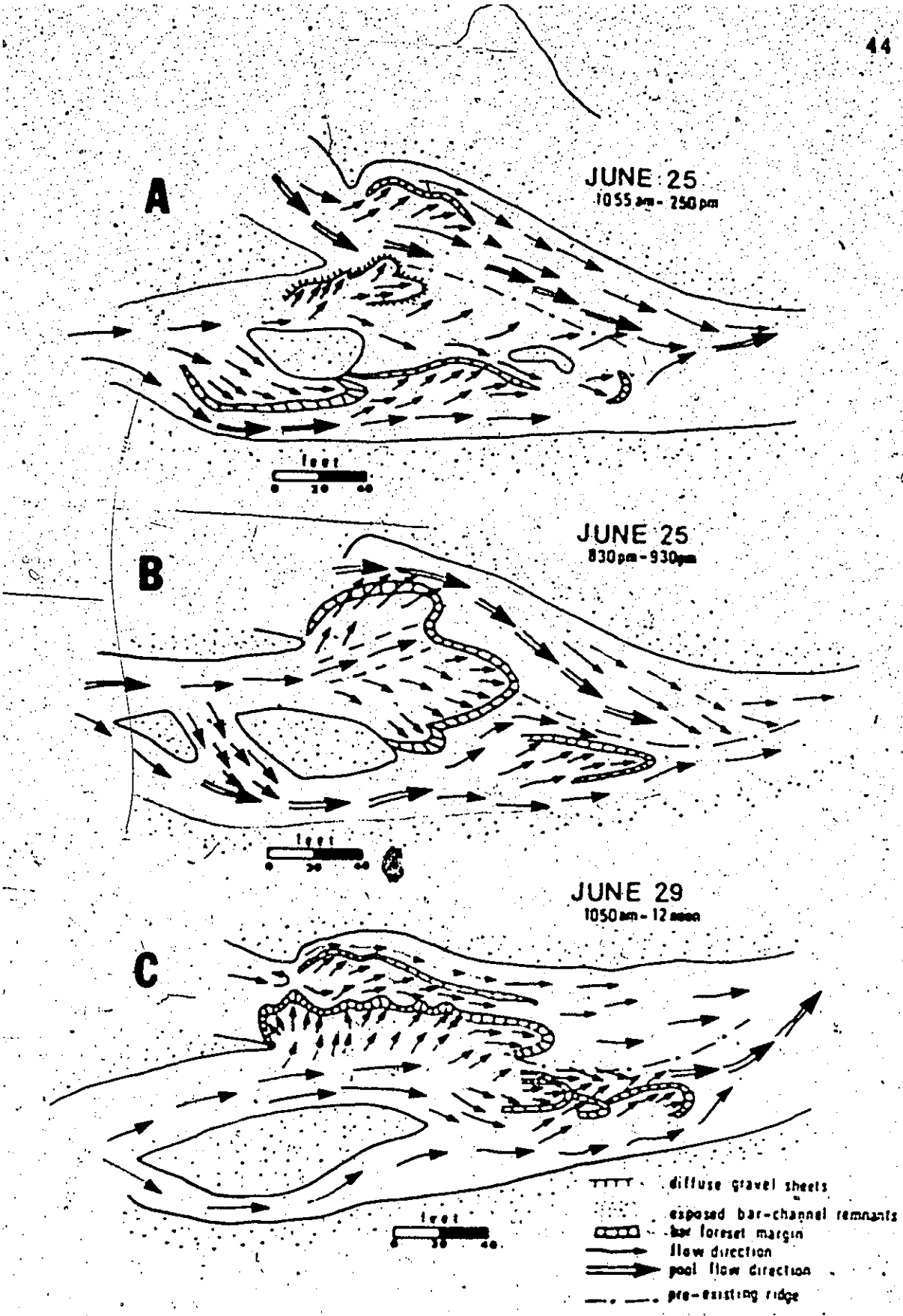
A
JUNE 25
1055 am - 250 pm
feet
B
JUNE 25
830 pm - 930 pm
feet
C
JUNE 29
1050 am - 12 noon
feet
diffuse gravel sheets
exposed bar-channel remnants
bar foreset margin
flow direction
pool flow direction
pre-existing ridge

were completely eroded away.

DISCUSSION:

Processes associated with bar development and destruction are illustrated schematically in Figure 20. Results from the present study suggest that bar development can be described as a three-stage process:

(1) Bars studied in all three reaches seem to initiate as diffuse gravel sheets in areas of flow divergence;

(2) Subsequent reworking of the diffuse sheet deposits and transport of finer debris results in incipient bar forms with barely discernable foreset margins;

(3) Coincident with continued lateral and downstream growth of the incipient bars, true bars evolve which display well-defined foreset or riffle margins.

The bar morphology that develops is a function of a complex interaction among many parameters (N. Smith, 1974), some of which include local flow competence, steadiness of the flow, duration of the flow, proximity to stable banks, channel curvature and depth, and the erodability of the bank material.

Maintenance of a bar form depends upon the fluid discharge entering the bar system and the bar area. Observations by the author show that with significant lateral growth,

Figure 20. Idealized sketch illustrating proposed model for bar development and growth. Key is the same as in Figure 19.

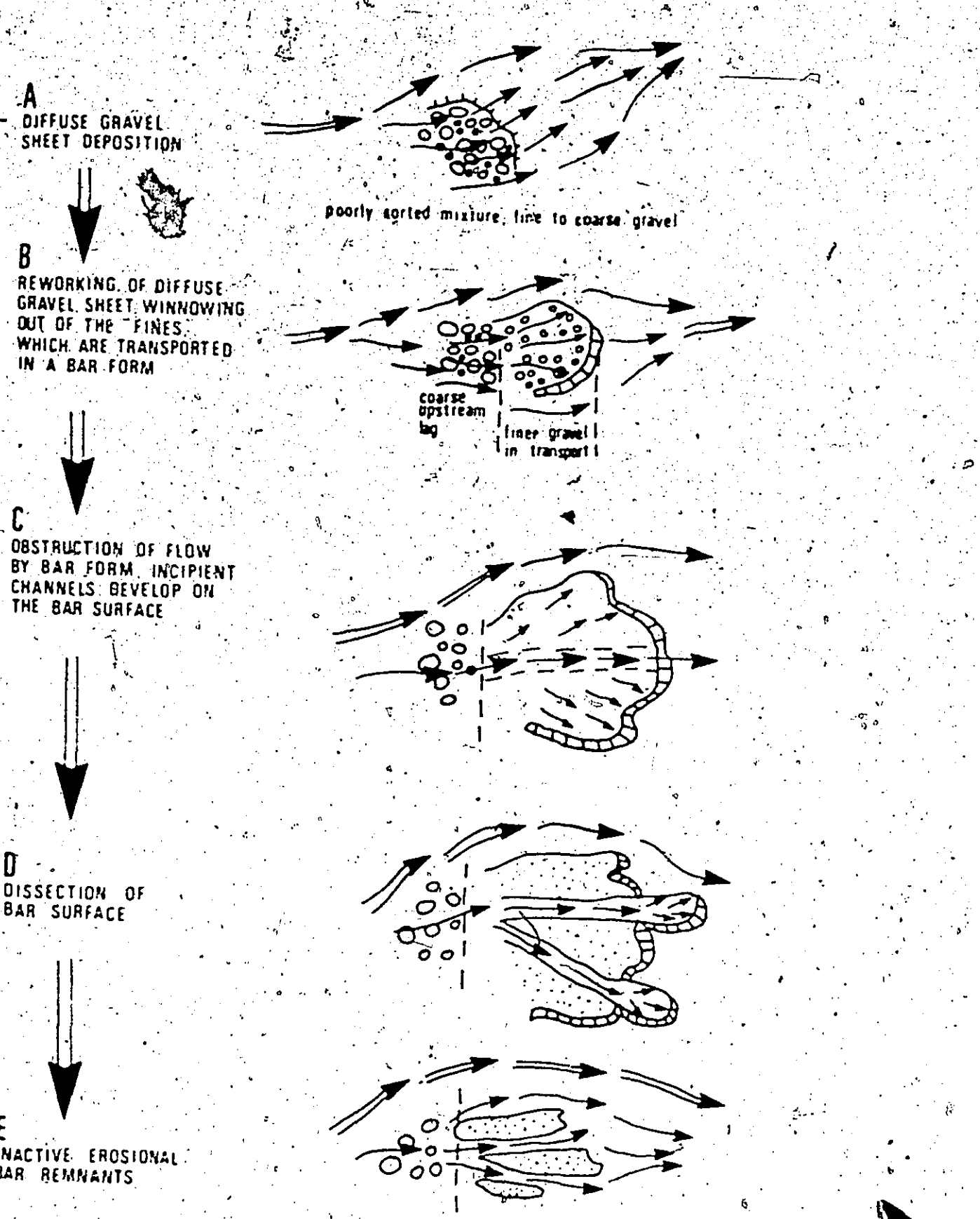
A
DIFFUSE GRAVEL SHEET DEPOSITION
poorly sorted mixture, fine to coarse gravel
B
REWORKING OF DIFFUSE GRAVEL SHEET WINNOWING OUT OF THE FINES WHICH ARE TRANSPORTED IN A BAR FORM
coarse upstream lag
finer gravel in transport
C
OBSTRUCTION OF FLOW BY BAR FORM. INCIPIENT CHANNELS DEVELOP ON THE BAR SURFACE
D
DISSECTION OF BAR SURFACE
E
INACTIVE EROSIONAL BAR REMNANTS

bars begin to obstruct the flow, resulting in a smaller cross-sectional flow area entering the bar system. Average velocities increase in these regions of concentrated flow. Bar size is limited as more sediment is transported in restricted flow regions. New channels are carved on the bar top as dissection of the original bar surface commences. Dissection of bar surfaces is quite rapid. Commonly material transported through the bar-top channels accumulates as small lobe extensions downstream from the original bar margin. Lateral migration of these bar-top channels results in almost total reworking of the original bar margin. Factors causing the decrease of discharge entering the bar system are:

(1) the shifting of main channel flows into adjacent channel systems;
(2) divergence of flows away from the bar by upstream flow obstructions;
(3) a general lowering of the total discharge of the river system during cooler weather conditions.

Results from this study indicate that systematic changes occur in bar morphologies from upstream to downstream reaches, where the dominant controls appear to be slope and grain size of the bed load. These data are summarized in Table 2. In steep coarse-grained upstream sections, diffuse gravel sheets with little or no margin development are the

Table 2. Hydrologic and channel characteristics of upstream, midstream and downstream reaches

Study Reach	Upstream	Midstream	Downstream
Slope	.0054	.0034	.0034
Mz	-5.6ø	-4.3ø	-2.7ø
Md	-6.0ø	-4.8ø	-3.7ø
Main channel system morphology	Single main channel somewhat meandering to braided form		Several main channels, down which main flows were alternately carried. Braided form
Secondary channel system morphology	Insignificant secondary channel flow	Significant secondary channel flow; braided form	
Channel cross-sectional morphology	Deep and Narrow	Shallow and Broad	
Minimum fluid discharge needed for significant bed load transport	2000cfs	1200cfs	1000cfs
Dominant active bar forms in main channel system	Diffuse gravel sheets; diagonal bars in protected areas	Diagonal bars are dominant Transverse bars are common	
Relative amount of bar-channel reworking during one field season	Very little		Extensive

predominant "bar" form. Diagonal bars occur occasionally in protective lee areas within the main channel. In low-slope, finer-grained midstream and downstream reaches pool-and-bar sequences occur in the main channel systems. The dominant bar form is the diagonal bar type. Transverse bars are also common. Channel geometry also changes from deep narrow somewhat meandering channel systems in upstream sections to shallower and broader braided channels in downstream reaches.

These differences in bar-and-channel morphologies in the river system can be explained as follows. In steep upstream coarse-grained reaches, gravel is in transport only during short periods of maximum flow conditions (Table 2). Fluid discharges needed for active bar-and-channel complexes in the reach were found to exceed 2,000 cfs. Since the bed load material is very coarse-grained, lower flows cannot remold the diffuse sheets into true bar forms. Coincidently, the lower discharge flows occupy the channel carved during high flow conditions. Hence, there is little lateral shifting of main flow transport between channel systems, resulting in a relatively stable main channel. Bars observed in the main channel are relict forms from the high flow conditions during the beginning of the summer discharge period, when contribution from snow melt areas was significant. The occasional diagonal bar forms are composed of finer sediment and occur in protective lee areas within the main

channel. Here sediment is temporarily deposited due to local flow incompetence; whereas in the open main channel areas the sediment would be transported further downstream.

In low slope finer-grained mid- and downstream reaches, lower fluid discharges are needed to transport the finer bed load material. Consequently, original diffuse gravel sheet deposits within the main channels have an opportunity of being reworked throughout most of the warm summer months, resulting in extensive true bar formation. There is significant lateral exchange of main flow transport between adjacent channel systems, yielding the complex braided channel pattern.

Similar transitions from ill-defined bars in proximal areas to true bars with well-defined margins in distal reaches have been observed by Boothroyd (1972) in the Scott glacier outwash fan, northeast Gulf of Alaska.

CHAPTER 4

BEDLOAD TRANSPORT ON GRAVEL BARS: KICKING HORSE RIVER

INTRODUCTION

There are many aspects of sediment transport on shallow braid bars that are not understood, including the following:

(1) Most of the bars in the shallow braided complex of the Kicking Horse River migrate rapidly during short periods of rising discharge cycles. This episodic nature of bar migration suggests that there may be threshold values of certain flow parameters that must be exceeded before there is appreciable bedload transport and bar migration. What flow parameters are most important for bar migration in shallow gravel streams?

(2) Results from the plane table mapping project of braided patterns (Chapter 3) strongly suggested that bars originate as diffuse poorly-sorted gravel sheets. Upon subsequent reworking, finer material was winnowed out and remolded as a true bar form. If this is the process

associated with bar initiation and growth, then a coarse upstream lag layer should develop which exceeds the local competence of the stream. Is this hypothesis upheld by flow and sediment distribution patterns over active bar surfaces?

(3) Bars which are aligned parallel to the current commonly display marked downstream-fining trends in bedload grain size (N. Smith, 1974). Does this fining trend reflect the proposed winnowing out process of the finer sediment from original diffuse gravel sheets?

One aspect of the problem associated with bar migration and sediment sorting mechanisms is the difficulty in identifying the flow conditions needed for incipient gravel motion in shallow streams with high bed roughness elements. Since the publication of Gilbert's (1914) paper "The Transportation of Debris by Running Water" considerable work has been conducted on the mechanics of bedload transport (Hjulstrom, 1935; Shields, 1936; Rubey, 1937; Einstein, 1950; Sundborg, 1956; Gessler, 1965; Guy et al., 1966; Williams, 1967; Harms, 1969). Most of these bedload studies have been concentrated on sand-size sediment transport, because it is very difficult to measure coarse bedload movement. Several workers have applied well-known transport formulae and established hydraulic relations to natural channels with

coarse bedload sediments (Fahnestock, 1963; Helley, 1969; Boothroyd, 1972). Other studies have been concerned with the application of these "established" relations to ancient coarse-grained deposits in order to infer former flow conditions (Birkeland, 1968; Baker, 1973; Eynon and Walker, 1974). Few studies, however, have actually tried to discern the main controls of sediment transport and flow conditions characteristic of gravel streams (Kellerhals, 1967; Helley, 1969; Hollingshead, 1971; Wilcock, 1971). Most of these studies have been conducted in water depths between 3 and 30 ft, and it may not be correct to apply the same hydraulic formula to the shallow (0.5-3.0 ft deep) gravelly channels of the Kicking Horse River system.

Obvious difficulties in applying hydraulic formulae to shallow systems arise from interactions between large roughness elements and the flow. For example, turbulent eddies shed from the large bed particles probably disrupt the entire flow and the assumption of a logarithmic velocity profile may no longer be valid, and frictional contribution from the bed irregularities may be very high. Also, interactions between particles in transport and bed roughness elements may have a significant effect on the initiation and maintenance of gravel movement.

Lack of confidence in applying existing sediment transport theory to coarse-grained shallow stream systems

also prompted an investigation of gravel transport on shallow braid bars. It is doubtful that studies of sediment and fluid dynamics will be able to predict accurately sediment motion of coarse sediments, but hopefully relatively crude sediment transport models can be used for interpretation of ancient and recent deposits. It was hoped that in situ measurements of flow parameters, bedload grain size and bar migration rates would allow some limited prediction of incipient motion of coarse particles.

PROCEDURE

The purpose of this investigation was to try to determine hydraulic conditions necessary for bar growth and development, to determine migration rates of bars during single discharge cycles and to examine the sorting of bedload material on bar surfaces. The observations were restricted to transverse bars monitored during rising daily discharge cycles. These bars were chosen for study because of their relative simple morphology and flow distribution patterns. The downstream study section was chosen, where most channels were accessible during maximum flows. Bars were studied during the Summer Diurnal Discharge Period, from August 2 to August 10, when daily diurnal discharge fluctuations varied

by a factor of 2 to 2.5.

The procedure consisted of surveying the bar margin during low flow periods. Two stations were established: one at the upstream contact with the convergence channel, and one at the downstream foreset margin (Figure 21A). During rising flows the following measurements were made at approximately 15 minute intervals at the bar stations: water surface elevations, velocity measurements (with a standard Gurley-Price current meter, 0.2 ft above the bar surface), water depth, dimensions of the ten largest pebbles on the bar surface and the downstream migration of the foreset margin. The ten largest pebbles were selected from hand-grab samples of sediment on the bar surface. Due to the high suspended sediment concentration, it was impossible to see the pebbles on the bar surface. Because pebbles were returned to the original sample site after measurement, it was possible to recognize pebble lags upon recurrent sampling of the same particles. Random velocity profiles were measured during rising flow conditions on several bars. During low flow conditions the following day, the bar outline was resurveyed and the stations re-established. On the average, bars could only be monitored during two cycles, as flow conditions changed so rapidly that bars either became emergent, inactive or were completely eroded away.

N. Smith (1974) also studied bar evolution during

Figure 21A. Field sketch of sample stations on transverse bars, high flow conditions

Figure 21B. Field sketch of sample stations on diagonal bars, low flow conditions

A TRANSVERSE BAR

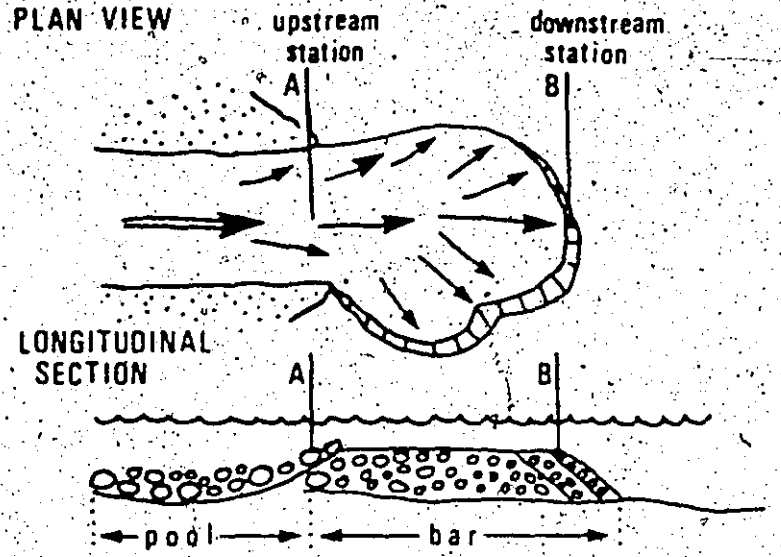

B DIAGONAL BAR

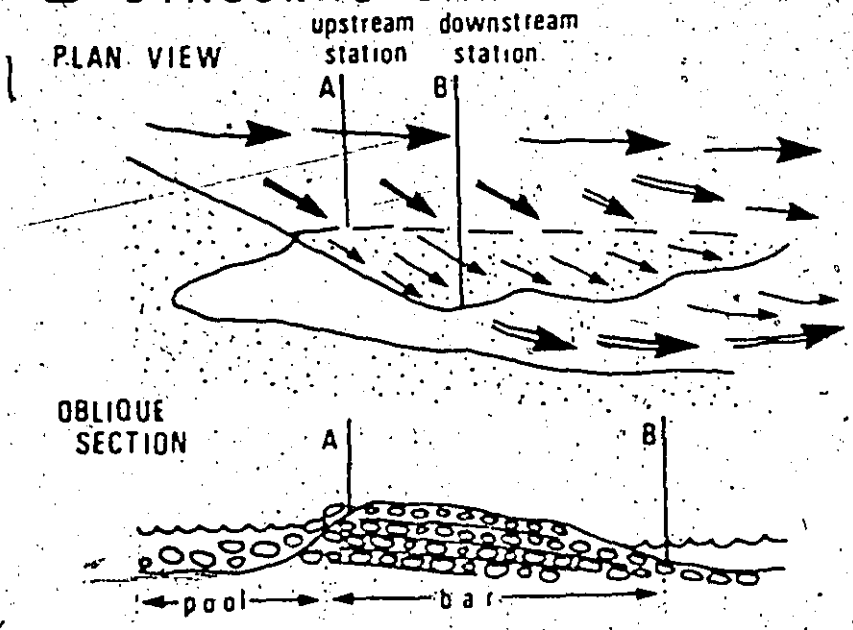

rising stages in the Kicking Horse River. The essential contrast between these two studies is that the present study measured flow conditions and bar migration continually during rising stages, whereas N. Smith's data were basically instantaneous measurements at peak flows. It was hoped that by measuring flow conditions at only two stations on the bar surface and rates of migration of the foreset, that the controls of gravel transport on bar surfaces could be better understood.

Sorting on diagonal bars was not examined under active gravel transport conditions, due to the more complex flow patterns over these bars. Under low flow conditions measurements of the dimensions of the ten largest pebbles were made at two stations: one at the upstream bar-channel boundary and one on the riffle margin, directly downstream from the other station (Figure 21B). Slopes of the bar surfaces were also measured between the two stations. Diagonal bars with foreset margins were not examined, because these bars are a transitional form between diagonal bars with riffle margins and transverse bars with foreset margins.

OBSERVED FLOW CONDITIONS OVER GRAVEL BEDS

A list of symbols used in this section is given in Table 3.

1. Estimates of Bed Roughness

Estimates of bed roughness can be calculated from semilog plots of velocity profiles, using the logarithmic velocity law, where

$$\frac{u}{u_*} = 8.50 + 5.75 \left(\log \left[\frac{y}{k_s}\right]\right) \quad (1)$$

$$= 5.75 \log \left(\frac{30.2y}{k_s}\right) \quad (2)$$

when $u = 0$, $y = k_s/30.2$ (3)

Velocity profile measurements are given in Appendix 1. Semilogarithmic plots of the measured velocity profiles are shown in Figure 22. Calculations of the estimates of bed roughness are shown in Table 4. The average k_s value was 0.596, where k_s estimates ranged from 0.178 to 0.875.

Alternatively, if it is assumed that all the resistance to flow is due to boundary roughness and given that the flow is a fully developed rough turbulent flow (large boundary Reynold's numbers), friction factors (f) for the bar surfaces can be determined from the following

Table 3. List of symbols used in Chapter 4

Symbol	Meaning	Dimensions
C_{max}	Maximum bedload sediment concentration by weight in parts per hundred thousand	
D	Depth of flow	L
d_i	Particle size at which i% (by weight) of the material is coarser	L
d_s	Average particle size of sediment	L
F^*	Froude Number $F^* = [\rho_f/(\rho_s - \rho_f)][\bar{u}^2/(gD)]$	
f	Darcy-Weisbach friction factor	
g	Gravitational acceleration	LT^{-2}
g_{bar}	Weight per unit surface area of downstream "bar" sediments	ML^{-2}
g_{lag}	Weight per unit surface area of upstream "lag" sediments	ML^{-2}
k_s	Roughness element height	L
q_{calc}	Probability of a given grain size remaining stationary	
S	Slope	
u	Velocity (unspecified depth)	LT^{-1}
$\bar{u}$	Average velocity (average of velocities measured at .2 and .8 of the total depth)	LT^{-1}
u_y	Velocity measured at height y measured above the bed	LT^{-1}
u_*	Shear velocity	LT^{-1}
u_{*c}	Critical shear velocity, calculated using Shield's criterion	LT^{-1}

Table 3/continued

Symbol	Meaning	Dimensions
y	Height measured above bed	L
β	Shield's beta $\beta = \tau_o/(\gamma_s - \gamma_f)ds$	
γ_f	Unit weight of fluid	$ML^{-2}T^{-2}$
γ_s	Unit weight of sediment	$ML^{-2}T^{-2}$
Δ Grain Size	Difference in long axis measurements of ten largest pebbles between upstream and downstream sample locations	L
$\Delta P_{i\ bar}$	Individual percent (in decimal form) of grain size (i) in bed sample of downstream "bar" deposit	
$\Delta P_{i\ lag}$	Individual percent (in decimal form) of grain size (i) in bed sample of upstream "lag" deposit	
ρ_f	Mass density of fluid	ML^{-3}
ρ_s	Mass density of sediment	ML^{-3}
τ	Shear stress	$ML^{-1}T^{-2}$
τ_o	Shear stress acting on the bottom	$ML^{-1}T^{-2}$

Figure 22. Velocity profiles, downstream study section. Data are given in Appendix 1. Curves were drawn from equations generated by a computer program (Biomed BMD02R) using multiple linear regression analysis.

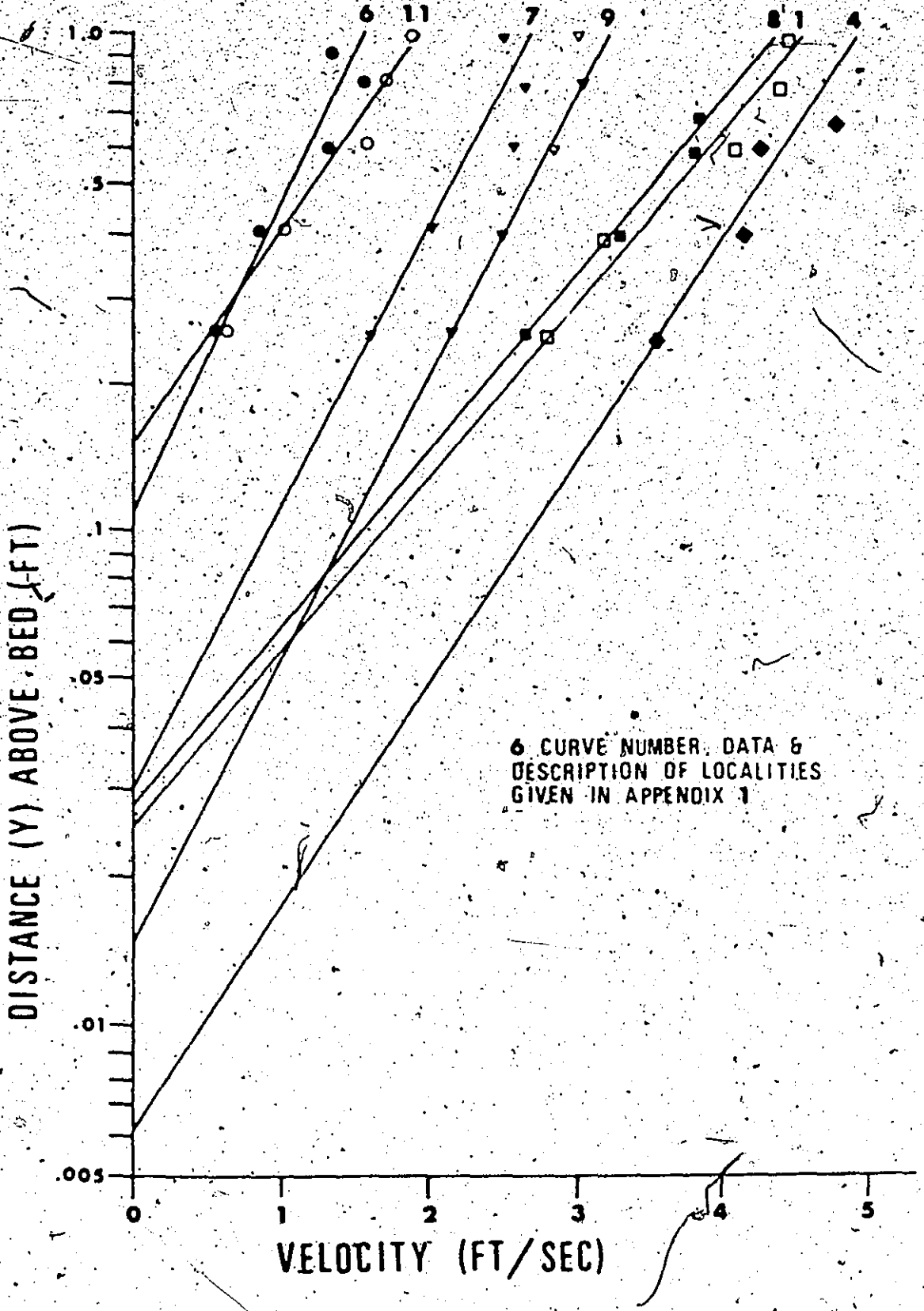
6
11
7
9
8
1
4
1.0
.5
.1
.05
.01
.005
0
1
2
3
4
5
DISTANCE (Y) ABOVE BED (FT)
VELOCITY (FT/SEC)
6 CURVE NUMBER. DATA & DESCRIPTION OF LOCALITIES GIVEN IN APPENDIX 1

Table 4. Bed roughness estimates from velocity profile data

Curve	y intercept (ft)	(30.2)y $= k_s$ (ft)	$u_{.25ft}$ (ft/sec)	u_* (ft/sec)	$\bar{u}$ (ft/sec)	$\frac{u_*}{\bar{u}}$	f eqtn(6)
1	0.023	0.695	2.76	0.20	3.73	0.054	0.023
4	0.0059	0.178	3.50	0.16	3.81	0.042	0.014
7	0.029	0.875	1.59	0.13	2.06	0.063	0.032
8	0.026	0.785	2.62	0.20	3.14	0.064	0.033
9	0.0148	0.447	2.15	0.13	2.58	0.050	0.020
		$\bar{k}_s$ = 0.596					
6	0.1	3.02	0.61	0.09	1.04	0.086	0.059
							$\bar{f}$ = 0.030

equation (Daily and Harleman, 1966, p.272):

$$f^{-0.5} = 2 \log \left(\frac{D}{k_s}\right) + 2.1 \qquad (4)$$

where f values are determined from the Chezy equation:

$$f = \frac{8gDS}{\bar{u}} \qquad (5)$$

The average f value determined from the velocity, depth and slope measurements on bar surfaces (1) at upstream stations was 0.327 (range: 0.098-0.582); (2) at downstream stations was 0.368 (range: 0.079-0.906). Calculations of these f values are shown in Tables 5-10. Using an average f value of 0.347 and equation (4), k_s values were found to vary between 0.64-3.50 ft.

Because the flow was very turbulent with surface boils and eddies, water surface slope measurements may not be reliable. Anomalous slope (S) values in equation (5) may account for the wide range of f values obtained at upstream and downstream stations on bar surfaces. Alternatively, the following equation can be used with the velocity profile data to obtain other estimates of friction factors on bar surfaces:

$$\frac{\bar{u}}{u_*} = \left(\frac{8}{f}\right)^{0.5}, \text{ where } f = 8\left(\frac{u_*}{\bar{u}}\right)^2 \qquad (6)$$

Calculations of f values are shown in Table 4. The average f value was 0.03 (range: -0.014-0.059), yielding an average k_s value of .019 (upstream) and .013 (downstream) (Tables 5-10).

Bed roughness is commonly thought to correspond to the 35 percentile of the grain size distribution of the bedload sediment. Grain size values corresponding to this percentile are only 0.05 ft, which is much less than estimates of roughness from equations (1) and (4). Kellerhals (1967) in his studies of the regime theory of gravel-paved channels, found that the Nikuradse equivalent grain roughness is approximately equal to the 10th percentile of the grain size distribution. Results from this study show that the grain size of sediment in the 10th percentile (Figure 23) (1.57 ft) is higher than the size of roughness elements estimates from equation (1), but correspond to the size of roughness heights obtained from equation (4). A summary of the various estimates of bed roughness is given in Table 11.

Use of the method involving the velocity profile and equation (1) assumes a logarithmic velocity distribution which may not be valid for large relative roughness heights in gravel streams. This may account for the low k_s value. Comparisons of the estimates of roughness heights suggest that those estimates derived from the Chezy equation (5) and equation (4) correspond very well with the size of sediment in the 10th percentile of the grain size distribution curve.

Figure 23. Cumulative frequency curve of average bed sample, downstream study reach (modified after N. Smith, 1974)

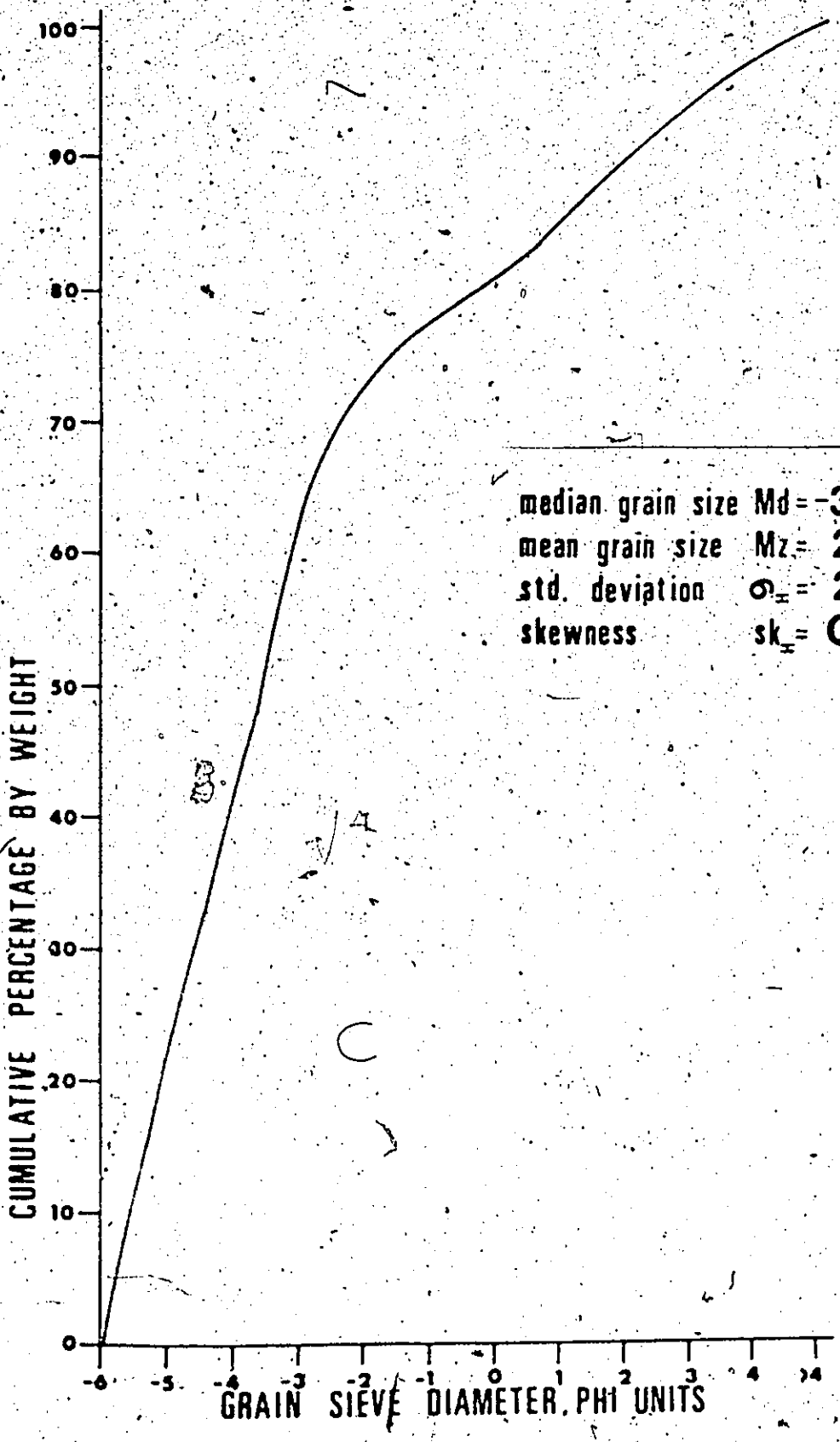

median grain size M_d = -3.59 Ø
mean grain size M_z = 2.76 Ø
std. deviation σ_I = 2.98
skewness sk_I = 0.448

2. Bottom Velocity - Average Velocity and Bottom Velocity-Shear Velocity Relations

Bottom velocity measurements on active bar surfaces were obtained with a standard Gurley-Price current meter at a depth 0.20 ft from the bed. Because most equations involving sediment transport utilize the average or shear velocities, relations between these parameters and measured bottom velocities had to be determined.

An empirical relation between bottom velocity measurements and average velocities were obtained from the velocity profile data (Figure 22, Appendix 1). The average velocity is defined as the average of the velocities measure at depths corresponding to 0.2 and 0.8 of the total depth. These calculations are given in Appendix 2. A linear regression between bottom velocity measurements and average velocities, calculated from the velocity profiles) gives the following relation:

$$\log \bar{u} = 0.18\, u_{0.2y} - 0.018 \qquad (7)$$

The relationship between the measured bottom velocity and the shear velocity was obtained from equation (2), where

$$u_{0.2y} = 5.75 \log \left(\frac{30.2 \times 0.2}{k_s}\right) u_* \qquad (8)$$

If k_s = 1.57 ft (corresponding to the 10th percentile of the grain size distribution),

$$u'_{0.2y} = 3.36\, u_* \qquad (9)$$

Calculations of the shear and average velocities from measured bottom velocity data are shown in Tables 5-10.

RESULTS AND DISCUSSION

1. Grain Movement

In order to determine flow conditions needed for incipient motion of coarse grains on bar surfaces, field measurements of bottom velocities, depth, slope and sediment grain size were made at upstream and downstream stations on transverse bars. Grain sizes were determined from the ten largest pebbles on the bar surface. The largest upstream particles were interpreted as gravel lags, where the same pebbles were quite commonly encountered in recurrent bedload samples. Largest downstream pebbles were seen to be actively transported in migrating bar lobe fronts. These qualitative observations support the proposed hypothesis that bars initiate from reworking of diffuse gravel sheet deposits. It was thought that measured hydraulic data during the periods of active bar growth might show that flow conditions were capable of transporting the downstream sediments but incompetent to move upstream deposits.

Most studies on initiation of grain movement conclude

Table 5. Calculations of flow parameters from measured field data, active transverse bars

Bar 2 August 3

Time (p.m.)	Depth (ft)	$u_{0.2y}$ (ft/sec)	Slope	Intermediate axis (mm)	f eqtn (5)	k_s eqtns (6),(4) (ft)	$\bar{u}$ (ft/sec) eqtn (7) (5),(4)		u_* eqtn (9) (ft/sec)	τ eqtn (10)
Upstream Station										
4:20	1.4	3.41	.0108	46.4	.257	.020	2.25	3.89	1.01	0.943
4:45	1.6	3.78	.0105	48.5	.211	.023	2.54	4.53	1.13	1.05
5:15	1.6	3.60	.0039	52.1	.091	.023	2.54	4.21	1.07	0.394
5:40	1.6	4.10	.0053	53.2	.082	.023	2.54	5.17	1.22	0.530
5:55	1.8	3.03	.0015	51.8	.063	.026	2.86	3.33	0.90	0.172
6:30	1.5	2.80	.0017	49.7	.072	.022	2.38	3.03	0.83	0.159
6:50	1.8	2.76	.0005	50.9	.026	.026	2.86	2.98	0.82	0.061
8:00	1.7	2.73	.0009	51.5	.045	.025	2.70	2.94	0.81	0.094
8:20	1.8	2.41	.0004	50.2	.028	.026	2.86	2.58	0.72	0.004
9:11	1.8	1.84	.0003	47.9	.033	.026	2.86	2.04	0.55	0.031
Downstream Station										
4:30	0.9	3.71	.0108	33.9	.129	.013	1.43	4.04	1.10	0.607
4:55	1.0	3.63	.0105	40.4	.149	.015	1.59	4.26	1.08	0.655
5:20	1.4	3.26	.0039	33.7	.105	.020	2.23	3.66	0.97	0.341
5:45	1.4	2.76	.0053	39.2	.215	.020	2.23	2.98	0.82	0.463
6:10	1.1	3.13	.0015	39.0	.035	.016	1.75	3.47	0.93	0.103
6:35	1.3	2.25	.0017	41.7	.097	.019	2.07	2.42	0.67	0.140
7:05	1.3	3.20	.0005	34.3	.013	.019	2.07	3.57	0.95	0.041
8:10	1.3	2.95	.0009	33.8	.029	.019	2.07	3.22	0.88	0.073
8:30	1.1	3.13	.0004	37.8	.010	.016	1.75	3.47	0.93	0.003
9:20	1.1	2.51	.0003	41.6	.012	.016	1.75	2.69	0.75	0.021

Table 6. Calculations of flow parameters from measured field data, active transverse bars

Bar 2 August 4

Time (p.m.)	Depth (ft)	$u_{0.2y}$ (ft/sec)	Slope	Intermediate axis (mm)	f, eqtn (5)	k_s (ft) eqtns (6), (4)	$\bar{u}$ (ft/sec) eqtn (7)		u_* eqtn (9) (ft/sec)	τ eqtn (10)
							(5), (4)			
Upstream										
3:45	1.8	1.59	.0061	54.7	.833	.026	2.86	1.84	.473	.687
4:10	1.8	1.55	.0061	53.1	.861	.026	2.86	1.81	.461	.687
4:25	1.8	1.36	.0044	53.9	.727	.026	2.86	1.68	.405	.491
4:45	1.7	1.50	.0019	54.2	.263	.025	2.70	1.78	.446	.200
5:05	1.6	2.00	.0033	54.5	.286	.023	2.54	2.18	.595	.325
5:35	1.6	1.67	.0040	55.1	.455	.023	2.54	1.90	.497	.404
6:00	1.6	2.00	.0053	53.2	.459	.023	2.54	2.18	.595	.531
6:35	1.8	2.95	.0080	41.4	.357	.026	2.86	3.22	.878	.897
7:15	1.9	2.51	.0101	43.8	.684	.028	3.02	2.69	.747	1.198
7:45	2.2	2.41	.0105	38.8	.894	.032	3.50	2.58	.717	1.444
Downstream										
3:50	1.1	3.03	.0061	39.8	.156	.016	1.75	3.33	.902	.419
4:15	1.2	2.48	.0061	41.2	.267	.017	1.91	2.66	.738	.457
4:30	1.3	2.35	.0044	39.1	.232	.019	2.07	2.52	.699	.357
4:55	1.2	2.51	.0019	36.4	.081	.017	1.91	2.69	.747	.142
5:10	1.4	2.15	.0033	41.2	.221	.020	2.23	2.32	.640	.288
5:45	1.4	2.15	.0040	39.9	.268	.020	2.23	2.32	.640	.349
6:10	1.2	2.51	.0053	37.2	.226	.017	1.91	2.69	.747	.397
7:05	1.4	2.69	.0080	38.8	.344	.020	2.23	2.90	.801	.699
7:25	1.5	2.35	.0101	40.4	.615	.022	2.38	2.52	.699	.945
7:55	1.5	2.08	.0105	36.4	.798	.022	2.38	2.25	.619	.983

Table 7. Calculations of flow parameters from measured field data, active transverse bars

Bar 3 August 6

Time (p.m.)	Depth (ft)	$u_{0.2y}$ (ft/sec)	Slope	Intermediate axis (mm)	f eqtn (5)	k_s eqtns (ft)		$\bar{u}$ (ft/sec) eqtn (7)	u_* eqtn (9) (ft/sec)	τ eqtn (10)
						(6), (4)	(5), (4)			
Upstream										
4:10	1.0	2.84	.0119	53.5	.323	.015	1.59	3.08	.845	.741
4:30	1.1	3.16	.0123	46.2	.282	.016	1.75	3.51	.940	.843
5:00	1.1	3.56	.0152	47.7	.251	.016	1.75	4.14	1.059	1.045
5:20	1.2	2.51	.0118	41.7	.504	.017	1.91	2.69	.747	.885
6:30	1.2	2.51	.0113	40.4	.483	.017	1.91	2.69	.747	.844
Downstream										
4:20	0.4	3.71	.0119	42.1	.063	.006	.636	4.40	1.104	.297
4:40	0.4	3.50	.0123	41.5	.078	.006	.636	4.04	1.041	.307
5:05	0.5	3.07	.0152	37.1	.171	.007	.795	3.39	.914	.474
5:23	0.5	3.16	.0118	40.1	.123	.007	.795	3.51	.940	.368
6:45	0.5	2.73	.0113	36.3	.168	.007	.795	2.94	.813	.353

Table 8. Calculations of flow parameters from measured field data, active transverse bars

Bar 3 August 8

Time (p.m.)	Depth (ft)	$u_{0.2y}$ (ft/sec)	Slope	Intermediate axis (mm)	f eqtn (5)	k_s eqtns (ft) (6),(4)	$\bar{u}$ (ft/sec) eqtn (7) (5),(4)		u_* eqtn (9) (ft/sec)	τ eqtn (10)
Upstream										
3:45	1.0	3.26	.0171	51.0	.329	.015	1.59	3.86	.970	1.067
4:10	1.0	2.69	.0166	50.0	.510	.015	1.59	2.90	.801	1.033
4:45	1.0	2.93	.0144	43.1	.363	.015	1.59	3.20	.872	.901
5:40	0.9	2.85	.0076	39.6	.184	.013	1.43	3.09	.848	.425
6:15	0.7	3.94	.0111	38.1	.085	.010	1.11	4.84	1.173	.487
6:35	0.8	4.00	.0152	39.0	.127	.012	1.27	4.96	1.190	.759
7:00	0.8	2.59	.0113	37.0	.302	.012	1.27	2.78	.771	.564
7:35	0.8	3.40	.0092	41.3	.126	.012	1.27	3.88	1.011	.457
8:00	1.0	2.76	.0124	36.8	.360	.015	1.59	2.98	.821	.770
8:25	0.9	2.19	.0113	40.0	.471	.013	1.43	2.36	.652	.635
8:40	0.9	2.35	.0109	37.6	.398	.013	1.43	2.52	.699	.614
Downstream										
3:55	1.5	1.67	.0171	39.2	1.822	.022	2.38	1.90	.497	1.554
4:20	1.5	1.86	.0166	39.1	1.514	.022	2.38	2.06	.554	1.438
5:00	1.6	1.79	.0144	40.4	1.482	.023	2.54	2.00	.533	.759
5:50	1.6	1.84	.0076	34.2	.751	.023	2.54	2.04	.548	.762
6:20	1.1	2.23	.0111	37.3	.548	.016	1.75	2.40	.664	1.138
6:45	1.2	2.23	.0152	37.6	.818	.017	1.91	2.40	.664	.846
7:05	1.2	2.28	.0113	40.9	.583	.017	1.91	2.45	.679	.574
7:45	1.0	2.15	.0092	39.3	.441	.015	1.59	2.32	.640	.774
8:05	1.0	2.12	.0124	35.2	.609	.015	1.59	2.29	.631	.776
8:30	1.1	1.90	.0113	34.1	.731	.016	1.75	2.09	.565	.776
8:50	1.2	2.08	.0109	33.9	.663	.017	1.91	2.25	.619	.816

Table 9. Calculations of flow parameters from measured field data, active transverse bars

Bar 6 August 10

Time (p.m.)	Depth (ft)	$u_{0.2y}$ (ft/sec)	Slope	Intermediate axis (mm)	f eqtn(5)	k_s eqtns (ft) (6),(4)	(5),(4)	$\bar{u}$ (ft/sec) eqtn (7)		u_* eqtn (9) (ft/sec)	τ eqtn(10)
Upstream											
4:10	1.6	3.10	.0085	46.9	.298	.023	2.54	3.43		.923	.849
4:30	1.6	2.55	.0091	46.9	.502	.023	2.54	2.73		.759	.905
4:45	1.6	3.55	.0011	46.4	.027	.023	2.54	4.12		1.056	1.102
5:05	1.6	2.99	.0101	47.8	.388	.023	2.54	3.28		.890	1.011
5:20	1.7	3.03	.0098	48.0	.387	.025	2.70	3.33		.902	1.041
5:30	1.6	3.30	.0099	50.9	.295	.023	2.54	3.72		.982	.994
Downstream											
4:15	0.8	1.59	.0085	29.6	.576	.012	1.27	1.84		.473	.424
4:35	0.8	1.20	.0091	33.4	.760	.012	1.27	1.57		.357	.454
4:55	0.9	1.84	.0011	34.7	.061	.013	1.43	2.04		.548	.462
5:15	0.9	1.29	.0101	36.1	.882	.013	1.43	1.63		.383	.567
5:25	1.0	1.40	.0098	35.5	.869	.015	1.59	1.70		.417	.612
5:35	1.0	1.59	.0099	35.1	.751	.015	1.59	1.84		.473	.618

Table 10. Calculations of flow parameters from measured field data, active transverse bars

Bar 7 August 11

Time (p.m.)	Depth (ft)	$u_{0.2y}$ (ft/sec)	Slope	Intermediate axis (mm)	f eqtn (8)	k_s eqtns (ft) (6),(4)	k_s eqtns (ft) (5),(4)	$\bar{u}$ (ft/sec) eqtn (7)	u_* eqtn (9) (ft/sec)	τ eqtn (10)
Upstream										
4:00	0.8	2.69	.0075	48.8	.184	.012	1.27	2.90	.801	.375
4:20	0.8	2.23	.0076	46.6	.273	.012	1.27	2.40	.664	.380
4:55	0.8	2.00	.0074	44.6	.320	.012	1.27	2.18	.595	.370
5:30	0.9	2.23	.0073	50.8	.295	.013	1.43	2.40	.664	.407
6:00	0.9	2.23	.0074	53.4	.299	.013	1.43	2.40	.664	.413
6:15	0.9	2.15	.0072	49.1	.310	.013	1.43	2.32	.640	.405
6:30	0.9	2.04	.0076	49.7	.359	.013	1.43	2.22	.607	.429
6:45	0.9	1.90	.0076	48.4	.402	.013	1.43	2.09	.565	.428
Downstream										
4:05	0.3	2.10	.0075	33.9	.112	.004	.477	2.27	.625	.140
4:25	0.3	2.00	.0076	37.2	.123	.004	.477	2.18	.595	.142
5:00	0.3	1.84	.0074	39.5	.137	.004	.477	2.04	.548	.139
5:35	0.4	2.19	.0073	37.1	.135	.006	.636	2.36	.652	.182
6:05	0.4	2.04	.0074	38.2	.155	.006	.636	2.28	.607	.185
6:20	0.4	2.10	.0072	35.2	.114	.006	.636	2.27	.625	.180
6:35	0.4	1.90	.0076	37.8	.179	.006	.636	2.09	.565	.190
6:55	0.4	1.94	.0076	39.2	.173	.006	.636	2.13	.577	.190

Table 11. Bed roughness estimates

Method	Roughness size
Velocity profiles and equation (1)	k_s = 0.58 ft
Chezy equation (5) and equation (4)	k_s = 0.64-3.5 ft
Equation (6) and equation (4)	k_s = 0.016 ft
Grain Size distribution - 35 percentile	d = 0.05 ft
Grain Size distribution - 10 percentile	d = 1.57 ft

that the boundary tractive force or shear stress is an essential parameter to define conditions of grain motion. The shear stress, τ, is given by:

$$\tau = \gamma_f DS \qquad (10)$$

It was hoped that shear stress calculations (Tables 5-10) using equation (10) would differentiate upstream from downstream stations in terms of flow conditions necessary for sediment transport. However, shear stresses calculated from equation (10) show no relation to the average size of the ten largest bedload particles.

The reasons for this lack of correlation are thought to be the difficulty in accurate determination of depth and slope relations with such shallow (1-3 ft) depths, large roughness factors, rapidly fluctuating velocities and strong eddy development (which probably disrupt the entire flow) producing locally non-uniform, unsteady conditions. Kellerhals (1967) found that with large bedload roughness elements, there is a radical change in phases of bedload transport and in formulae correlating various river dimensions with flow parameters. His findings further decrease confidence in the application of hydraulic equations developed for essentially "two-dimensional" uniform flow conditions to flows which are unsteady, non-uniform and three-dimensional.

Although calculations of tractive force showed no relation with grain size on the bar surface, a plot of bottom velocity (0.2 ft above the gravel bed) versus average intermediate diameter of the ten largest pebbles does separate the upstream lag deposits from the downstream gravels in transport (Figure 24). This plot suggested that perhaps the shear velocity impinging upon the grains was the main controlling factor in the initiation of bedload movement. For this reason, measured bottom velocities were converted to shear velocities, using equation (9) and data were replotted in Figures 25A-25F.

Other estimates of the shear velocity based upon velocity profile measurements or from shear stress calculations give spurious results, which are less than Shield's criterion by a factor of 1 or 2.

Assuming that Shield's relations are valid for this system, Shield's criterion was used to calculate the initial shear velocity for bedload movement using the following relations.

$$\tau_c = \beta(\gamma_s - \gamma_f)d_s \qquad (11)$$

$$\tau_c = \rho_f u_{*c}^2 \qquad (12)$$

For fully developed turbulent flow, $\beta = 0.06$; by substitution,

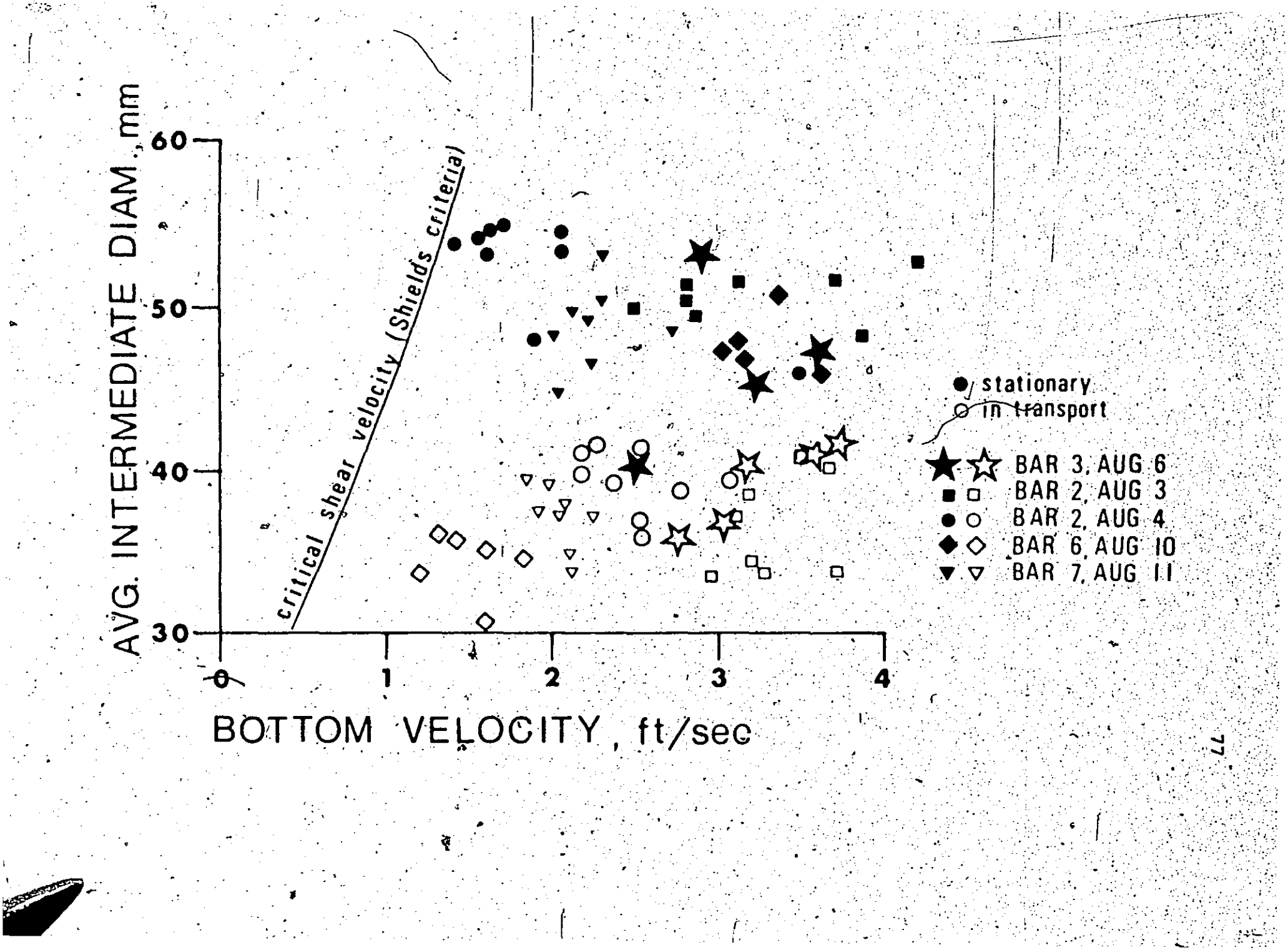
AVG. INTERMEDIATE DIAM., mm
60
50
40
30
0
1
2
3
4
BOTTOM VELOCITY, ft/sec
critical shear velocity (Shields criteria)
stationary
in transport
BAR 3, AUG 6
BAR 2, AUG 3
BAR 2, AUG 4
BAR 6, AUG 10
BAR 7, AUG 11

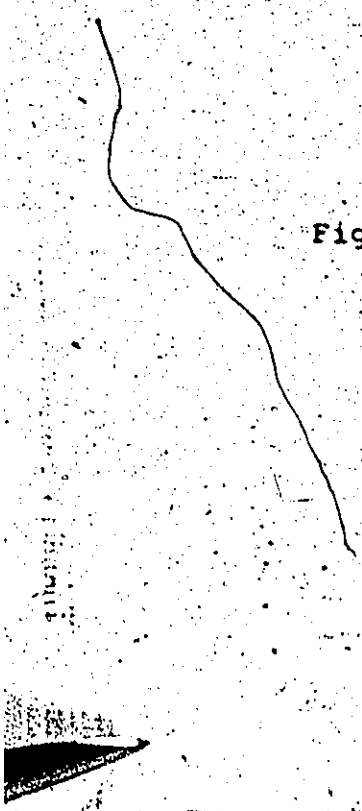

Figure 25. Plot of Grain Size versus Shear Velocity, active transverse bars.

A Bar 2, August 4

B Bar 2, August 3

C Bar 7, August 11

D Bar 3, August 8

E Bar 3, August 6

F Bar 6, August 10

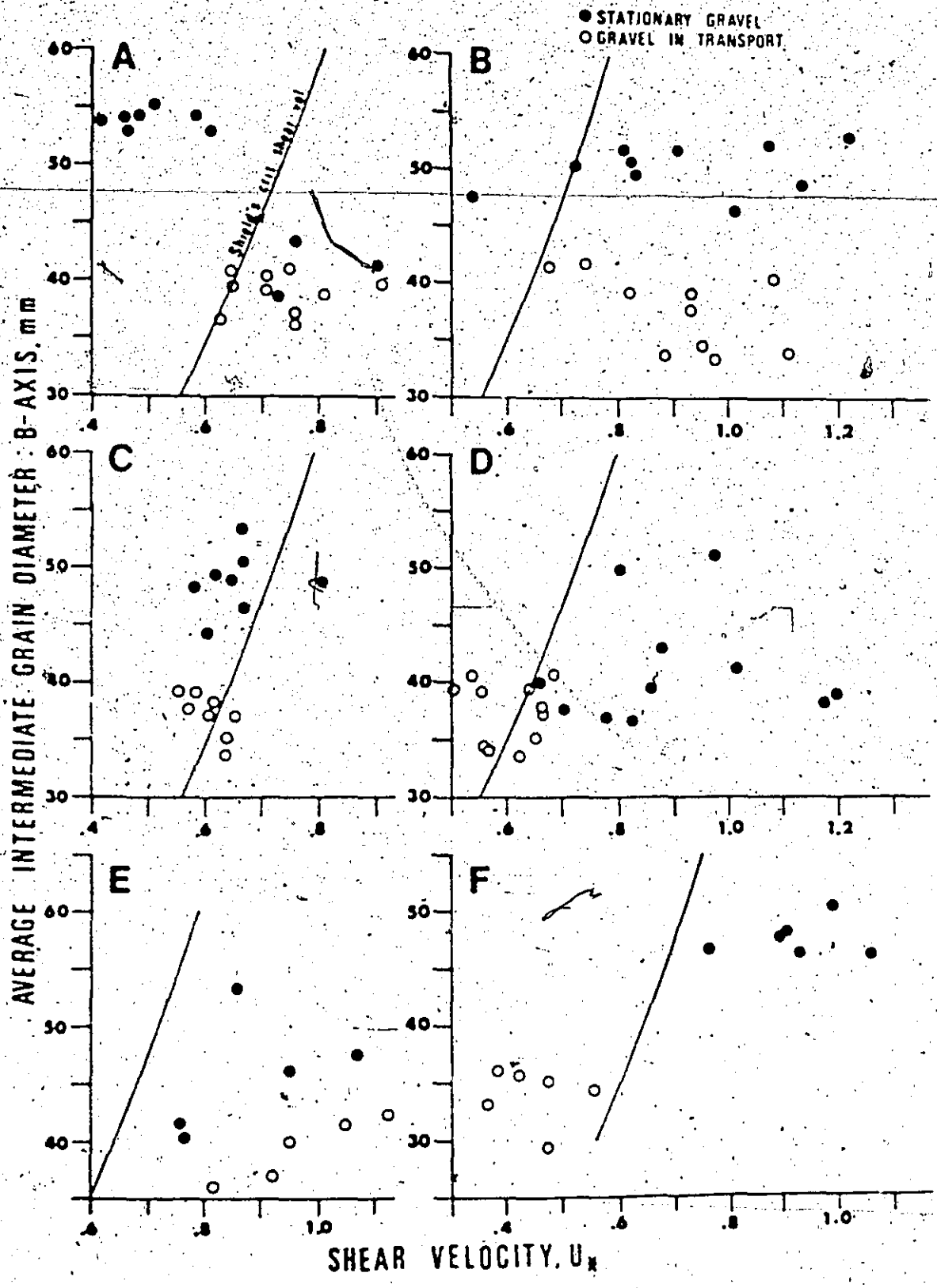
● STATIONARY GRAVEL
○ GRAVEL IN TRANSPORT
A
B
C
D
E
F
AVERAGE INTERMEDIATE GRAIN DIAMETER : B-AXIS, mm
SHEAR VELOCITY, U*

$$\rho_f u_{*c}^2 = 0.06\,(\gamma_s - \gamma_f)d_s \qquad (13)$$

Rearranging,

$$u_{*c} = \left[\frac{0.06(g[\rho_s - \rho_f]d_s)}{\rho_f}\right]^{0.5} \qquad (14)$$

Because most of the bedload sediment was dolomitic in composition, the density of dolomite (2.84 g/cc) was assumed to be the average density of the sediment (ρ_s). Water temperatures and suspended sediment concentrations were measured at various stages of the flow to determine the fluid density (ρ_f). Results from these calculations are plotted in Figure 25 as the critical shear velocity curve.

Comparisons with the field data (Figure 25) show that despite the fact that critical erosion velocities for initiation of bedload movement were reached, in most cases, at the upstream stations, sediment was not transported as predicted from Shield's criterion. This discrepancy is thought to be primarily due to (1) the interaction between particles and large bed roughness elements, where pivoting or overturning of particles may greatly affect the velocities at which bedload transport commences, and (2) the difficulty in obtaining a true estimate of average bedload grain size.

2. Bar Migration Rates and Bedload Discharge Calculations

In situ data obtained during the rising discharge cycles on transverse bars are presented in Appendix 3. Qualitatively, by examination of the plots, the following observations are made:

(1) Water depths are fairly constant at both upstream and downstream stations throughout the rising discharge period;

(2) Slight increases in average grain size of the ten largest pebbles at both stations correspond to upstream velocity increases;

(3) Bars migrate downstream with an average rate of 0.062 ft/min. The advance rates varied from 0.04 ft/min to 0.137 ft/min;

(4) Bars migrate downstream in spurts, rather than continuously, through rising flow conditions. Maximum downstream migration rates of bar foreset margins coincide most closely with maximum rates of velocity increase at the upstream station.

A plot of gravel discharge versus rate of increase of velocity at the upstream station support the above relation between bar migration rates and upstream velocity fluctuations (Figure 26). Gravel discharges per unit bar width were

Figure 26. Plot of Gravel Discharge versus Rate of Increase of Bottom Velocity, active transverse bars.

Figure 27. Comparison of calculated and measured gravel discharges

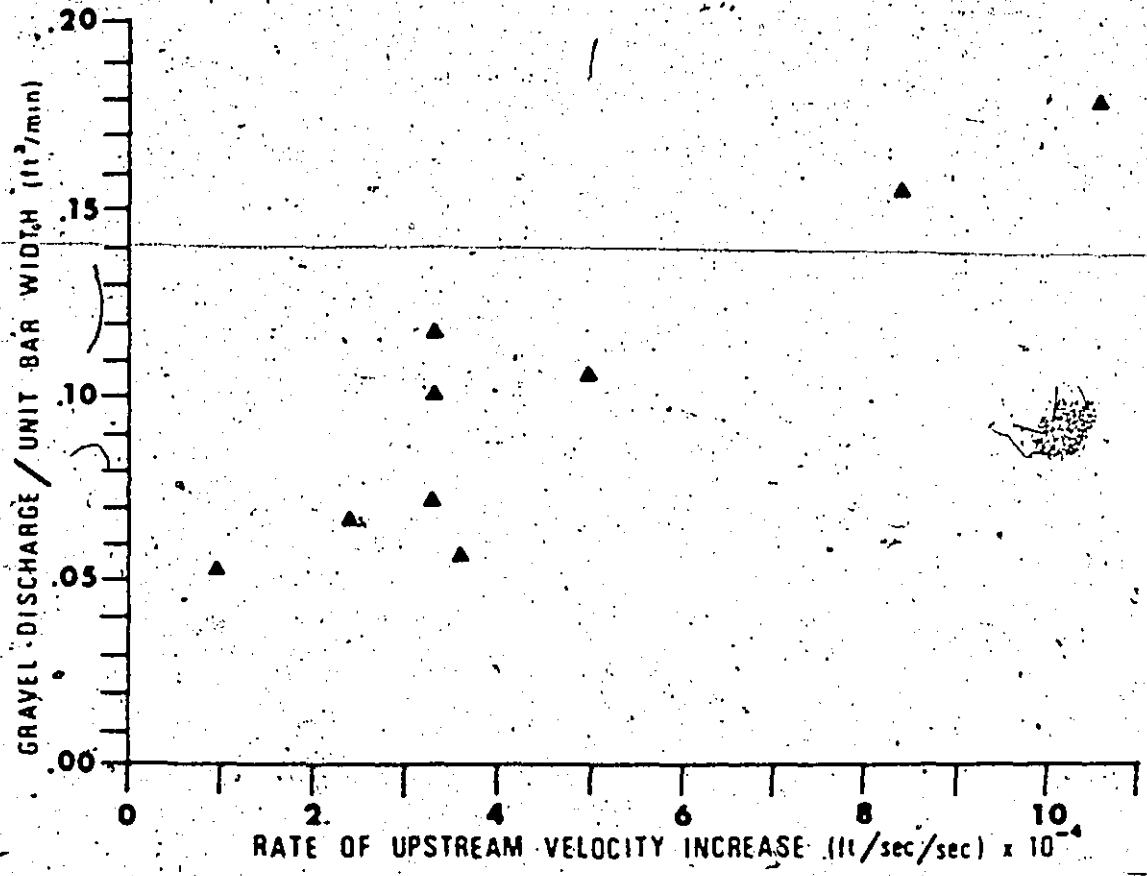
.20
.15
.10
.05
.00
GRAVEL DISCHARGE / UNIT BAR WIDTH (ft²/min)
0
2
4
6
8
10
RATE OF UPSTREAM VELOCITY INCREASE (ft/sec/sec) x 10⁻⁴

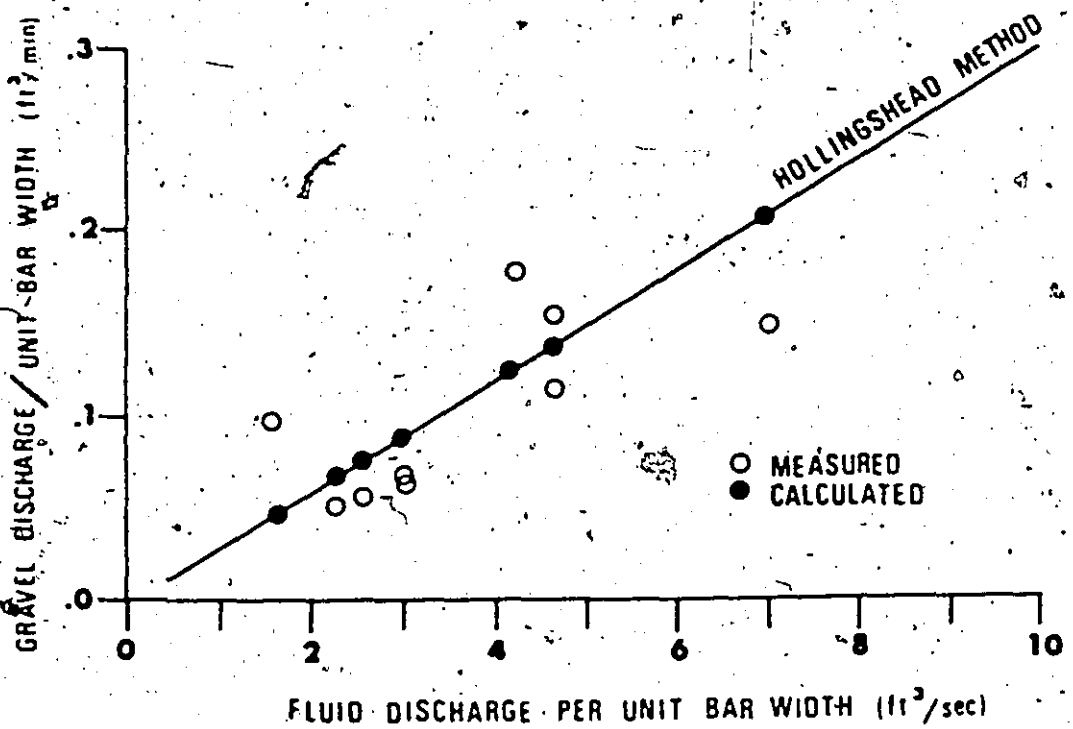
.3
.2
.1
.0
GRAVEL DISCHARGE / UNIT BAR WIDTH (ft²/min)
HOLLINGSHEAD METHOD
MEASURED
CALCULATED
0
2
4
6
8
10
FLUID DISCHARGE PER UNIT BAR WIDTH (ft³/sec)

calculated as the product of bar height times bar advance rates. Gravel discharges per unit bar width ranged from 0.052 ft^3/min to 0.178 ft^3/min, with the average gravel discharge equal to 0.08 ft^3/min. Gravel discharges show no relation with calculated stream power values, which probably reflects the gross inaccuracy of the shear stress values obtained from the measured field data.

The observed correlation between bar migration rates and upstream velocity fluctuations can be explained in terms of the diffuse gravel sheet model. Since the diffuse gravel sheets consist of a poorly sorted mixture of bed material, smaller particles are lodged in between the larger pebbles. A certain high velocity increase is needed to jostle and pivot the larger particles, exposing finer grained sediment, which is then transported downstream as a bar form. As a result of this initial winnowing of the top gravel layer, a large coarse-grained pavement is developed in upstream sections, which protects underlying finer sediment from being transported. Further downstream migration of the bar front depends upon recurrent high velocity increases in upstream sections, which dislodge the larger particles, again exposing finer sediments to competent flows. For this reason, bar fronts seem to advance in spurts, rather than continuously during a rising discharge cycle, where high rates of upstream velocity

increases occur only occasionally.

Because it was impossible to obtain reasonable estimates of shear stress values or critical shear velocities, measured gravel discharges could not be compared with discharges predicted from well-known bedload transport formulae (i.e. the Einstein or Meyer-Peter bedload transport formulae). Hollingshead (1971) in his study of sediment transport in gravel rivers of the Alberta foothills proposed an alternate method to calculate bedload discharge in coarse-grained streams. This method is based on a field determination of partial fluid discharges contributing to the bedload transport and on analysis of flume data of Cooper (1970). The Hollingshead (1971) method is described as follows:

(1) Partial fluid discharges contributing to the bedload transport are calculated. Because field data in this study were obtained at points, the partial fluid discharge at the stations was computed as the product of the depth and average velocity.

(2) Cooper's (1970) flume data were used to obtain an estimate of the concentration by weight of the bed-material discharge in parts per hundred thousand. To use his data the following two quantities were calculated:

(i) Froude number $(F'') = [\rho_f/(\rho_s - \rho_f)][\bar{u}^2/gD]$ (15)

(ii) Ratio between the depth and the median grain size = D/Md grain size (16)

In the present study most of the Froude number values (F'') fell below the range of Cooper's flume data; consequently the maximum Froude number and Depth/Md grain size values were used, where:

$$F''_{max} = 0.4$$

$$D/Md \text{ grain size}_{max} = 30;$$

yielding, from Cooper's (1970) empirical relations, a maximum bed-material discharge concentration value of:

$$C_{max} = 0.00045$$

(3) The total bedload discharge is obtained as the product of the concentration C_{max} and the partial fluid discharge.

As shown in Figure 27, despite the fair amount of scatter, measured gravel discharges in the present study correspond closely with those values predicted by the Hollingshead (1971) method.

3. Sediment Sorting: Transverse Bars

As mentioned previously, there is some question about the actual sorting processes involved on bar surfaces. Most bars aligned parallel to the current display marked downstream-fining trends as shown by N. Smith in his studies of the Kicking Horse River bars (N. Smith, 1974). This fining trend downstream may reflect (1) differential transport of various size particles on the bar surface; (2) the winnowing out of finer sediment from upstream areas, leaving a coarse lag layer in upstream parts of bars, or (3) a combination of both processes.

In order to obtain a better estimate of sediment size distributions on bars, surface sediment samples were scraped from three foot square plots at upstream and downstream portions of exposed relatively unmodified transverse bar surfaces. Bars were sampled on gravel flats of the Kicking Horse River downstream from the Field bridge, with supplementary data obtained from the Bath Creek outwash flats. Samples were sieved at full phi (Ø) intervals for sieve diameters greater than -4Ø (16 mm). Sediments smaller than -4Ø (16 mm) were lumped together. It was thought that by looking only at the coarser particles, these would be more representative of single high flow deposits; whereas the finer particles could have been deposited between the larger grains during subsequent low flows. Cumulative frequency

curves are shown in Figure 28. Upstream stations are quite coarse, where an average of over 80% of the sample occurs in fractions greater than -4Ø (16 mm). Downstream samples have an average of 60% of the sediment occurring in fractions greater than -4Ø (16 mm).

Gessler (1965) in his flume studies on the stability of gravel channels, found that it was possible to determine the probability of moving a given size of sediment, given grain size distribution curves of lag and erosion sediments. If it is assumed that the coarse upstream samples from the exposed bars represent the distribution of lag deposits on active bars, and the downstream samples from the exposed bars represent the eroded sediments from the diffuse sheets which were transported as bar lobes, then probabilities for movement of the grain sizes of sediment at upstream stations on the active bars can be estimated. The following relation (Gessler, 1965) was used to estimate the probability of not moving the sediment at upstream stations:

$$q_{calc.} = \frac{g_{lag}\Delta P_{i\ lag}}{g_{lag}\Delta P_{i\ lag} + g_{bar}\Delta P_{i\ bar}} \qquad (17)$$

where

g_{lag} = 45.3 lbs/three foot square surface area

g_{bar} = 60.7 lbs/three foot square surface area

Figure 28. Cumulative frequency curves of average bed samples, upstream "lag" and downstream "bar" deposits, inactive transverse bars

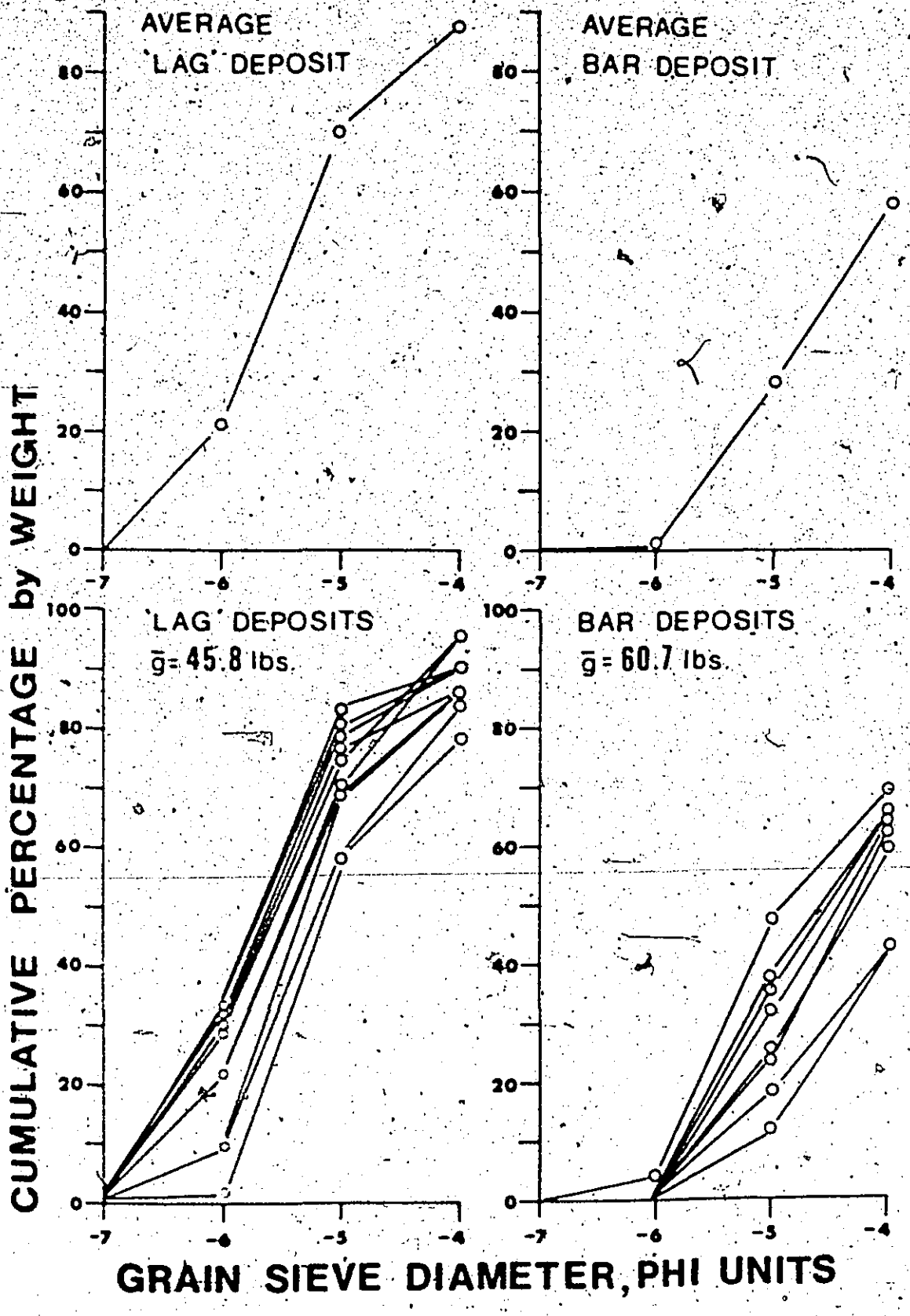
AVERAGE
'LAG' DEPOSIT
AVERAGE
BAR DEPOSIT
'LAG' DEPOSITS
$\bar{g}$= 45.8 lbs.
BAR DEPOSITS
$\bar{g}$= 60.7 lbs.
CUMULATIVE PERCENTAGE by WEIGHT
GRAIN SIEVE DIAMETER, PHI UNITS

The grain sizes that were used in this analysis were those recorded at upstream stations during periods of maximum bar transport rates. Two estimates were made of the probability of a given grain size (q_{calc}) remaining stationary, corresponding to maximum, minimum percentages of the given grain size on the cumulative frequency curve envelopes (Figure 28). Results from this analysis show that the upstream pebbles have an average probability of $q_{calc} = 0.628$ (range: 0.452-0.811) for remaining stationary during periods of most active bar growth. This analysis supports the idea that the downstream fining trend in the coarser tails of grain size distribution curves may reflect the development of upstream lag gravel pavements during periods of active bar growth. However, the overall downstream-fining trend is more probably attributable to both lag development in coarser tails and differential transport of the finer sediments across bar surfaces.

4. Sediment Sorting: Diagonal Bars

Sorting of sediment on bars which parallel currents is somewhat understood. However, the most common bar form in the outwash flats of this study region is the diagonal bar form, which migrates obliquely to main current directions. Sediment sorting on these bars is not understood. N. Smith (1974) stated that there were no obvious size sorting trends on diagonal bar surfaces. This aspect of the present study

was undertaken to examine in greater detail the sorting of sediments across diagonal bar surfaces. As with the transverse bars, surface samples were scraped from three foot square plots in upstream and downstream sections of exposed relatively unmodified diagonal bar surfaces. Only bars with preserved riffle margins were sampled. Dimensions of the ten largest pebbles encountered in the surface samples were measured. Slopes of the bar surface were also measured between the upstream and downstream sample stations. Forty-six diagonal bars were examined in the outwash flats of the Kicking Horse River, of Bath Creek and of the North Saskatchewan River.

Results of this study are plotted in Figure 29. The difference in grain size (Δ Grain Size) is the difference in long axis measurements of the ten largest pebbles between upstream and downstream sample stations. Negative values of Δ Grain Size indicate that the marginal sediments are finer-grained than the upstream sediments; positive values of Δ Grain Size indicate that the marginal sediments are coarser-grained than the upstream deposits. As shown in Figure 29, the sorting trends on diagonal bar surfaces seem to vary with bar depositional slope. On bar surfaces with slopes less than 0.06 sediment fines downstream; on slopes approximately equal to 0.06 there is no difference in grain size in downstream directions; on slopes greater than 0.06 there is a

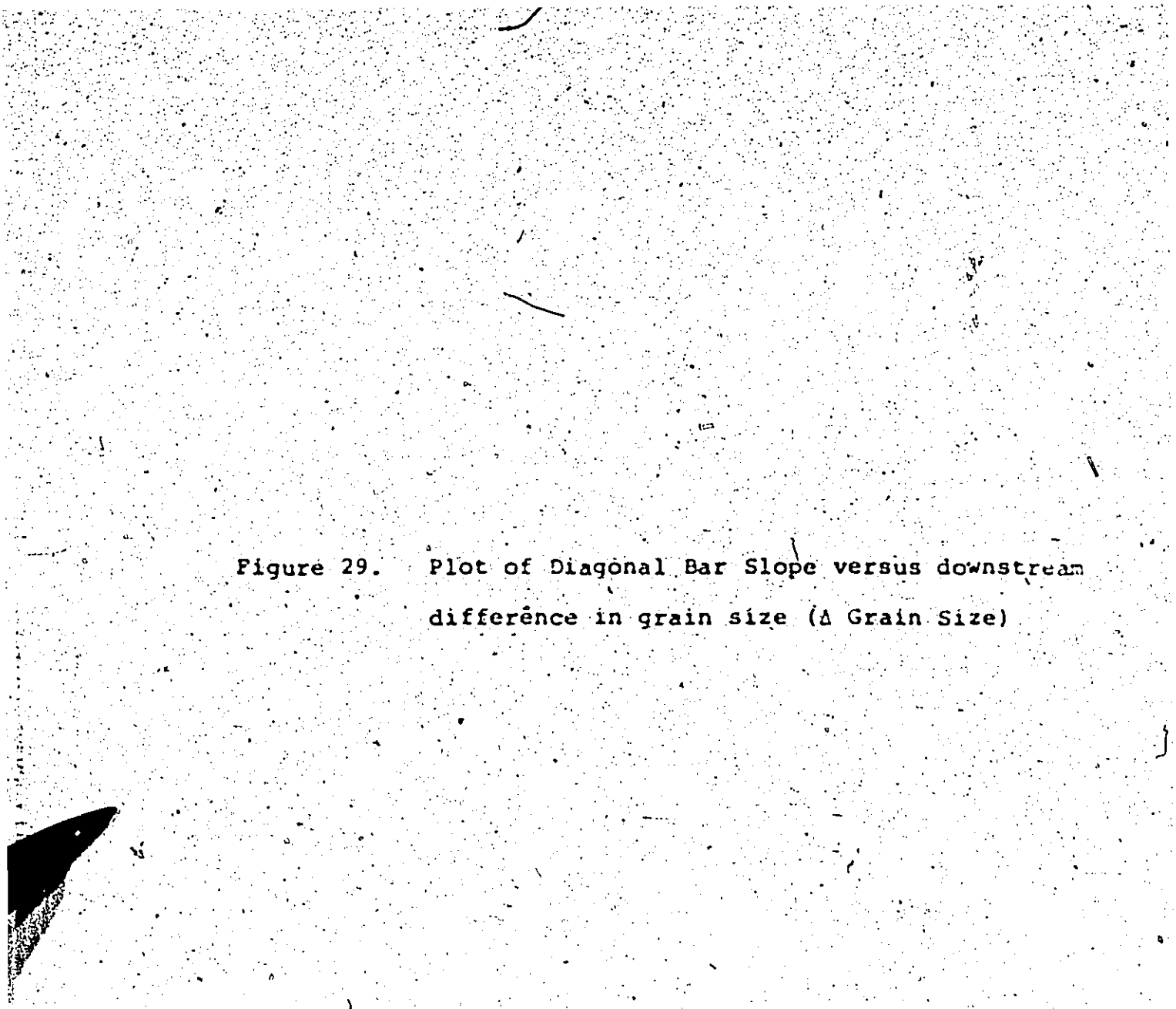

Figure 29. Plot of Diagonal Bar Slope versus downstream difference in grain size (Δ Grain Size)

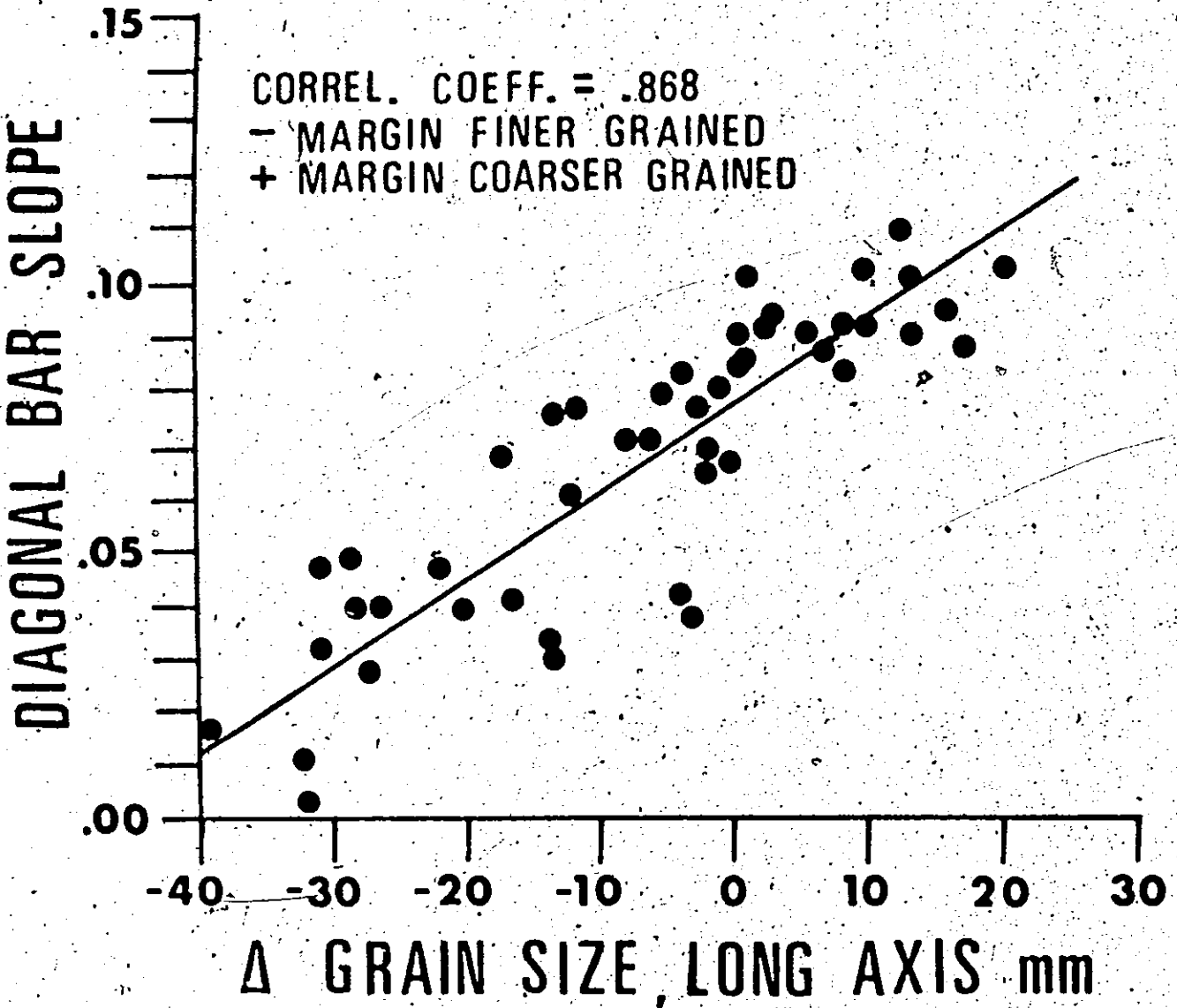
CORREL. COEFF. = .868
- MARGIN FINER GRAINED
+ MARGIN COARSER GRAINED
DIAGONAL BAR SLOPE
.15
.10
.05
.00
-40
-30
-20
-10
0
10
20
30
Δ GRAIN SIZE, LONG AXIS mm

downstream coarsening trend.

The relation between slope and sorting of sediment on these bars can only be hypothesized as these data were obtained during inactive low flow conditions. Perhaps on bars with low slopes, the sorting is similar to that on transverse bars. Here finer sediment is winnowed out from upstream areas and carried downstream as a diagonal bar form. Upstream sediments would be mainly a lag pavement, resulting in an overall downstream fining trend toward the bar riffle margin. With an increase in slope, perhaps there is an added momentum contributed to the bed material in transport and almost all of the sediment is transported on bar surfaces with slopes about 0.06. Bars with higher slopes (greater than 0.06) may start to behave as foreset margins, where the coarser particles during avalanche roll to the foot of the slope, resulting in an inverse grading in downstream direction across the bar surface.

5. Conclusions

Inherent difficulties in adequately sampling coarse bedload material is a major obstacle to studies of hydraulic controls of bedload transport in gravel channels. However, despite the lack of good sampling procedures, general conclusions from the present study can be drawn about flow conditions and gravel transport in shallow (1-3 ft deep) braided reaches.

(1) Bed roughness elements approximated by the size of sediment corresponding to the 35 percentile of the grain size distribution are much lower than those estimates obtained by other methods. Nikuradse equivalent roughness elements (k_s) obtained from the logarithmic velocity law for fully developed turbulent flow, equation (4), and from velocity profile data, correspond to the size of the sediment in the 10 percentile of the grain size distribution curve.

(2) Many of the basic relations of fluid flow do not apply in systems where bed roughness heights are large in comparison with flow depths.

(3) Field measurements of hydraulic conditions, bedload sediment size and bar migration rates, uphold the proposed hypothesis that bars are a result of reworking of original diffuse gravel sheets. Finer sediment is winnowed out of the poorly sorted upstream deposits and transported downstream as a true bar form. Development of a gravel pavement in upstream sections during this winnowing process limits the supply of bed material to the bar form and, hence, controls bar migration rates. Rapid rates of increase in velocities in upstream sections are required to disrupt the gravel pavement and expose

underlying finer sediment to flows capable of winnowing it out from the coarser lag particles. For this reason, maximum downstream migration rates correlated with maximum rates of upstream velocity increases.

(4) Computed gravel discharges across active transverse bars are closely approximated by the Hollingshead (1971) method of assessing bedload discharge in gravel rivers.

(5) Sorting of sediment on transverse bar surfaces seems to support the hypothesis that the bars are derived from reworking of diffuse gravel sheets.

(6) Sorting of sediment on diagonal bar surfaces is more complex and seems to correlate with bar depositional slope.

CHAPTER 5.

MODEL FOR PROXIMAL-DISTAL STRATIFICATION ORIGINS

Several workers have proposed sedimentary facies models for shallow meltwater fluvial-gravel environments (McDonald and Banerjee, 1971; Boothroyd, 1972; Rust, 1972; Clifton, 1973). The following features associated with the dominant gravel facies are thought to be characteristic of this environment: fining-upward, coarsening-upward, planar cross-stratified and massive gravels. Most of these models have been based upon observations of surficial sediment distributions on outwash flats during low flow conditions. Few workers have tried to correlate bar growth and gravel transport patterns on bar surfaces with these "characteristic" features (N. Smith, 1972, 1974). The following model is proposed for origins of stratification in proximal and distal reaches of outwash flats, based upon the results of the present study dealing with channel braiding patterns (Chapter 3) and gravel transport on bars (Chapter 4).

All bars observed in the present study fine downstream. Upstream sections of bars are characterized by a

coarse gravel lag pavement. In no cases were these coarse pebbles seen in transport over the downstream migrating lobe surface. During downstream migration of transverse bar lobes, planar cross-stratified gravels would be deposited on coarser-grained channel deposits. Upon subsequent reworking of transverse bar lobes, all vestiges of the cross-stratification may be destroyed, leaving a massive finer-grained bar deposit overlying the coarser-grained channel sediments. Vertical deposition on bar tops during waning flows could also produce fining-upward trends. Deposits associated with transverse bars would consist of predominantly fining-upward gravels, with lenses of cross-stratified sequences.

Fining-upward trends can also result from the infilling of secondary channels or pools by laterally-migrating longitudinal or point bar types, where grain sizes increase laterally from bar tops to the secondary channels. Vertical deposition in channels during waning flows would also yield fining-upward gravel sequences.

Gravel sorting on diagonal bars depends upon the bar depositional slope. Bars with low slopes fine downstream, where upstream deposits are interpreted as a lag deposit. Bars with intermediate slopes show no obvious size sorting. Bars with high slopes begin to behave as avalanche foresets, where coarser particles accumulate at the base of the foreset

margin. Upon lateral growth of these diagonal bars into adjacent secondary channels, fining-upward or massive gravels would probably be deposited. Strata would be very low angle to horizontally bedded.

Poorly sorted massive gravels are probably the result of high-flow diffuse gravel sheet deposition, which has had little opportunity of being reworked during subsequent low flow conditions. Massive gravels which appear better sorted and display ill-defined horizontal bedding are mostly attributable to extensive reworking of bar and channel outwash sediments. Gravel lags developed at upstream portions of bars would probably be manifest as coarse pebble to cobble-size stringers in section.

Coarsening-up sequences are difficult to account for. They may be a result of pool deposition during stages of increasing discharges, where the size of sediment left as a lag in the convergence channels or pools increases as the competence is increased. However, it is more probable that with increasing competence former finer-grained "lags" would be transported out of the convergence channels, resulting in a single layer deposit of coarse pebbles or cobbles. Most coarsening-up sequences reported from shallow braided gravel deposits may be only apparent where coarse gravels are deposited on remnants of formerly deposited finer-grained sediments. Accompanying the coarse pebble deposition there

was probably erosion of previous deposits, but because of the coarse pebbly nature of these fluvial gravels, it is impossible to discern erosional surfaces.

In coarse-grained proximal reaches most of the sediment is in transport only during high flow flood conditions. Gravel is transported as diffuse gravel sheets, one or two pebbles high, which display very little sediment sorting and no foreset development. Because of the large size of sediment in these upstream reaches, there is very little reworking of these diffuse sheet deposits during lower flows. In protected lee areas of the main channel there is some reworking of sediment into predominantly diagonal bar forms. Sediments in these proximal reaches would probably be poorly sorted gravels, with minor amounts of fining-upward and cross-stratified gravels.

In finer-grained downstream reaches sediment is transported during most of the warm summer months. There is extensive bar development. Bars seem to initiate as diffuse gravel sheets during higher flows. Subsequent reworking of these diffuse sheets yield true bar lobes, the morphology of which depend upon local flow conditions. Diagonal bars with riffle margins and transverse bars with foreset margins are the most common types. Distal outwash gravels would be predominantly cross-stratified with fining-up and massive low angle to horizontally bedded sequences.

CHAPTER 6

PRESERVABILITY OF STRATIFICATION IN MODERN OUTWASH DEPOSITS: NORTH SASKATCHEWAN RIVER

INTRODUCTION AND PROCEDURE

The capricious nature of the rapidly fluctuating environment of valley train glacial meltwater streams makes one wonder if it is at all possible to preserve recognizable sedimentary features in such a setting. Most models of shallow braided river facies have been based upon sediment distributions on outwash surfaces with very little attention given to the potential of such facies being incorporated in the ancient record. For this reason, the preservability of sedimentary features assumed to be characteristic of the dominant gravel facies was estimated by trenching exposed gravel flats of the North Saskatchewan River.

The study area was located on the upper North Saskatchewan River, about 5 miles upstream from the confluence with the Alexandra River (Figure 2). This particular reach was well suited for study as there were many relatively

unmodified bar-and-channel complexes. An area of approximately 135,000 square feet was mapped on the emergent flats. Shallow pits (average depth was 2.5 ft, range: 1.5-4.0 ft) were dug on a 50 foot grid pattern. Detailed stratigraphic sections were then measured in each trench. The following sedimentary features were measured (Figure 30): fining-upward and apparent "coarsening-upward" trends, horizontally and cross-bedded gravels, massive gravels with matrix, and massive gravels without matrix (termed open-work gravels). Coarse pebble or cobble stringers were also noted, termed coarse "lag" layers. Percentages of various sedimentary features in section were calculated. Areal percentages of bar-and-channel coverage on the surface of the study area were determined. Comparisons were then made between the surficial depositional features and types of stratification seen in section.

RESULTS AND DISCUSSION

The surficial base map of the study area is shown in Figure 31. Despite the fact that this upper reach has a high slope (0.0064) and large grain size (mean grain size = -4.7Ø) (D. Smith, 1973), the bar-and-channel forms resemble those found in the midstream section of the Kicking Horse River

Figure 30A. Trench section illustrating alternating open-work - closed-work gravel sequences. Ruler is one foot long

Figure 30B. Coarse-grained "lag" layer as seen in section. Scale is in "tenths of feet".

A

B

Figure 30C. Trench section illustrating coarse-grained planar cross-stratification. Ruler is one foot long.

Figure 30D. Longitudinal section of transverse bar lobe illustrating planar cross-stratified granules - small pebbles. Rule is one foot long.


C


D

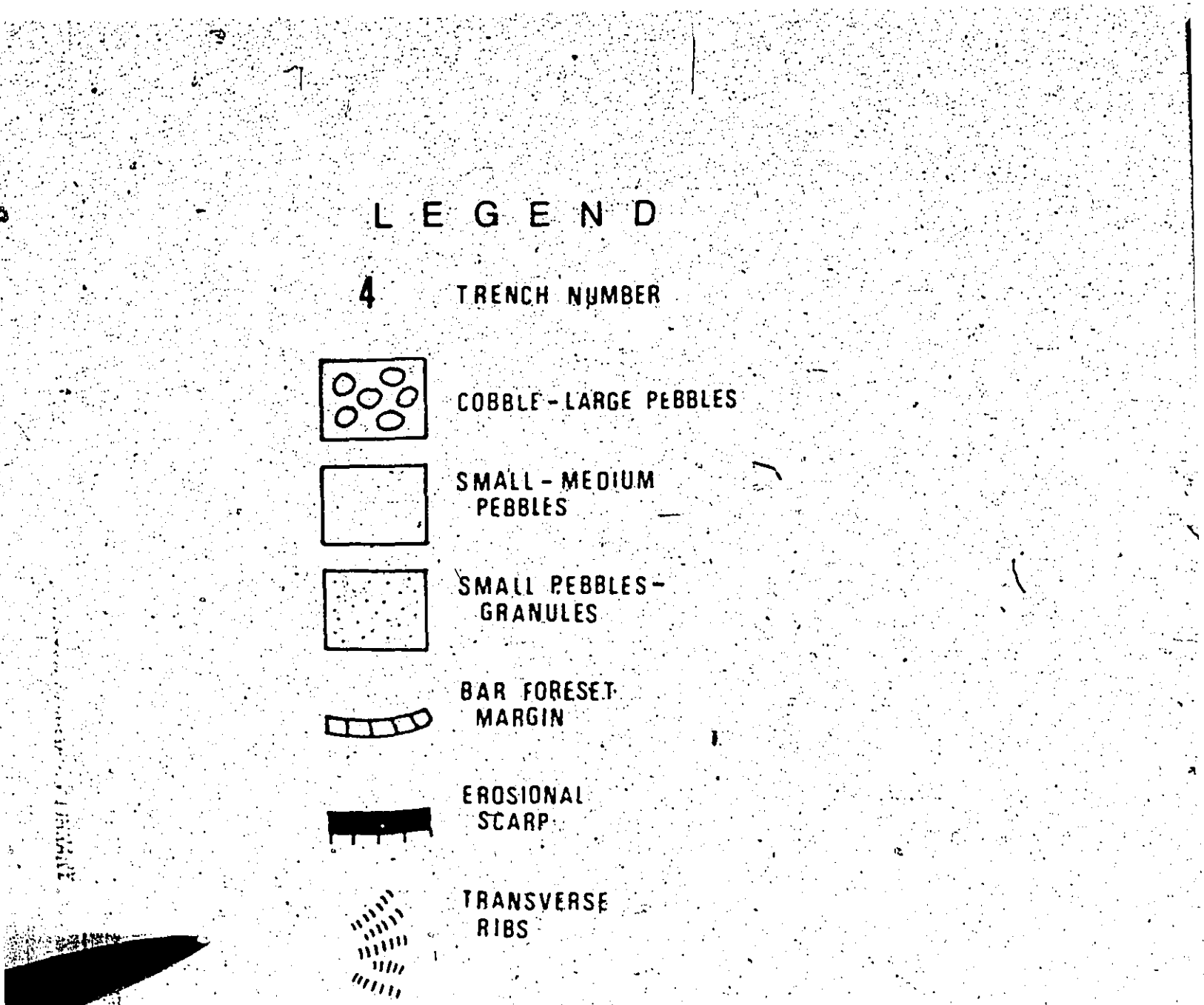

Figure 31. Surficial base map of exposed study reach, North Saskatchewan River

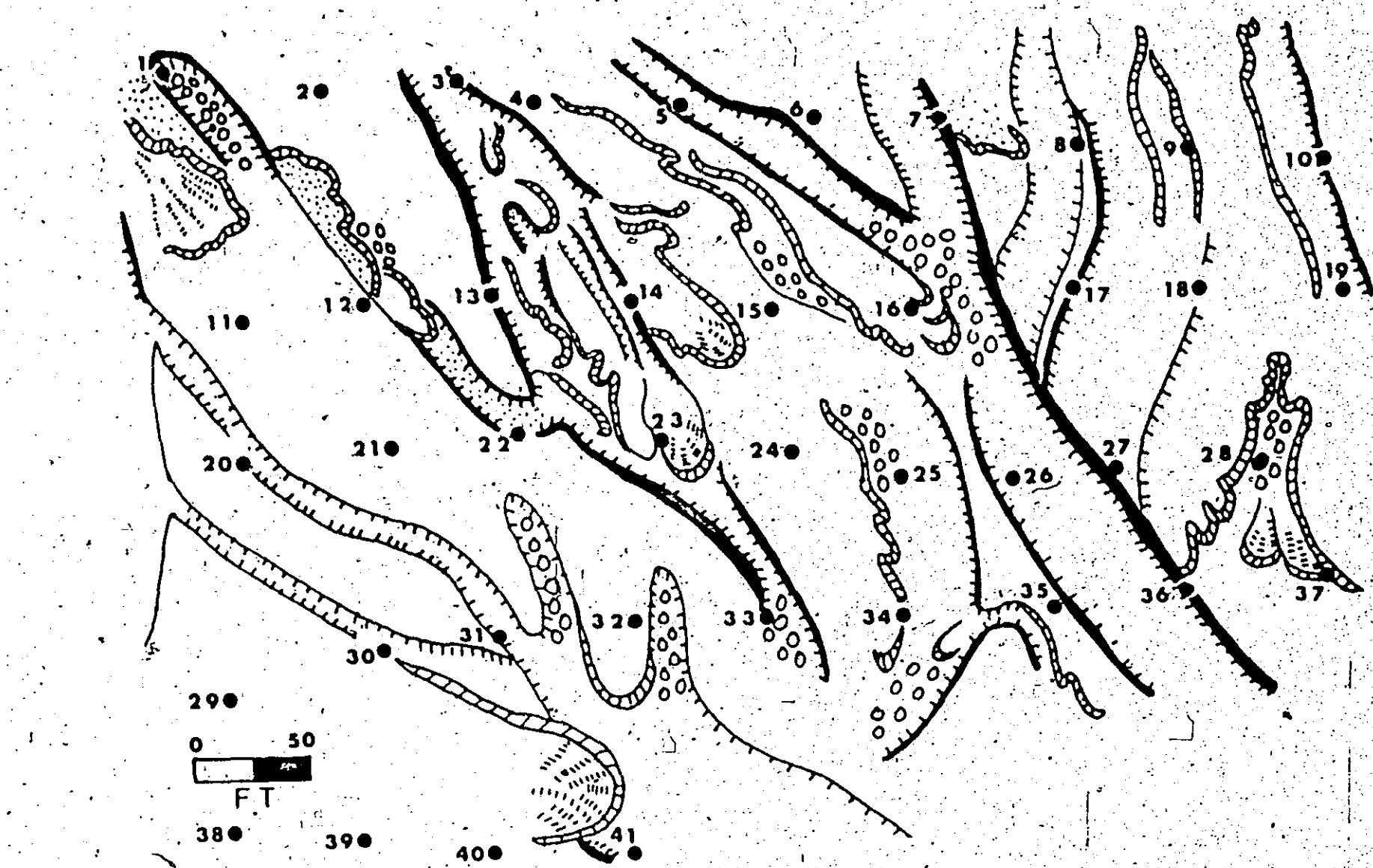
1
2
3
4
5
6
7
8
9
10
11
12
13
14
15
16
17
18
19
20
21
22
23
24
25
26
27
28
29
30
31
32
33
34
35
36
37
38
39
40
41
0
50
FT

(mean grain size = -4.3ϕ, slope = 0.0034). This suggests that grain size of the bed material or discharge fluctuations (which is impossible to evaluate) have a more pronounced affect on braiding patterns than slope. Because the braid patterns are similar, stratification types preserved in this study area would be representative of those associated with intermediate to distal outwash areas of the Kicking Horse River, where there is extensive bar formation and reworking of sediment in the warm summer months.

Surficial areal percentages show that in the North Saskatchewan study reach bars comprise 0.085% of the outwash area; convergence channels or pools account for 0.012%, and major channels comprise 0.085%. Reworked gravel flats of unknown origin account for 99.82% of the surface area.

Stratigraphic sections are given in Appendix 5. A summary diagram of the main sedimentary features measured in trenched sections is shown in Figure 32. Sedimentary feature percentages were calculated separately for pits that fell on bar, channel or unknown areas. It was hoped that the different subenvironments of the outwash plain could be distinguished on the basis of features associated with the gravel deposits. Bars display lower percentages of fining- and coarsening-up trends and slightly more cross-bedded gravels than the channeled areas. However, this analysis is not very accurate because it is impossible to determine in

Figure 32. Percentages of sedimentary features observed in trench sections, North Saskatchewan River

SEDIMENTARY FEATURE	AVG. %
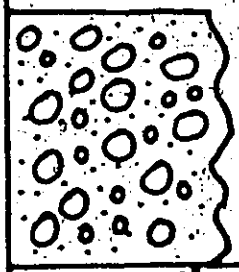 MASSIVE	50.9
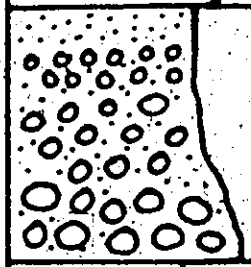 FINING-UPWARD	14.8
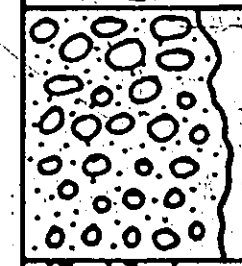 COARSENING-UPWARD	16.8
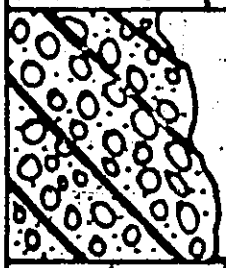 CROSS-BEDDED	15.4
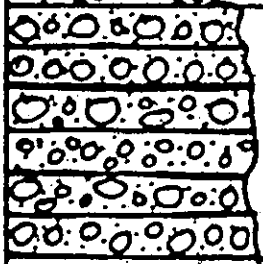 HORIZONTALLY BEDDED	1.6
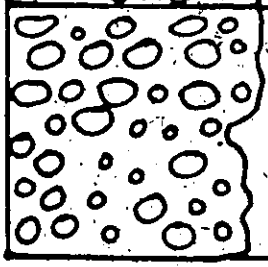 OPEN-WORK	4.6

section how much of the vertical exposure is attributable to surface bars and channels and how much is relict.

Total percentages of the entire reach (Figure 32) indicate that in modern coarse-grained intermediate to distal outwash plains, massive gravels comprise about 50% of the dominant gravel sediment type. The remaining percentage is almost equally composed of coarsening-upward, fining-upward and cross-bedded gravels, with minor amounts of horizontally bedded and open work gravels. The massive gravels display ill-defined horizontal bedding and are probably attributable to the extensive reworking of bar-and-channel complexes in outwash environments.

CHAPTER 7

SUMMARY: A PROPOSED MODEL FOR GLACIALLY-CONTROLLED BRAIDED RIVER DEPOSITION

In the present study, the following general aspects of bar formation and origins of stratification have been suggested:

(1) In coarse-grained proximal reaches gravel is mainly transported as diffuse gravel sheets, which display very little sediment sorting and no foreset development. Because of the large sediment size in proximal reaches, sediment is in transport only during flood conditions and there is little remolding of diffuse sheets into true bar forms during lower discharge periods. Occasionally, true bars may develop through winnowing processes active in protected areas within the channel system.

(2) In finer-grained medial to distal reaches, sediment is transported during most of the warm summer months. Extensive bar development characterizes these finer outwash flats. Diagonal and transverse bar types were the most common morphologies observed

in all the outwash systems examined in this study. Deposits associated with transverse bar migration would consist primarily of fining-upward massive gravels with a few lenses of planar cross-stratified sequences. Diagonal bar deposits would show fining-upward sequences or massive gravels with low angle to horizontal bedding.

(3) Bars develop from pre-existing diffuse gravel sheet deposits, where fine sediment is winnowed out of the poorly sorted upstream deposits and transported as true bar lobe. Upstream sections of bars are commonly characterized by coarse lag deposits.

(4) In modern medial to distal outwash plains, massive gravels comprise about 50 percent of the dominant sediment type preserved in section. Remaining percentages are equally composed of fining-upward and cross-stratified gravels with minor amounts of well-defined horizontally bedded and open-work gravels. The dominant massive gravels display an ill-defined horizontal bedding and are probably attributable to extensive reworking of gravel flats in confined outwash areas.

Because gravel bars are very transient features and rarely survive successive daily discharge cycles, deposits

associated with bars would lack well-defined extensive stratification. Most of the sediment would be quite channelized, have a massive appearance, and be characterized by lenticular bedding. Bars which initiate in shallow braided complexes, appear to originate from reworking of pre-existing diffuse gravel sheet deposits within the channel. Consequently, coarse-grained gravel lags would pass gradationally into finer sediments with lenses of cross-stratified gravels. Upstream bar lags are quite hard to distinguish from adjacent channel sediments; downstream bar sediments are much finer-grained than deposits in the channel.

Figure 33 gives typical stratigraphic columns which are thought to be associated with proximal versus medial-distal reaches. Coarse-grained proximal reaches would consist primarily of massive poorly sorted gravels derived from diffuse gravel sheet and channel deposition. Few traces of cross-bedding may be preserved, associated with true bar formation in protected areas. Downstream finer-grained reaches would have a decrease in massive gravels and a corresponding increase in planar cross-stratified sequences. Sediments would also be better sorted. Channel and bar sediments could be distinguished where downstream portions of bars are much finer-grained than adjacent channels. Cut-and-fill structures would be evident. Because of the many possible origins of fining-upward gravel sequences, no significant trends would

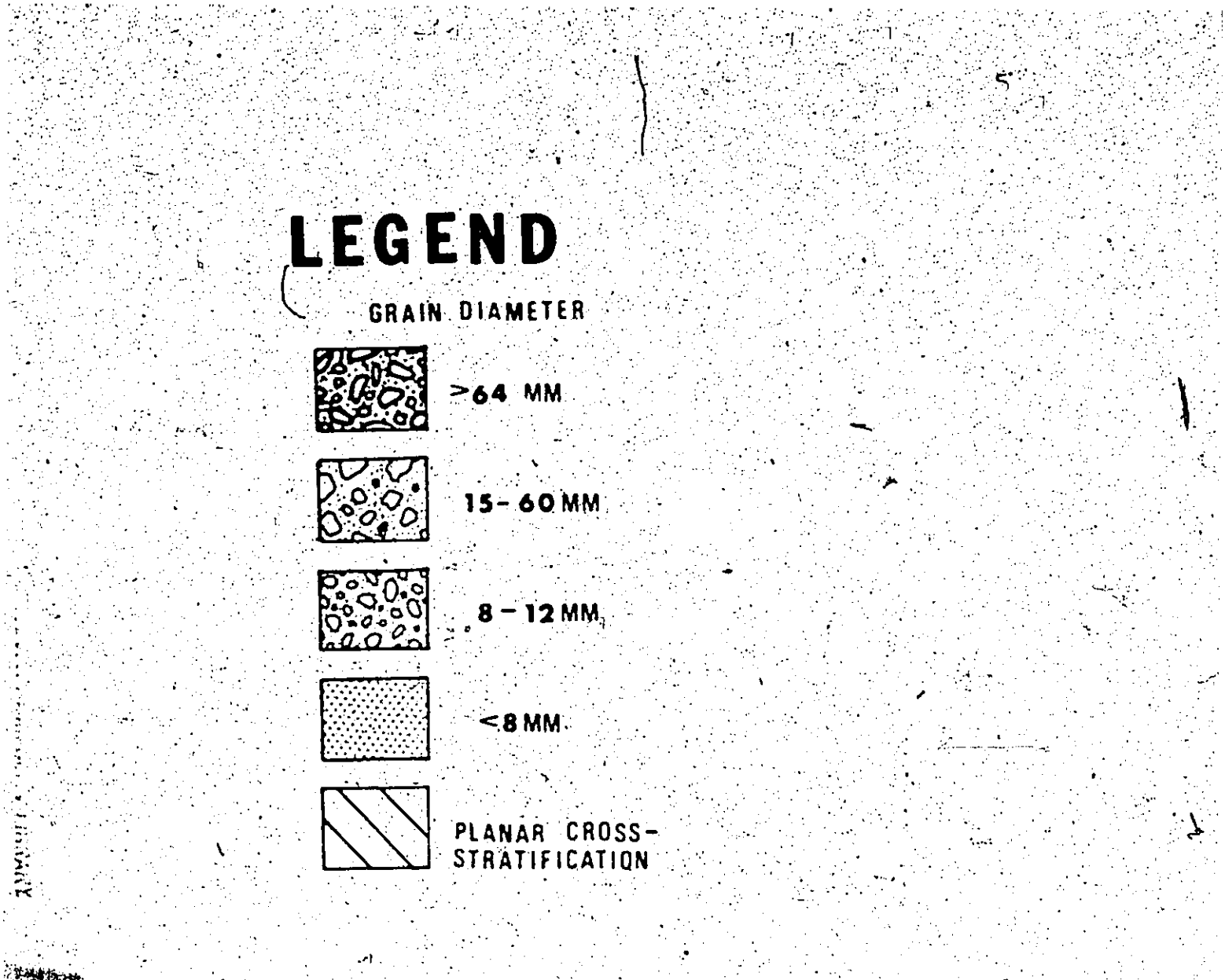

Figure 33. Idealized sketch of stratification types in Proximal versus Medial-Distal reaches. Sections are approximately 3 ft thick (corresponding to sedimentary deposits associated with one summer's flow). Horizontal scale is the same as Figure 16.

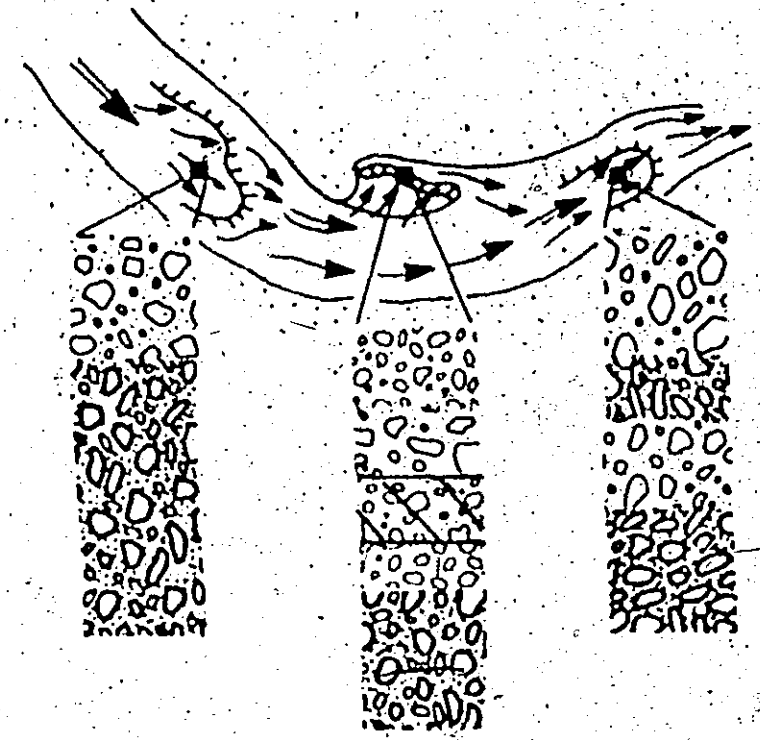

PROXIMAL COARSE GRAINED REACHES

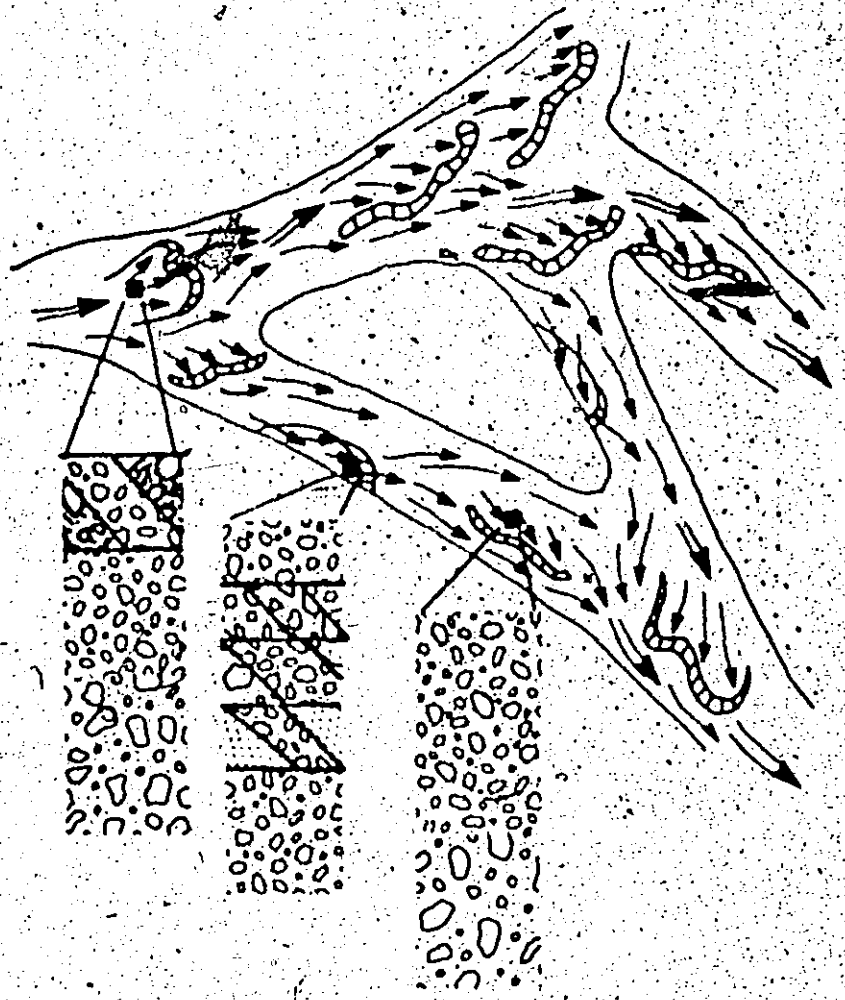

MEDIAL-DISTAL FINER GRAINED REACHES

be expected in this stratification type from proximal to more distal localities. Recognition of these differences in internal stratification types in coarse-grained fluvial outwash gravel sediments would aid in paleogeographic reconstruction.

COMPARISONS WITH OTHER FLUVIAL SYSTEMS

N. Smith (1974) suggested in his discussion of the distinction between glacial meltwater and non-glacially controlled fluvial deposits that the presence of the following features would indicate the rapidly fluctuating flow conditions characteristic of glaciofluvial environments: (1) reactivation structures; (2) alternating open-work and matrix filled gravel sequences; (3) graded growth increments in planar cross-strata, and (4) graded sand-silt laminations. However, the results of the present study indicate that these features have a low probability of being incorporated into the record of coarse-grained outwash systems. The bulk of confined valley-train glaciofluvial sediments appears to be composed of massive gravels with little or no bedding.

The major distinction between glacial meltwater and nonglaciofluvial systems is in the periodicity of discharge fluctuations. Both systems have high spring melt floods. The glaciofluvial environment is also characterized by daily summer

diurnal fluctuations in discharge, which constantly rework previous bar-channel deposits. Non meltwater rivers are subject to more sporadic high rainfall flooding. Both systems would probably yield massive gravel deposits which display some crude horizontal bedding and occasional sedimentary structures. Beds may be somewhat more lenticular in the glacial environment where reworking of sediments is more frequent. However, these distinctions are quite subtle and may not be recognizable in coarse-grained fluvial deposits.

Distinctions between the environments may be in the association of meltwater fluvial deposits with glaciolacustrine influenced deposits. In certain areas catastrophic ice-dam lake breakouts (termed jökulhlaups) flood associated valley-train deposits. Very little work has been done on jökulhlaup influenced rivers (Church, 1972; Baker, 1973; Fahnestock and Bradley, 1973). It is thought that a sudden surge of high flood discharges into the fluvial system would probably completely remobilize the bed material and transport the bulk of sediment as bar forms. Rapid downstream migration of bars would probably result in extensive planar cross-stratified sequences (Fahnestock and Bradley, 1973; Baker, 1973). Lower normal summer meltwater flows would be incapable of reworking the catastrophic flood deposits and the extensive planar cross-stratification associated with the jökulhlaup - mobilized bar forms would eventually be incorporated

into the sedimentary record. Associated jökulhlaup features would also include huge scour pockets; ice floated debris and perhaps features associated with buried ice debris. The occurrence of these structures in coarse-grained fluvial sediments would suggest glacially controlled flow conditions.

REFERENCES

ALLEN, J.A., 1914. Geology of Field map-area, British Columbia and Alberta: Geol. Surv. Canada, Mem. 55, 312p.

ALLEN, J.R.L., 1970. Physical Processes of Sedimentation: American Elsevier Pub. Co., Inc., 248p.

ARMSTRONG, A.J., and TIPPER, T.H., 1948. Glaciation in north central British Columbia: Amer. Jour. Sci., v. 246, p.283-310.

BAIRD, D.M., 1970. Banff National Park: Geol. Surv. Canada, Dept. Energy, Mines and Resources, Misc. Rept. 13, p.45-61.

BAKER, V.R., 1973. Paleohydrology and sedimentology of Lake Missoula flooding in eastern Washington: Geol. Soc. America, Spec. Paper 144, 79p.

BeMENT, W.O., 1972. The sedimentologic and paleogeographic history of the lower Kicking Horse River valley, southeast British Columbia, during deglaciation: Unpub. M.S. Thesis, Univ. Illinois at Chicago Circle.

BIRKELAND, P.W., 1968. Mean velocities and boulder transport during Tahoe-age floods of the Truckee River, California-Nevada: Geol. Soc. America Bull., v.79, p.137-192.

BLATT, H., MIDDLETON, G.V. and MURRAY, R.C., 1972. Origin of Sedimentary Rocks: Prentice-Hall, Englewood Cliffs, N.J., 634p.

BOOTHROYD, J.C., 1972. Coarse-grained sedimentation on a braided outwash fan, northeast Gulf of Alaska: Coastal Research Div. Tech. Rept. No. 6-CRD, Geography Programs, Office of Naval Research, U.S. Government. 127p.

BRADLEY, W.C., FAHNESTOCK, R.K. and ROWEKAMP, E.T., 1972. Coarse sediment transport by flood flows on Knik River, Alaska: Geol. Soc. America Bull., v.83, p.1261-84.

CHURCH, M.A., 1972. Baffin Island sandurs: a study of Arctic fluvial processes: Geol. Surv. Canada, Bull. 216, 208p.

CLIFTON, H.E., 1973. Pebble segregation and bed lenticularity in wave-worked versus alluvial gravel: Sedimentology, v.20, p.173-187.

COOPER, R.H., 1970. A study of bed-material transport based on the analysis of flume experiments: Unpub. Ph.D. Thesis, Univ. Alberta, Edmonton.

COSTELLO, W.R. and WALKER, R.G., 1972. Pleistocene sedimentology, Credit River, southern Ontario: a new component of the braided river model: Jour. Sed. Petrology, v.42, p.389-400.

DAILY, J.W. and HARLEMAN, D.R.F., 1966. Fluid Dynamics. Reading, England.

DOUGLAS, D.F., 1962. The structure and sedimentary deposits of braided rivers: Sedimentology, v.1, p.167-190.

EINSTEIN, H.A., 1950. The bed-load function for sediment transportation in open channel flows: U.S. Dept. Agric., Soil Conserv. Serv., Tech. Bull. No. 1026, 71p.

EYNON, G. and WALKER, R.G., 1974. Facies relationships in Pleistocene outwash gravels, southern Ontario: a model for bar growth in braided rivers: Sedimentology, v.21, p.43-70.

FAHNESTOCK, R.K., 1963. Morphology and hydrology of a glacial stream, White River, Mt. Rainier, Washington: U.S. Geol. Survey, Prof. Paper 422-A, 70p.

and BRADLEY, W.C., 1973. Knik and Matanuska Rivers, Alaska: a contrast in braiding. In Fluvial Geomorphology, Marie Morisawa (ed.). 4th Ann. Geomorphology Symposium, State Univ. New York, Binghamton, N.Y., p.220-250.

FULTON, R.J., 1971. Radio carbon geochronology of southern British Columbia: Geol. Surv. Canada, Paper 71-37, 28p.

GESSLER, J., 1965. The beginning of bedload movement of mixtures investigated as natural armoring in channels: Trans. by E.A. Prych, translation T-5, W.M. Keck Lab. of Hydraulics and Water Resources, Div. Engineering and Applied Sci., Calif. Inst. Tech., Pasadena, Calif., 89p.

GILBERT, G.K., 1914. The transportation of debris by running water: U.S. Geol. Survey, Prof. Paper 86, 261p.

GUY, H.P., SIMONS, D.B. and RICHARDSON, E.V., 1966. Summary of alluvial channel data from flume experiments, 1956-1961: U.S. Geol. Survey, Prof. Paper 462-I, 96p.

HARMS, J.C., 1969. Hydraulic significance of some sand ripples: Geol. Soc. America Bull., v.80, p.363-96.

HELLEY, E.J., 1969. Field measurements of the initiation of large bed particle movement in Blue Creek near Klamath, California: U.S. Geol. Survey, Prof. Paper 562-G, 19p.

HOLLINGSHEAD, A.B., 1971. Sediment transport measurements in a gravel river: Proc. Amer. Soc. Civil Engineers, Jour. Hydraulics Division, v.97, No. HY11, November, p.1817-34.

HJULSTROM, F., 1935. Studies of the morphological activity of rivers as illustrated by the River Fyris: Geol. Inst. Uppsala Bull., v.25, p.221-527.

KELLER, E.A., 1970. Bed-load movement experiments, Dry Creek, California: Jour. Sed. Petrology, v.40, p.1339-44.

_____, 1971. Areal sorting of bed-load material: the hypothesis of velocity reversal: Geol. Soc. America Bull., v.82, p.753-56.

_____ and MELHORN, W.N., 1973. Bedforms and fluvial processes in alluvial stream channels: selected observations. In Fluvial Geomorphology, Marie Morisawa (ed.). 4th Ann. Geomorphology Symposium, State Univ. New York, Binghamton, N.Y., p.253-84.

KELLERHALS, R., 1967. Stable channels with gravel-paved beds: Amer. Soc. Civil Engineers, Jour. Waterways and Harbours Division, v.93, p.63-83.

KRIGSTROM, A., 1962. Geomorphological studies of sandur plains and their braided rivers in Iceland: Geograf. Ann., v.44, p.328-46.

McDONALD, B.C. and BANERJEE, I., 1971. Sediments and bed forms on a braided outwash plain: Canadian Jour. Earth Sci., v.8, p.1282-1301.

McPHERSON, H.J., 1970. Landforms and glacial history of the upper North Saskatchewan valley, Alberta, Canada: Canadian Geographer, v.14, p.10-26.

ORE, H.T., 1964. Some criteria for recognition of braided stream deposits: Univ. Wyoming, Contrib. Geology, v.3, p.1-14.

RUBEY, W.W., 1937. The force required to move particles on a stream bed: U.S. Geol. Survey, Prof. Paper 189-E, p.E121-E140.

RUST, B.R., 1972. Structure and process in a braided river: Sedimentology, v.18, p.221-245.

SHIELDS, A., 1936. Anwendung der Ähnlichkeitsmechanik und der Turbulenzforschung auf die Geschiebewegung. Berlin Preuss Versuchsanstalt für Wasser, Erd und Schiffbau, no. 26, 26p.

SMITH, D.G., 1972. Aggradation and channel patterns of the Alexandra-North Saskatchewan River, Banff National Park, Alberta. In Mountain Geomorphology, Univ. British Columbia Geographic Series 14, p.177-185.

_____, 1973a. Aggradation and channel braiding in the North Saskatchewan River, Alberta, Canada: Ph.D. Thesis, Johns Hopkins Univ., 84p.

_____, 1973b. Aggradation of the Alexandra-North Saskatchewan River, Banff Park, Alberta. In Fluvial Geomorphology, Marie Morisawa (ed.). 4th Ann. Symposium on Geomorphology, State Univ. New York, Binghamton, N.Y., p.201-20.

_____, in preparation. Neoglacial history of Sunwapta Pass, Jasper Park, Canada.

SMITH, N.D., 1970. The braided stream depositional environment: comparison of the Platte River with some Silurian clastic rocks, north-central Appalachians: Geol. Soc. America Bull., v.81, p.2993-3014.

_____, 1971. Transverse bars and braiding in the lower Platte River, Nebraska: Geol. Soc. America Bull., v.82, p.3407-20.

_____, 1972. Sedimentology of the upper Kicking Horse River, British Columbia: a braided meltwater stream: Geol. Soc. America, Abstr. Northeastern Section, Buffalo, N.Y., p.45-6.

_____, 1974. Sedimentology and bar formation in the upper Kicking Horse River, a braided outwash stream: Jour. Geology, v.82, p.205-223.

SUNDBORG, A., 1956. The River Klarälven: a study of fluvial processes: Geograf. Ann., v.38, p.127-316.

WESTGATE, J.A. and DREIMANIS, A., 1967. Volcanic ash layers of Recent age at Banff National Park, Alberta, Canada: Canadian Jour. Earth Sci., v.4, p.155-61.

WILCOCK, D.N., 1971. Investigation into the relations between bedload transport and channel shape: Geol. Soc. America Bull., v.82, 2159-76.

WILLIAMS, G.P., 1967. Flume experiments on the transport of a coarse sand: U.S. Geol. Survey, Prof. Paper 562-B, 31p.

WILLIAMS, P.F. and RUST, B.R., 1969. The sedimentology of a braided river: Jour. Sed. Petrology, v.39, p.649-79.

APPENDIX 1

VELOCITY PROFILE DATA
DOWNSTREAM STUDY REACH, KICKING HORSE RIVER

Curve 1. Locality 1. Transverse Bar Upstream Station, 7 August 1973; 1:20 p.m.

Curve 2. Locality 1. 7 August 1973; 1:45 p.m.

Curve 3. Locality 2. Transverse Bar Upstream Station, 11 August 1973; 12:15 p.m.

Curve 4. Locality 2. 11 August 1973; 12:25 p.m.

Curve 5. Locality 3. Secondary Channel, 11 August 1973; 12:30 p.m.

Curve 6. Locality 4. Transverse Bar Upstream Station, 11 August 1973; 1:30 p.m.

Curve 7. Locality 5. Main Channel, 2:00 p.m.

Curve 8. Locality 6. Transverse Bar Downstream Station, 4 August 1973; 12:20 p.m.

Curve 9. Locality 6. Transverse Bar Upstream Station, 4 August 1973; 12:10 p.m.

Curve 10. Locality 6. Transverse Bar Upstream Station, 4 August 1973; 3:10 p.m.

Curve 11. Locality 6. Transverse Bar Downstream Station, 4 August 1973; 3:30 p.m.

Appendix 1/continued

Curve 1

Distance Above Bed (y) (ft)	Velocity (ft/sec)
0.25	2.76
0.40	3.13
0.60	4.06
0.80	4.32
1.00	4.35
1.20	4.39
1.40	4.75
1.60	5.51

Curve 2

Distance Above Bed (y) (ft)	Velocity (ft/sec)
0.25	1.97
0.40	1.86
0.60	2.37
0.80	2.23
1.00	1.97
1.20	1.62

Curve 3

Distance Above Bed (y) (ft)	Velocity (ft/sec)
0.25	2.76
0.40	2.55
0.60	2.37
0.80	3.26
1.00	4.25
1.20	3.63
1.40	3.95

Curve 4

Distance Above Bed (y) (ft)	Velocity (ft/sec)
0.25	3.50
0.40	4.08
0.60	4.14
0.70	4.70

Appendix 1/continued

Curve 5

Distance Above Bed (y) (ft)	Velocity (ft/sec)
0.25	3.10
0.40	3.41
0.60	3.45
0.80	3.16
0.25	2.93
0.40	3.26
0.50	3.60

Curve 6

Distance Above Bed (y) (ft)	Velocity (ft/sec)
0.25	0.61
0.40	0.84
0.60	1.30
0.80	1.51
0.90	1.33

Curve 7

Distance Above Bed (y) (ft)	Velocity (ft/sec)
0.25	1.59
0.40	2.00
0.60	2.51
0.80	2.59
1.00	2.45

Curve 8

Distance Above Bed (y) (ft)	Velocity (ft/sec)
0.25	2.62
0.40	3.24
0.60	3.75
0.70	3.77

Appendix 1/continued

Curve 9

Distance Above Bed (y) (ft)	Velocity (ft/sec)
0.25	2.15
0.40	2.45
0.60	2.80
0.80	2.99
1.00	2.93
1.20	2.95
1.40	2.73

Curve 10

Distance Above Bed (y) (ft)	Velocity (ft/sec)
0.25	1.55
0.40	2.00
0.60	2.51
0.80	2.65
1.00	2.84
1.20	3.10
1.40	3.03
1.60	2.45

Curve 11

Distance Above Bed (y) (ft)	Velocity (ft/sec)
0.25	3.71
0.40	4.54
0.60	5.04
0.70	5.81

APPENDIX 2

BOTTOM VELOCITY-AVERAGE VELOCITY RELATIONS, ACTIVE TRANSVERSE BARS*

(1) Curve No.	(2) Depth	(3) 0.6x (depth)	(4) Velocity at 0.6x (depth)	(5) 0.8x (depth)	(6) Velocity at 0.8x (depth)	(7) 0.2x (depth)	(8) Velocity at 0.2x (depth)	Avg Vel**	Bottom Velocity
1	1.6	0.96	4.35	1.28	4.52	0.32	2.95	3.73	2.75
2	1.2	0.72	2.29	0.96	2.03	0.24	2.74	2.38	2.74
3	1.4	0.84	2.97	3.87	1.12	0.28	1.93	1.52	1.95
4	0.7	0.42	4.06	0.56	4.13	0.14	3.50	3.81	3.50
5	0.8	0.48	3.44	0.64	3.40	0.16	3.10	3.25	3.10
6	0.9	0.54	1.17	0.72	1.46	0.18	0.63	1.04	0.63
7	1.0	0.60	2.52	0.80	2.59	0.20	1.54	2.06	1.54
8	0.7	0.42	3.25	0.56	3.67	0.14	2.62	3.14	2.62
9	1.4	0.84	2.96	1.12	2.95	0.28	2.22	2.58	2.13
10	1.6	0.96	2.82	1.28	3.07	0.32	1.82	2.44	1.59
11	0.7	0.42	4.60	0.56	4.96	0.14	3.72	4.34	3.72

*Depth in feet. Velocities in feet/sec.
**Avg Vel = [Col(8)+Col(6)]/2

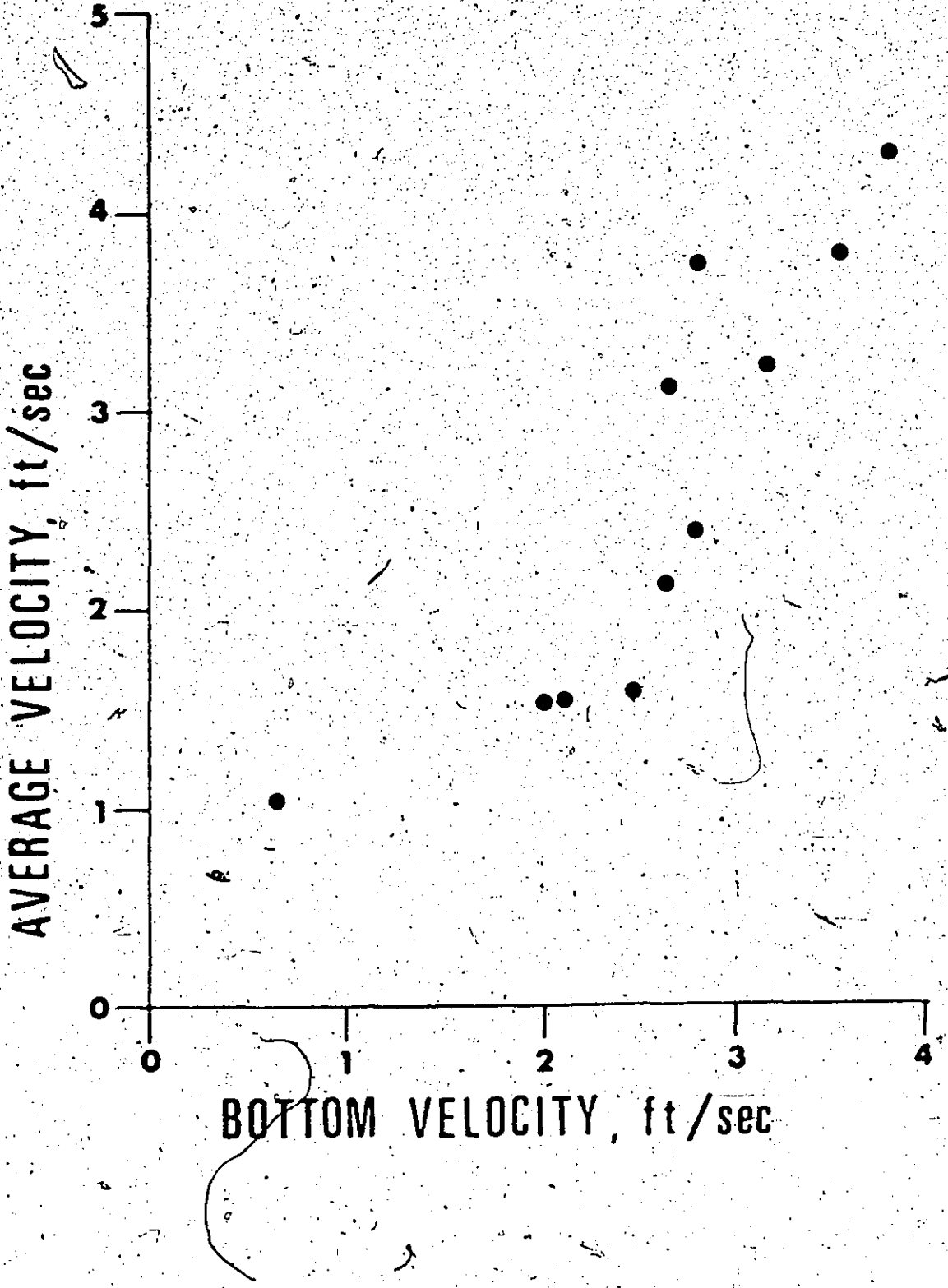
AVERAGE VELOCITY, ft/sec
BOTTOM VELOCITY, ft/sec
0
1
2
3
4
5

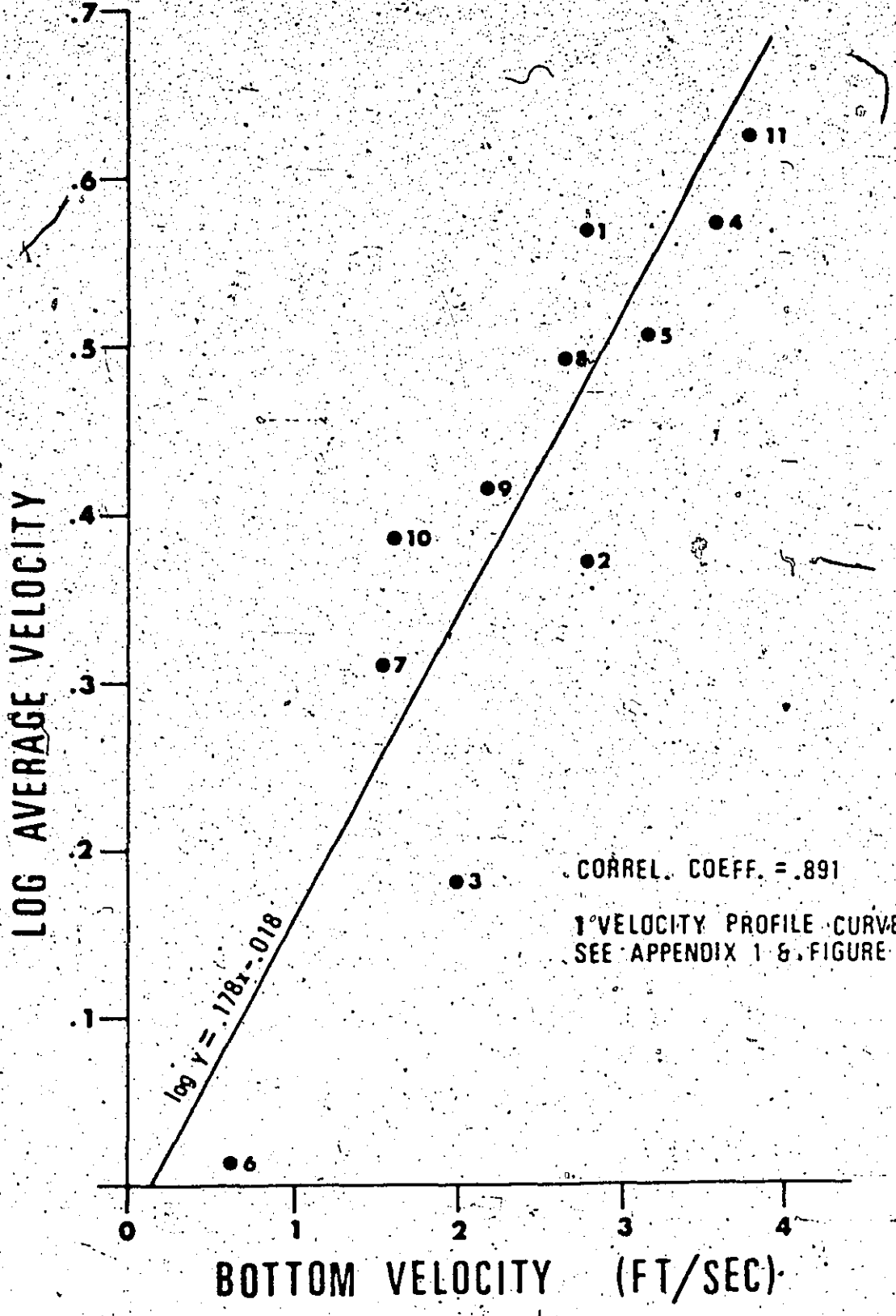

CORREL. COEFF. = .891

1°VELOCITY PROFILE CURVE.
SEE APPENDIX 1 & FIGURE 22

APPENDIX 3

IN SITU HYDROLOGIC AND GRAVEL TRANSPORT MEASUREMENTS, ACTIVE TRANSVERSE BARS

BAR 2, AUG 2

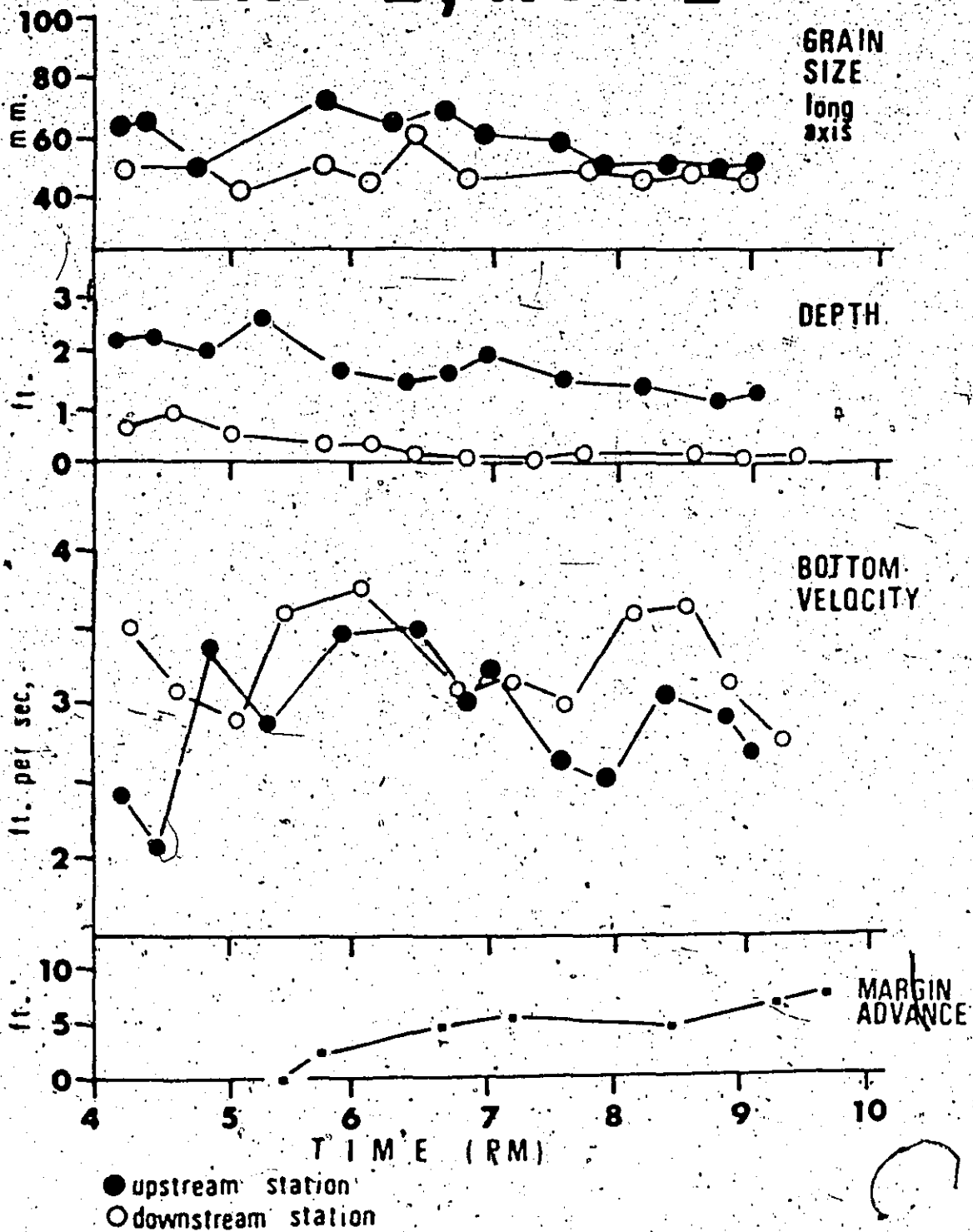
GRAIN SIZE long axis
mm.
100
80
60
40
DEPTH
ft.
3
2
1
0
BOTTOM VELOCITY
ft. per sec.
4
3
2
MARGIN ADVANCE
ft.
10
5
0
4
5
6
7
8
9
10
TIME (RM)
upstream station
downstream station

BAR 2, AUG 3

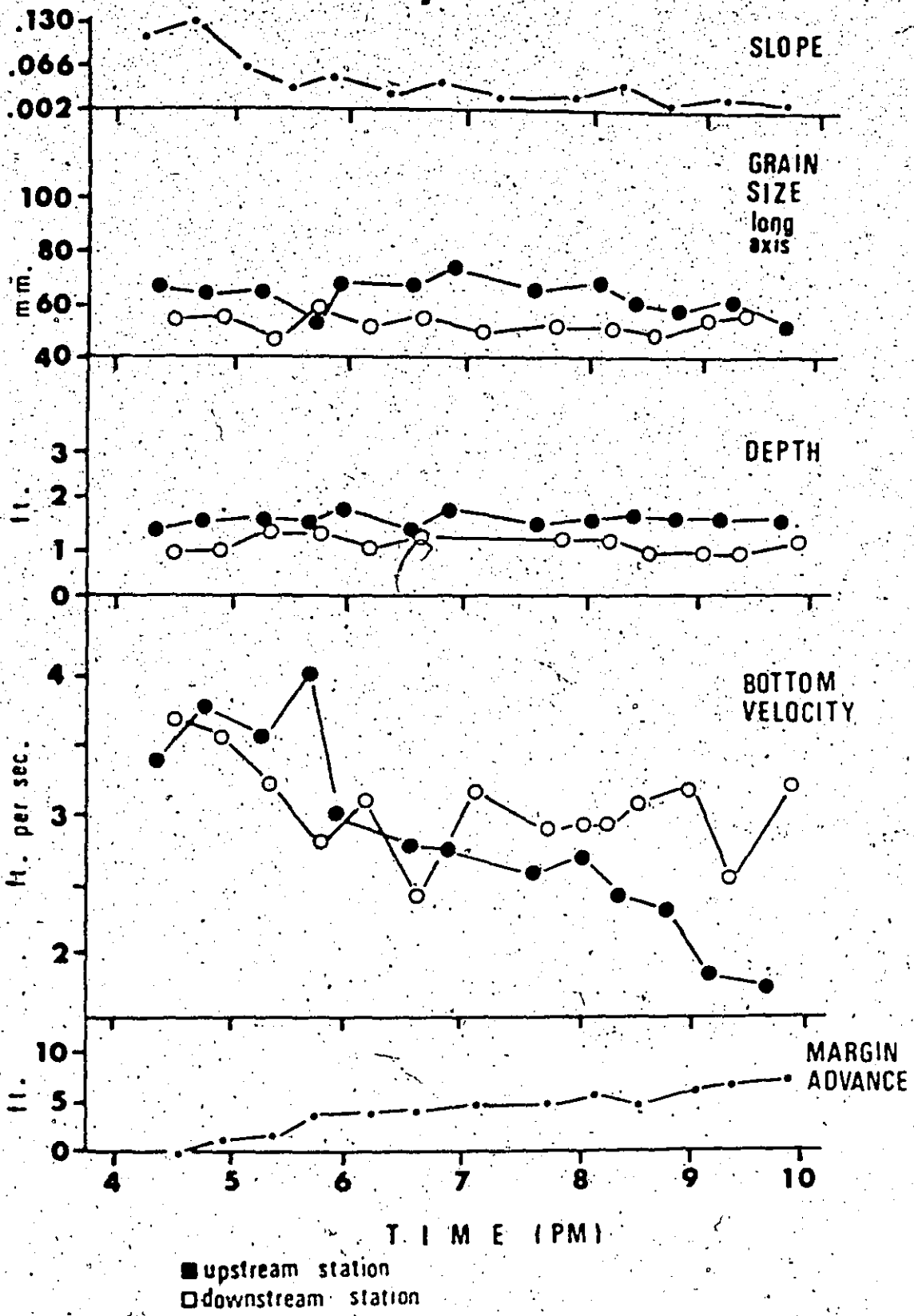
.130
.066
.002
SLOPE
GRAIN SIZE long axis
100
80
60
40
mm.
DEPTH
3
2
1
0
ft.
BOTTOM VELOCITY
4
3
2
ft. per sec.
MARGIN ADVANCE
10
5
0
ft.
4
5
6
7
8
9
10
TIME (PM)
upstream station
downstream station

BAR 2, AUG 4

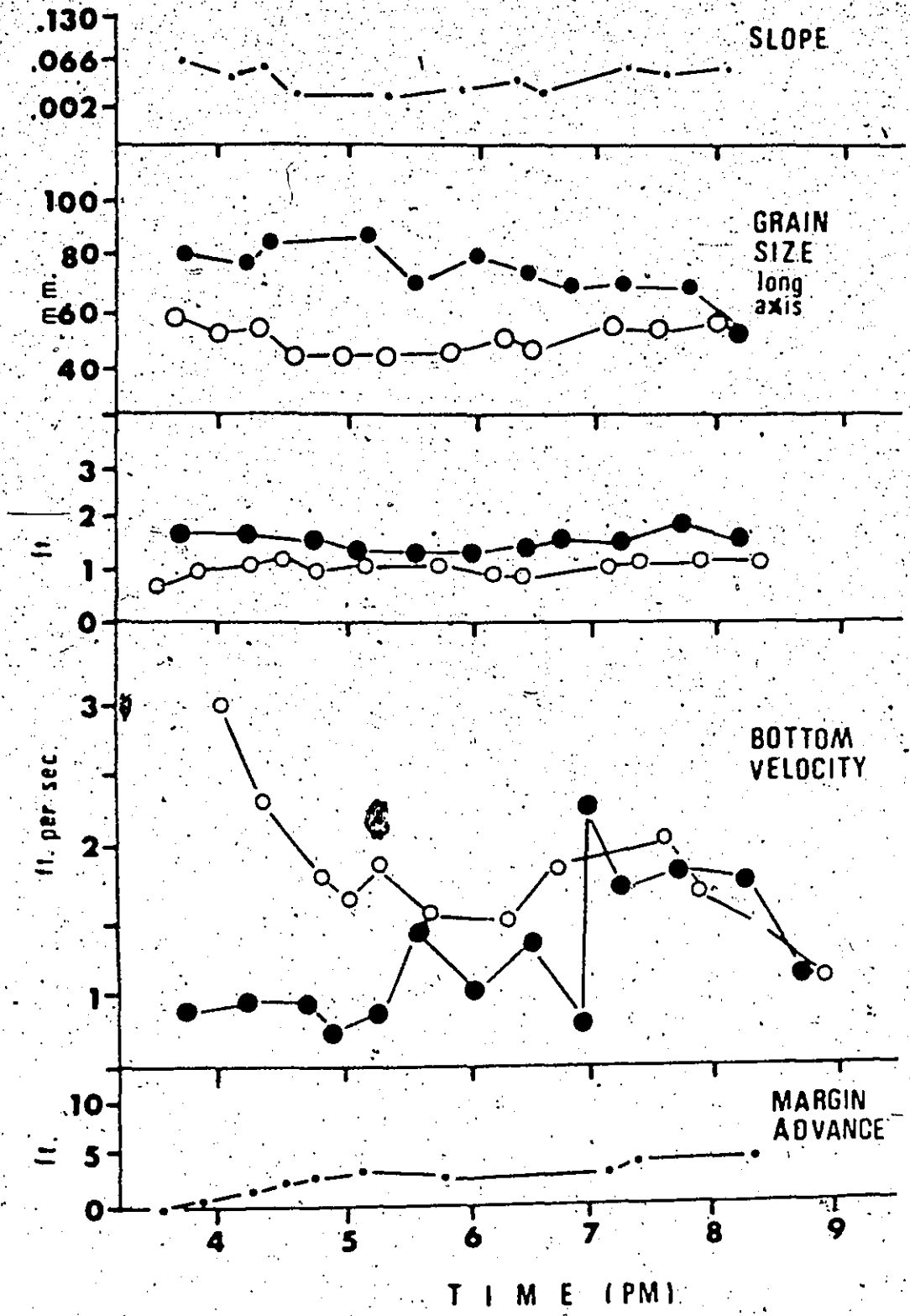
.130
.066
.002
SLOPE
100
80
60
40
mm.
GRAIN SIZE
long axis
3
2
1
0
ft.
3
2
1
ft. per sec.
BOTTOM VELOCITY
10
5
0
ft.
MARGIN ADVANCE
4
5
6
7
8
9
TIME (PM)
upstream station
downstream station

BAR 3, AUG 8

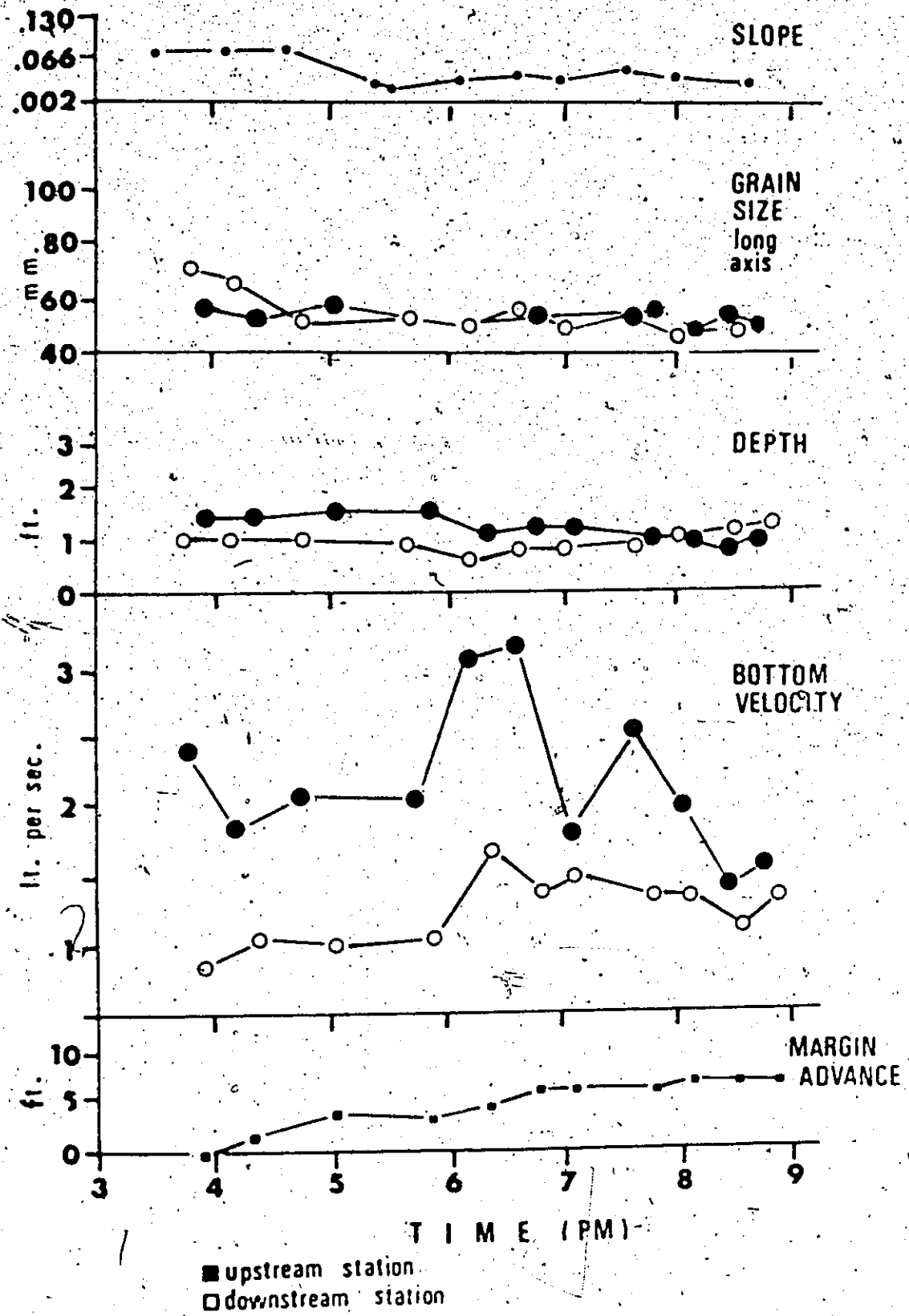
.130
.066
.002
SLOPE
100
80
60
40
mm
GRAIN SIZE long axis
3
2
1
0
ft.
DEPTH
3
2
1
ft. per sec.
BOTTOM VELOCITY
10
5
0
ft.
MARGIN ADVANCE
3
4
5
6
7
8
9
TIME (PM)
upstream station
downstream station

BAR 3, AUG 6

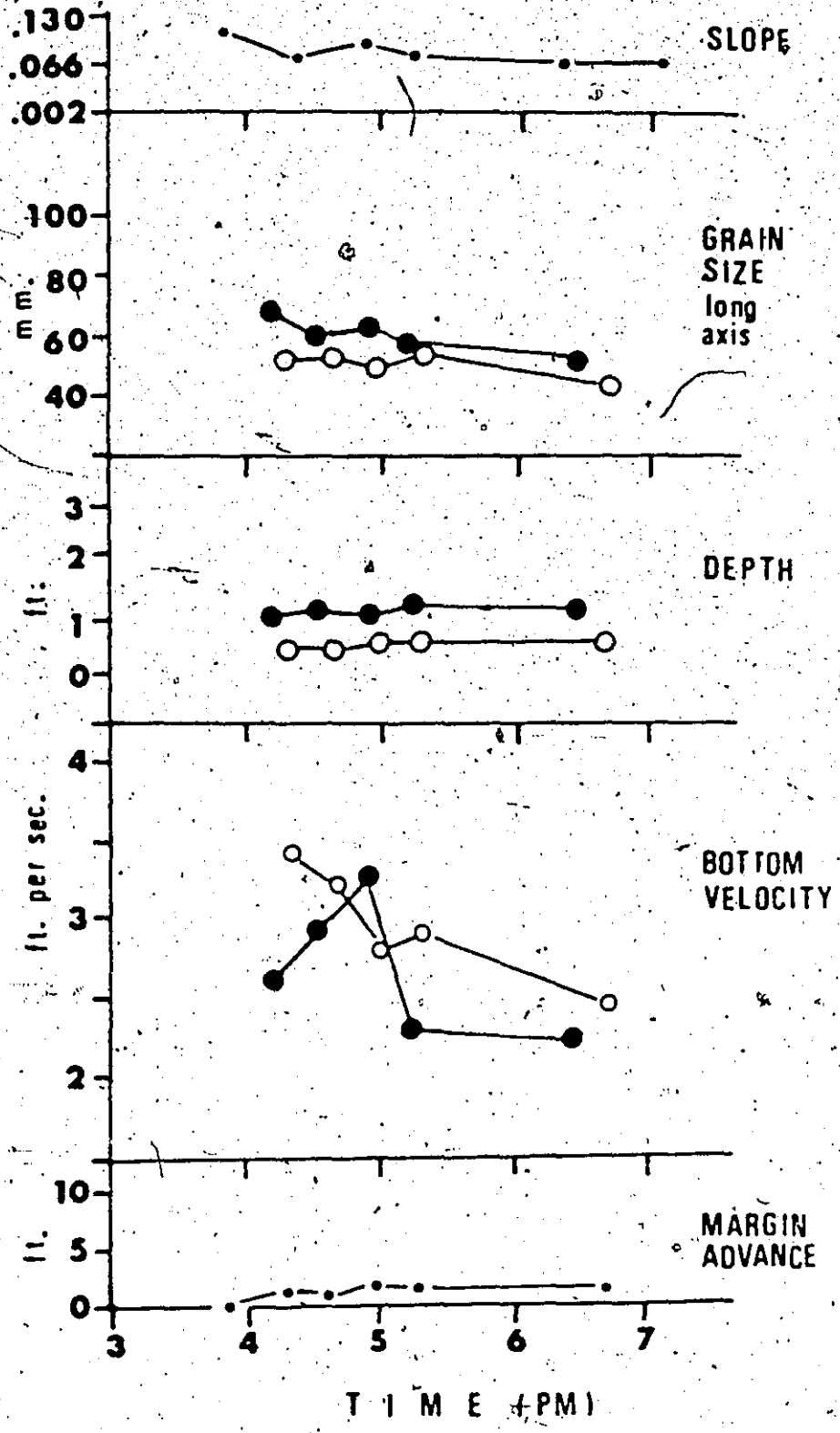
.130
.066
.002
SLOPE
100
80
60
40
mm
GRAIN SIZE long axis
3
2
1
0
ft.
DEPTH
4
3
2
ft. per sec.
BOTTOM VELOCITY
10
5
0
ft.
MARGIN ADVANCE
3
4
5
6
7
TIME (PM)
upstream station
downstream station

BAR 6, AUG 10

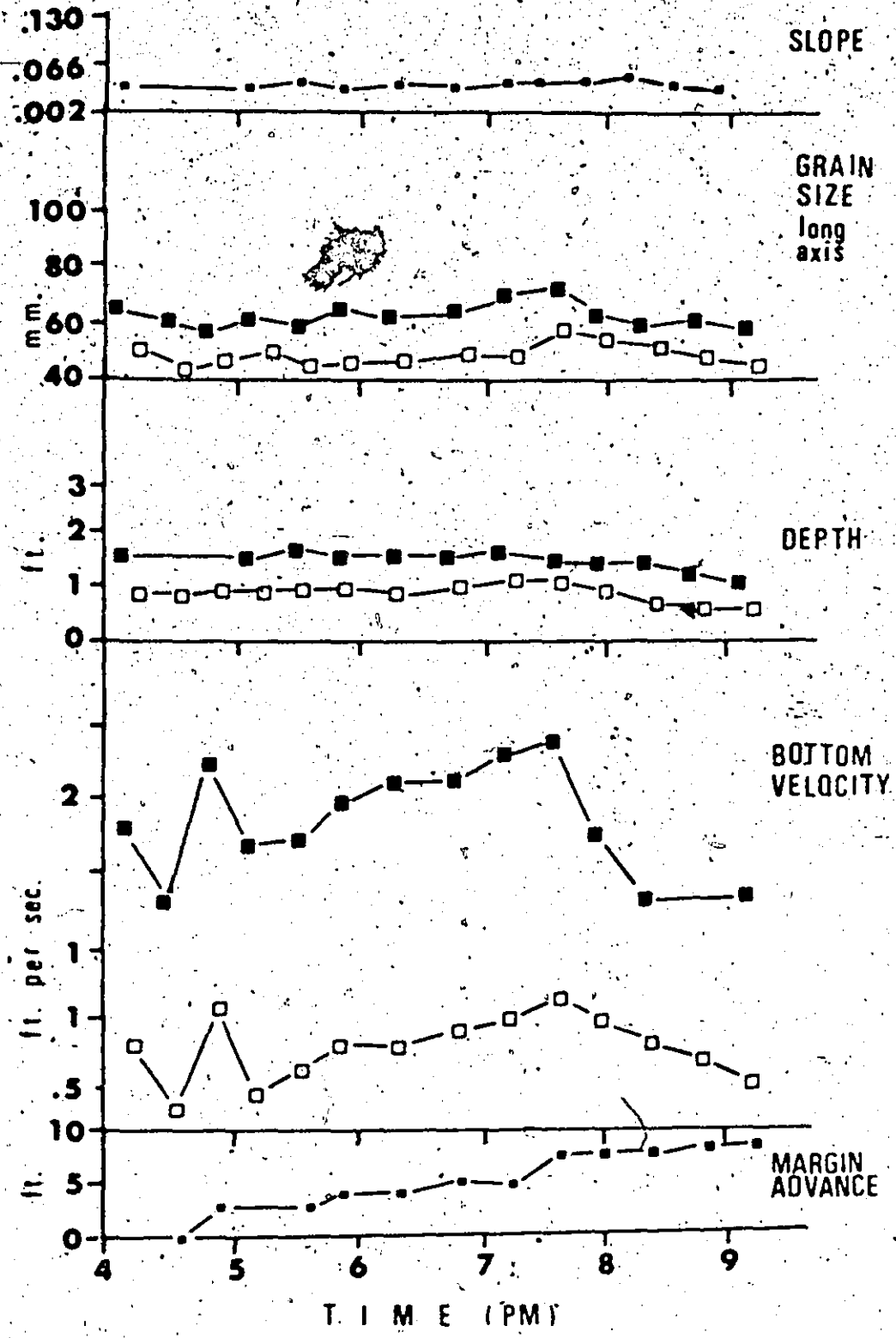
.130
.066
.002
SLOPE
100
80
mm. 60
40
GRAIN SIZE long axis
3
2
ft. 1
0
DEPTH
2
ft. per sec. 1
1
.5
BOTTOM VELOCITY
10
5
ft. 0
MARGIN ADVANCE
4
5
6
7
8
9
T I M E (PM)
upstream station
downstream station

APPENDIX 4

CALCULATIONS OF THE PROBABILITY OF UPSTREAM SEDIMENT ON ACTIVE TRANSVERSE BARS REMAINING STATIONARY

"Minimum Percentage" Probability*

Grain size** (mm)	Δp_{lag}	$\bar{g}_{lag}\Delta p_{lag}$	Δp_{Bar}	$\bar{g}_{Bar}\Delta p_{Bar}$	$\bar{g}_{lag}\Delta p_{lag} + \bar{g}_{Bar}\Delta p_{Bar}$	q	Avg. q
52.1	0.23	10.419	0.04	2.428	12.847	0.811	0.796
53.2	0.17	7.701	0.03	1.821	9.522	0.809	
51.0	0.28	12.684	0.05	3.035	15.719	0.807	
50.0	0.28	12.684	0.05	3.035	15.719	0.807	
43.1	0.40	18.120	0.08	4.856	22.976	0.789	
39.6	0.45	20.385	0.09	5.464	25.848	0.789	
38.1	0.45	20.385	0.09	5.463	25.848	0.789	
39.0	0.45	20.385	0.09	5.463	25.848	0.789	
46.9	0.34	15.402	0.07	4.249	19.651	0.784	
46.4	0.34	15.402	0.07	4.249	19.651	0.784	

*Based upon minimum percentages of given grain sizes on the cumulative frequency curve envelopes, Fig. 28

**Intermediate axis (B-axis)

Appendix A/continued

"Maximum Percentage" Probability*

Grain size** (mm)	Δp_{lag}	$\bar{q}_{lag}\Delta p_{lag}$	Δp_{Bar}	$\bar{q}_{Bar}\Delta p_{Bar}$	$\bar{q}_{lag}\Delta p_{lag} + \bar{q}_{Bar}\Delta p_{Bar}$	q	Avg. q
52.1	0.22	9.966	0.19	11.533	21.499	0.464	0.461
53.2	0.17	7.701	0.14	8.498	16.199	0.475	
51.0	0.27	12.231	0.23	13.961	26.192	0.467	
50.0	0.27	12.231	0.23	13.961	26.192	0.467	
43.1	0.37	16.761	0.33	20.031	36.792	0.456	
39.6	0.42	19.026	0.38	23.066	42.092	0.452	
38.1	0.42	19.026	0.38	23.066	42.092	0.452	
39.0	0.42	19.026	0.38	23.066	42.092	0.452	
46.9	0.32	14.496	0.28	16.996	31.492	0.460	
46.4	0.32	14.496	0.28	16.996	31.492	0.460	

$q_{calc} = \beta_{lag}\Delta p_{i\ lag}\ \bar{q}_{lag}\Delta p_{i\ lag} + \bar{q}_{Bar}\Delta p_{i\ Bar}$

$\bar{q}_{lag} = 45.3$ lbs

$\bar{q}_{Bar} = 60.7$ lbs

*Based upon maximum percentages of given grain sizes on the cumulative frequency curve envelopes, Fig. 28

**Intermediate axis (B-axis)

APPENDIX 5

STRATIGRAPHIC SECTIONS MEASURED IN SHALLOW PITS TRENCHED IN EXPOSED NORTH SASKATCHEWAN RIVER OUTWASH FLATS

LEGEND

1 SECTION NUMBER

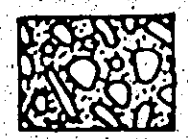

64 – 150 CLOSED WORK GRAIN DIAMETER IN MM

15 – 60

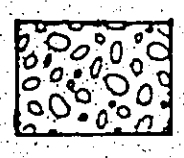

8 – 12

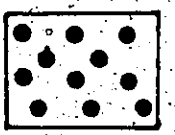

3 – 5

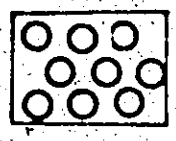

15 – 60 OPEN WORK GRAIN DIAMETER IN MM

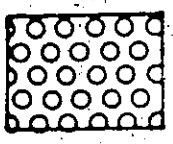

8 – 12

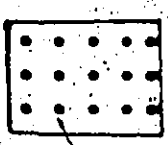

3 – 5

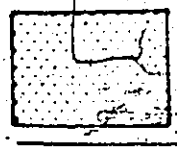

< 3 SAND

PLANAR CROSS-STRATIFICATION

TROUGH CROSS-STRATIFICATION

BAR TRENCH SECTIONS

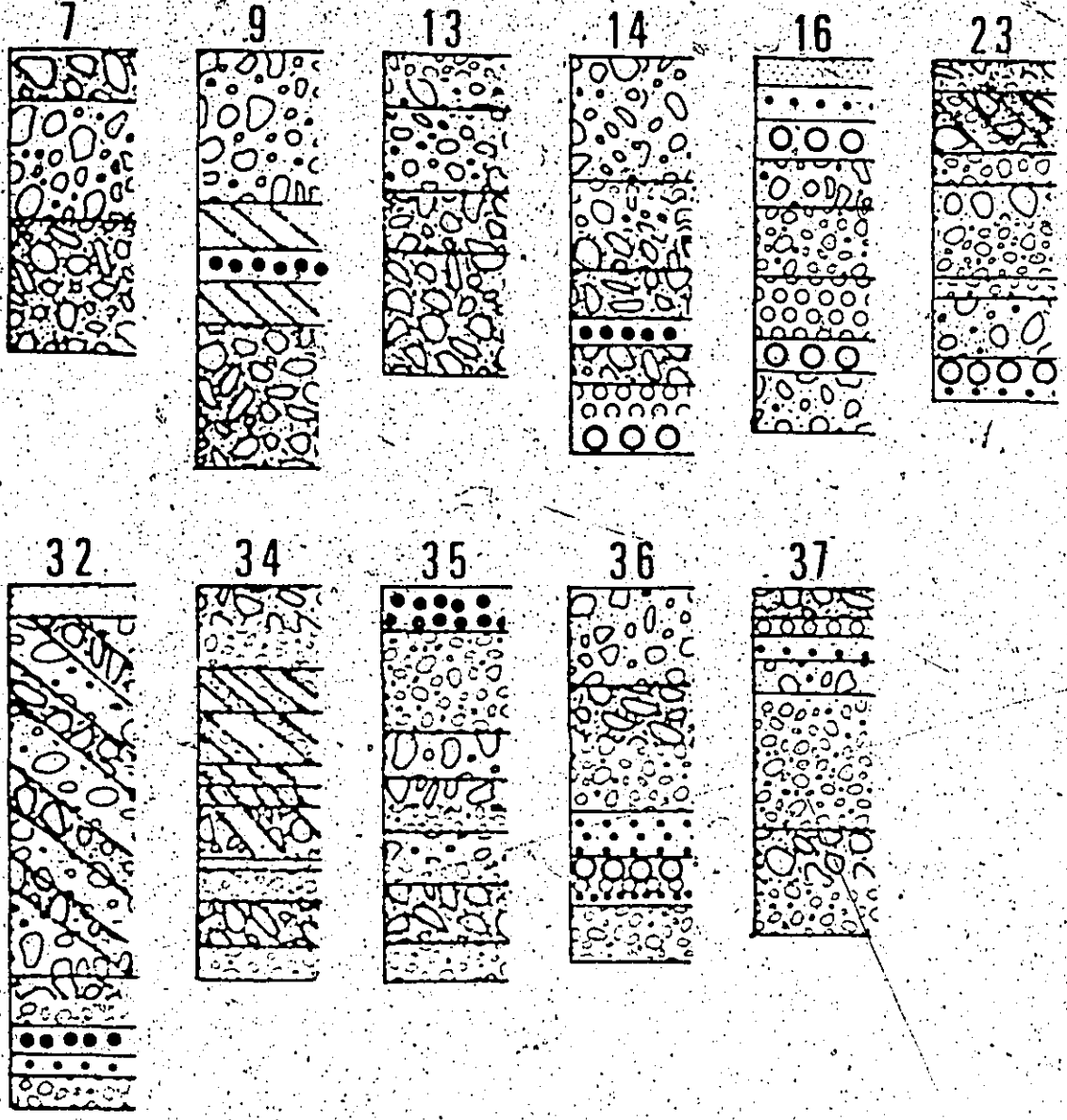

LEGEND

1 SECTION NUMBER

64 – 150 CLOSED WORK GRAIN DIAMETER

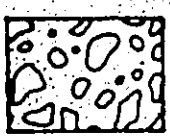

15 – 60 IN MM

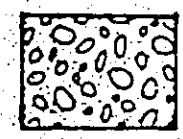

8 – 12

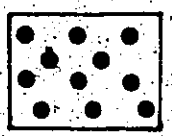

3 – 5

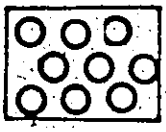

15 – 60 OPEN WORK GRAIN DIAMETER IN MM

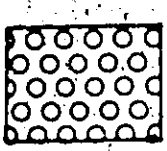

8 – 12

3 – 5

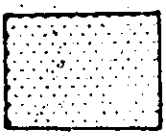

< 3 SAND

PLANAR CROSS-STRATIFICATION

TROUGH CROSS-STRATIFICATION

CHANNEL TRENCH SECTIONS

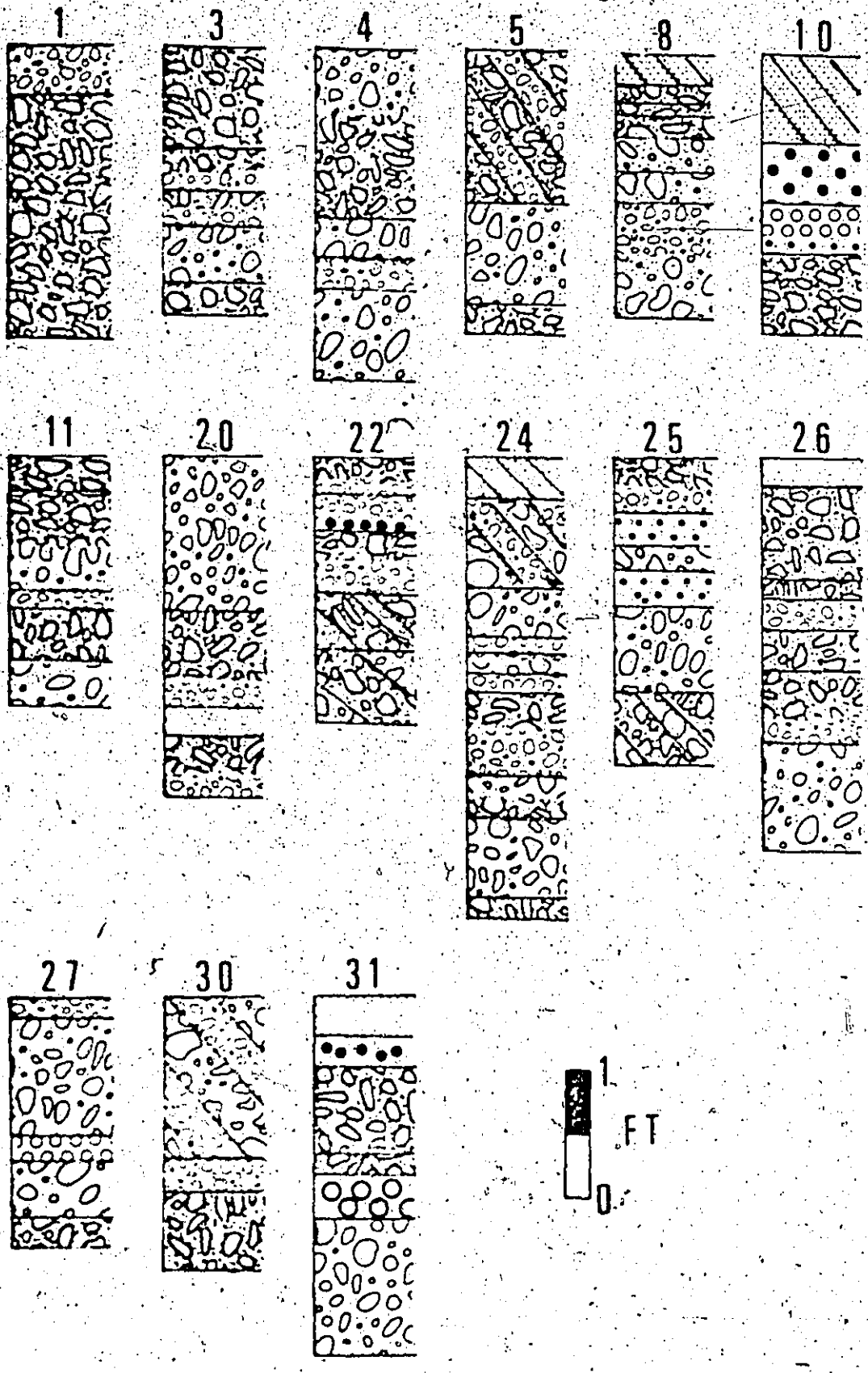

LEGEND

1 SECTION NUMBER

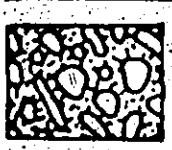

6·4 – 150 CLOSED WORK GRAIN DIAMETER IN MM

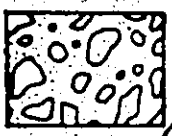

15 – 60

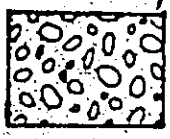

8 – 12

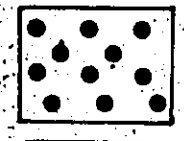

3 – 5

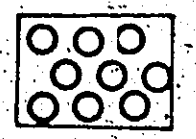

15 – 60 OPEN WORK GRAIN DIAMETER IN MM

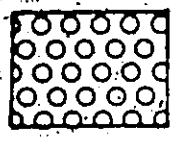

8 – 12

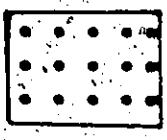

3 – 5

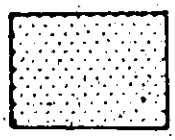

< 3 SAND

PLANAR CROSS-STRATIFICATION

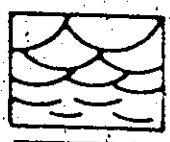

TROUGH CROSS-STRATIFICATION

? BAR-CHANNEL TRENCH SECTIONS